MARTEC™

Smart Solutions for Engineering,
Science and Computing

Near Field Effects of Tidal Power Extraction on Extreme Events and Coastline Integrity in the Bay of Fundy

Final Report

Martec Technical Report #TR-11-01 Rev 01

March 2011

Prepared for:

Offshore Energy Research Associations
5151 George Street, Suite 400
Halifax, NS
B3J 3P7

Martec Limited
1888 Brunswick Street, Suite 400
Halifax, Nova Scotia B3J 3J8 Canada

tel. 902.425.5101
fax. 902.421.1923
email. martec-info@lr.org
www.martec.com

REVISION CONTROL

REVISION	REVISION DATE
01	**March 18, 2011**

PROPRIETARY NOTICE

This report was prepared under the Contract dated January 6, 2010 between **Offshore Energy Research Associates** and Martec Limited and contains information proprietary to Martec Limited.

The information contained herein may be used and/or further developed by **Offshore Energy Research Associates** for their purposes only.

Complete use and disclosure limitations are contained in the Contract dated January 6, 2010 between **Offshore Energy Research Associates** and Martec Limited.

SIGNATURE PAGE

NEAR FIELD EFFECTS OF TIDAL POWER EXTRACTION ON EXTREME EVENTS AND COASTLINE INTEGRITY IN THE BAY OF FUNDY

Technical Report # TR-11-01 Rev 01
18 March 2011

Prepared by: R. Watanabe **Date:** MARCH 18/11

R. Watanabe
Senior Engineer

Reviewed by: J.L. Warner **Date:** March 18/11

J.L. Warner
Consultant

Approved by: J.D. Covill **Date:** March 18/11

J.D. Covill
Team Leader, Field Services

EXECUTIVE SUMMARY

The objective of this project is to quantify the near-field effects of large scale tidal power extraction from the Bay of Fundy by the use of tidal energy extraction devices on the resulting effects of extreme storm events and coastline integrity by implementing a spectral wave model to numerically simulate wave transformation for operational (with turbines) and non-operational (without turbines) tidal conditions. The predicted current fields for the operational and non-operational conditions were obtained directly from the hydrodynamic modeling of the Bay of Fundy produced by Fisheries and Oceans Canada (Dr. David Greenberg). Time-dependent current predictions for the near and far-field models were input directly into the wave spectral model to assess the effects of power extraction on wave transformation. The wave-current modelling analysis was organized into three phases.

- Phase I Seasonal (Non-Storm) Wave Conditions
- Phase II Storm Wave Conditions
- Phase III Extreme Wave Conditions

A spectral wave model (one-dimensional and two-dimensional) was integrated with the existing circulation models for tidal currents in the Bay of Fundy to simulate the wave-current interaction. The overall objective of the work is to assess the changes in wave conditions caused by the extraction of energy from tidal currents, which will indicate the effect of the tidal energy turbines on shoreline erosion and coastline integrity.

The results of the analysis carried out using the SwanOne wave model (a one-dimensional model) show that changes in the current affect the spectral shape of the waves and redistribute wave energy to different frequency bands. As expected, changes in the current produce a net change in the characteristics of energy propagating through the model. More detailed analysis of the transformations occurring, particularly the redistribution of energy to the various frequency bands, was carried out using two-dimensional models.

The modelling of the wave-current interaction using the 2-dimensional STWAVE model with the BIO tidal current model is shown to be a powerful tool to quantify expected changes in wave energy throughout the model domain. The modelling and refinement of the wave-current model was carried out to help define areas of interest in regards to shoreline response to changing conditions. Some of the modelling results from the on-going BIO/Acadia research were integrated into our analysis to incorporate any expected changes in the flow field with the introduction of tidal energy extraction devices. In particular, the extreme case of an intense concentration of 225 turbines installed across Minas Passage had shown a decrease of up to 20% in current magnitude in close proximity to the turbines. Using this value of change in the current field in a portion of Minas Passage and combining with a series of wave conditions, nearshore effects produced only small localized changes in wave energy levels at the adjacent shoreline. Based on the analysis carried out on potential changes in wave patterns as a result of current changes and caused by a set of 225 tidal turbines positioned offshore from Cape Split across a portion of Minas Passage, the resulting nearshore effects observed in the model were small decreases in energy levels at the adjacent shoreline. Therefore, it can be expected that under the conditions analyzed, the energy extraction could cause increased deposition of

suspended sediment in some near-field regions of the Minas Basin channel and Passage. Far field effects of tidal changes were not considered as part of this study.

Small changes shown in the analysis carried out could still represent more significant changes in sedimentation or erosion as a cumulative effect over the longer term. More detailed information on flow and sediment properties are required. Details of the flow field surrounding the individual turbines and the resultant details of flow around an array require further characterization. Sediment properties in the regions of flow changes should be better quantified for predictive effects of deposition or scour due to flow changes.

TABLE OF CONTENTS

LIST OF FIGURES

LIST OF TABLES

1.0 INTRODUCTION

Large-scale tidal power extraction from the Bay of Fundy has the potential to directly influence the behavior of the near-resonant tidal system and alter the physical and ecological environment. Extreme storm events that pass through the Gulf of Maine and Bay of Fundy Region can cause significant coastal flooding, shoreline erosion and sediment re-distribution due to the combined influence of storm waves and currents. Relatively small changes in tidal flows due to power extraction will influence the wave refraction and shoaling patterns in the near-field and cause variations of wave energy levels. Focusing of wave rays causes changes in wave direction, increases in wave energy and decreases in directional wave spreading. This effect has implications not only for the design conditions of the "operational" power extracting units but also the potential for significant changes in shoreline wave energy and the development of sections of increased erosion or accretion.

Martec has undertaken a study to quantify the near-field effects of power extraction on the resulting effects of extreme storm events and coastline integrity by implementing a spectral wave model to numerically simulate wave transformation for operational (with turbines) and non-operational (without turbines) tidal current conditions. The predicted current fields for the operational and non-operational conditions will be obtained directly from the hydrodynamic modeling efforts proposed by Dalhousie University (Dr. Keith Thompson- Far Field Effects) and Fisheries and Oceans Canada (Dr. David Greenberg – Near Field Effects). Time-dependent current and water level predictions for the near and far-field models will be input directly into the wave spectral model to assess the effects of power extraction on wave transformation.

In this project, a spectral wave model will be integrated with the existing circulation models for tidal currents in the Bay of Fundy (see Figure 1-1) to simulate the wave-current interaction. The overall objective of the work is to assess the changes in wave conditions caused by the extraction of energy from tidal currents, which will indicate the effect of the tidal energy turbines on shoreline erosion and coastline integrity. During this study, the data used in our analysis are updated with on-going results from new current modeling programs that are carried out related to the effect of tidal extraction devices.

The wave - current modeling analysis is organized into three phases.

- Phase I Seasonal (Non-Storm) Wave Conditions – Initial implementation of the spectral wave model to numerically simulate wave transformation in detail for non-storm conditions with no tidal energy extraction to calibrate the model, followed by test cases to include energy extraction.
- Phase II Storm Wave Conditions – Incorporation of operation conditions from numerical tidal models produced by others (e.g., Dalhousie, BIO, Acadia) and the addition of 'storm' events to determine areas of increased waver intensity and sediment transport along the coastline.
- Phase III Extreme Wave Conditions – Establish extreme wave conditions at the energy extraction locations to establish overall effect of wave and current changes due to the

operation of the tidal devices and the resultant effect of these changing fields on the integrity of the structures.

The specific technical objectives of the three phases are:

- Understand and quantify the interaction between the tidal flows and surface waves under existing conditions in the Bay of Fundy
- Assess effects of any changes in tidal flows (due to energy extraction) on wave conditions in the region
- Detail any changes in resultant shoreline wave energy levels

The work activities in Phases I, II and III are discussed in this report. The methodology is described in Section 2 and the results of the analysis are presented in Section 3. Conclusions and recommendations are summarized in Section 4.

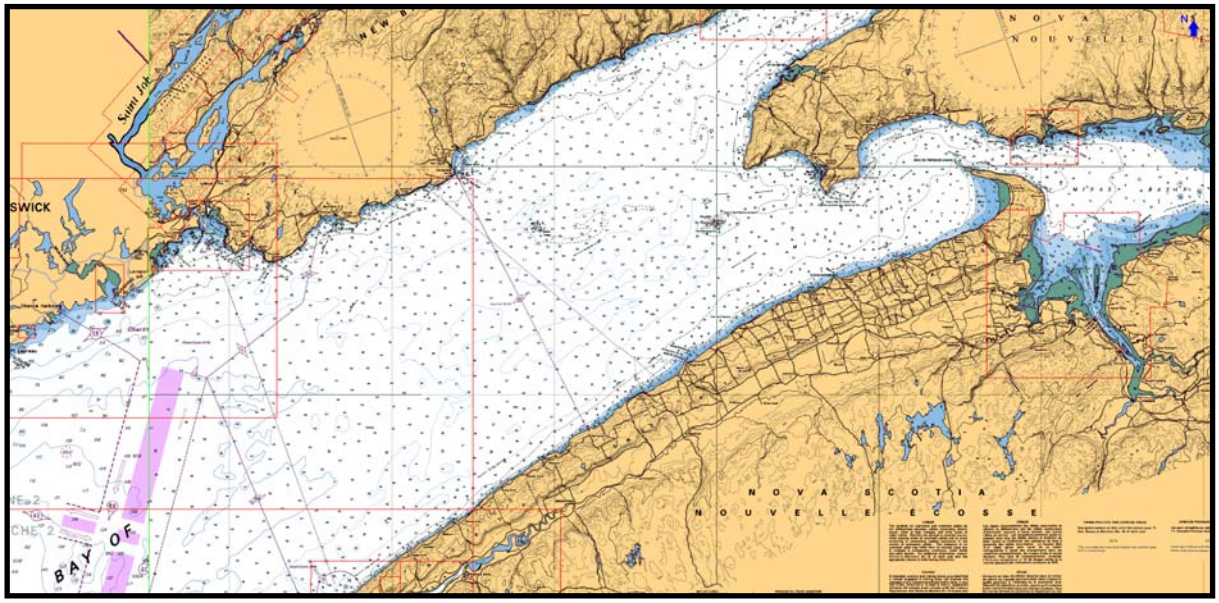

(a) Overall Area of Wave and Current Input

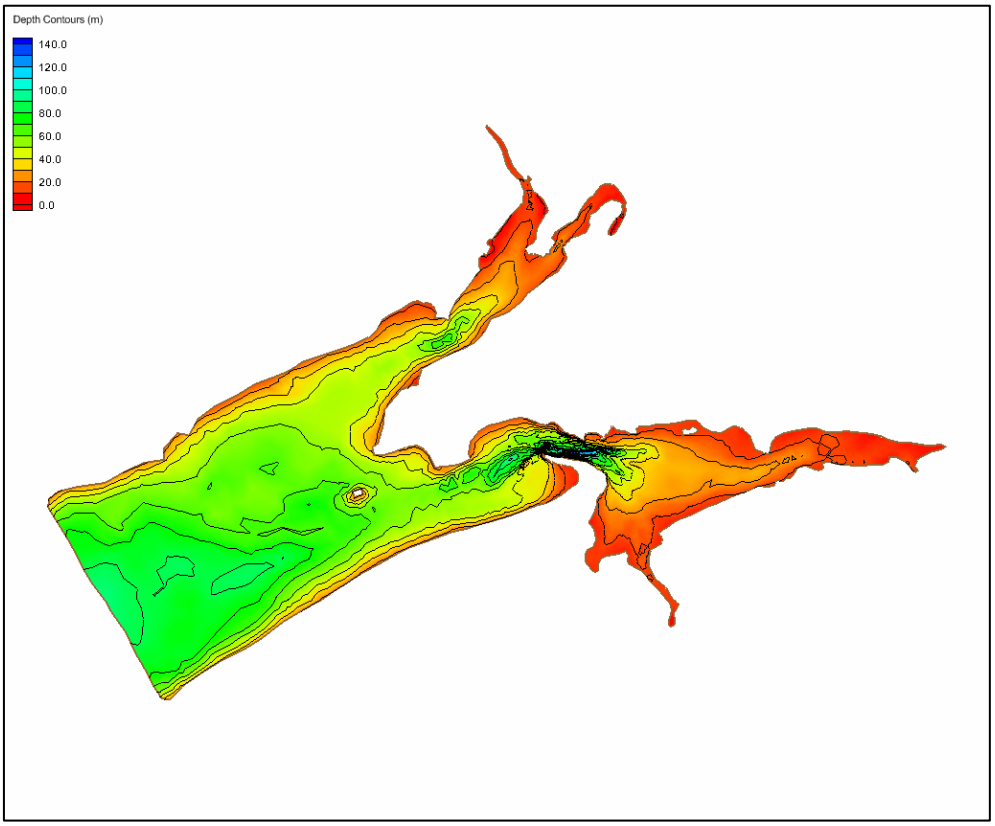

(b) Bathymetry of Overall Study Area

Figure 1-1: Study Domain – Bay of Fundy

2.0 METHODOLOGY

Wave action is one of the predominate factors influencing the magnitude of loads on marine structures, coastal erosion and sediment transport. Thus any changes in wave characteristics are important to quantify in order to predict subsequent environmental consequences. These potential changes have to be part of any risk assessment of modifications to the variability of the marine environment.

In the Bay of Fundy, large tidal currents and the wind-driven waves interact in a complex relationship producing the existing random but bounded effects on erosion and sediment transport. The approach to be used in this assessment is to utilize the detailed grid of tidal currents produced by the hydrodynamic modeling groups and integrate on that current grid a wave prediction scheme with the appropriate physics of interaction to obtain a field of wave spectra (and associated wave height) establishing the resultant energy distribution useful for predicting any changes in erosion and sediment transport on the coastlines.

To simulate the effects of tidal currents on the wave conditions in the Bay of Fundy, it is necessary to couple the models for tidal currents and ocean waves, which may use different grid types, geographical coordinate systems, domains and grid resolutions. In order to exchange data between the tidal current model and the wave model, data on the tidal current mesh must be interpolated to the computational grid for the waves.

In Phase I, output from the existing tidal current model developed by Dave Greenberg of Fisheries and Oceans Canada (BIO model) (grid detail is shown in Figure 2-1) is integrated with output developed from the MSC50 wave hindcast model to establish any changes in wave energy magnitudes and concentration along the coastline. Sample tidal current data from the BIO model are shown in simplified form in Figure 2-2.

Wave conditions for the Bay of Fundy Region are derived primarily from Environment Canada's MSC50 data set for the period 1955 to 2005 and from DFO wave buoy measurements at selected locations within the model domain. The MSC50 data set is a 50 year continuous hindcast for the Northern Hemisphere that includes shallow water effects. Joint frequency distributions of significant wave height and spectral period by direction were generated to assess the seasonal wave climatology in the Bay of Fundy. Wave hindcast locations selected for use in this study are shown in Figure 2-3 and their coordinates and water depths are shown in Table 2-1.

A spectral wave model based on the wave action balance equation (STWAVE and SWAN) is used to predict more detailed wave transformation due to refraction, shoaling, breaking and non-linear wave-current interactions in coastal regions of the Bay of Fundy. Information about the sea surface is contained in the wave variance spectrum, which defines the distribution of wave energy over all frequencies and directions. The wave energy density is not conserved when waves propagate on an ambient current, but the wave action density is conserved. The STWAVE (Smith et al., 2001) and SWAN (TU Delft 2009) models are based on the spectral action balance equation, which includes the effects of refraction and frequency shifts induced

by the current. Since the strong tidal currents can greatly change wave conditions, but waves only weakly impact the currents, a one-way interaction will be used to pass tidal current data from the circulation model to the wave model. Model calibration will be performed for seasonal wave conditions with no tidal extraction devices.

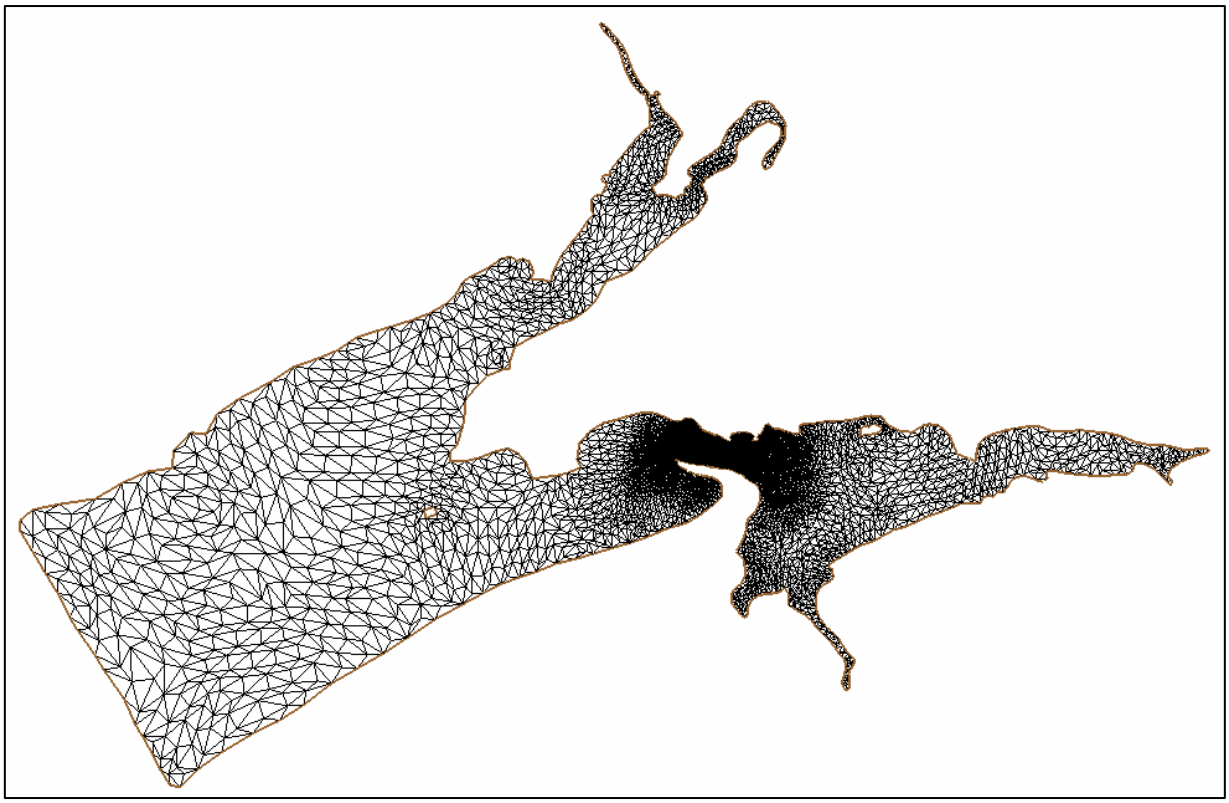

Figure 2-1: Grid for Currents from BIO Model

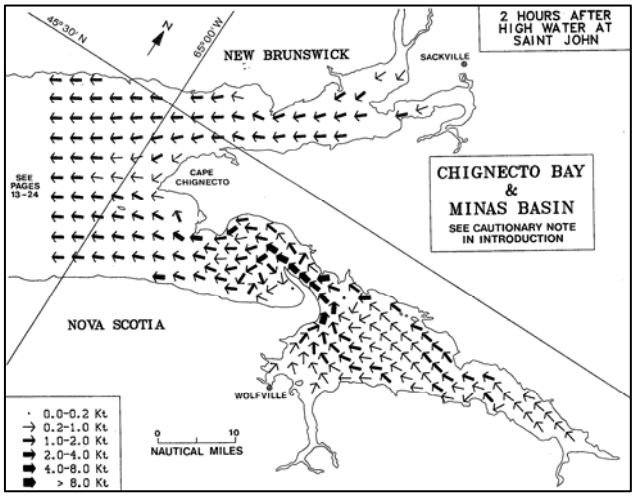

(a) 2 Hours after High Water at Saint John

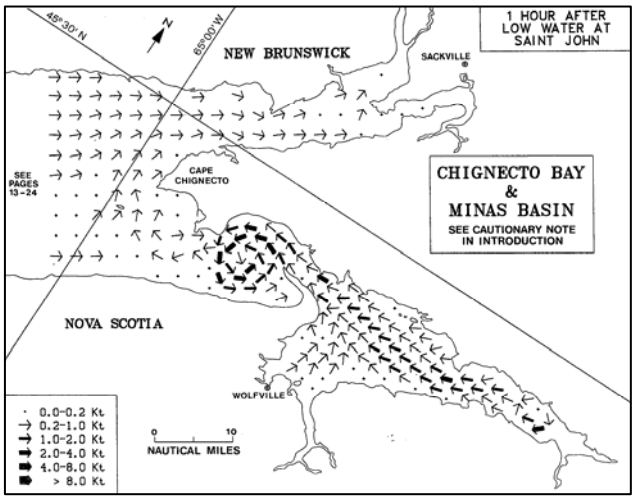

(b) 1 Hour after Low Water at Saint John

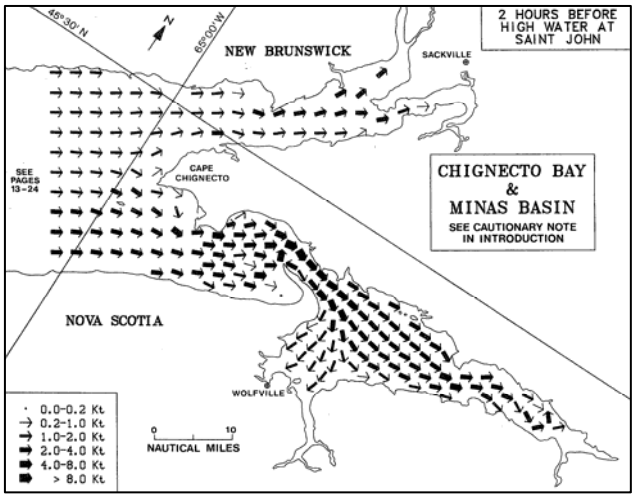

(c) 2 Hours before High Water at Saint John

Figure 2-2: Sample Tidal Current Data

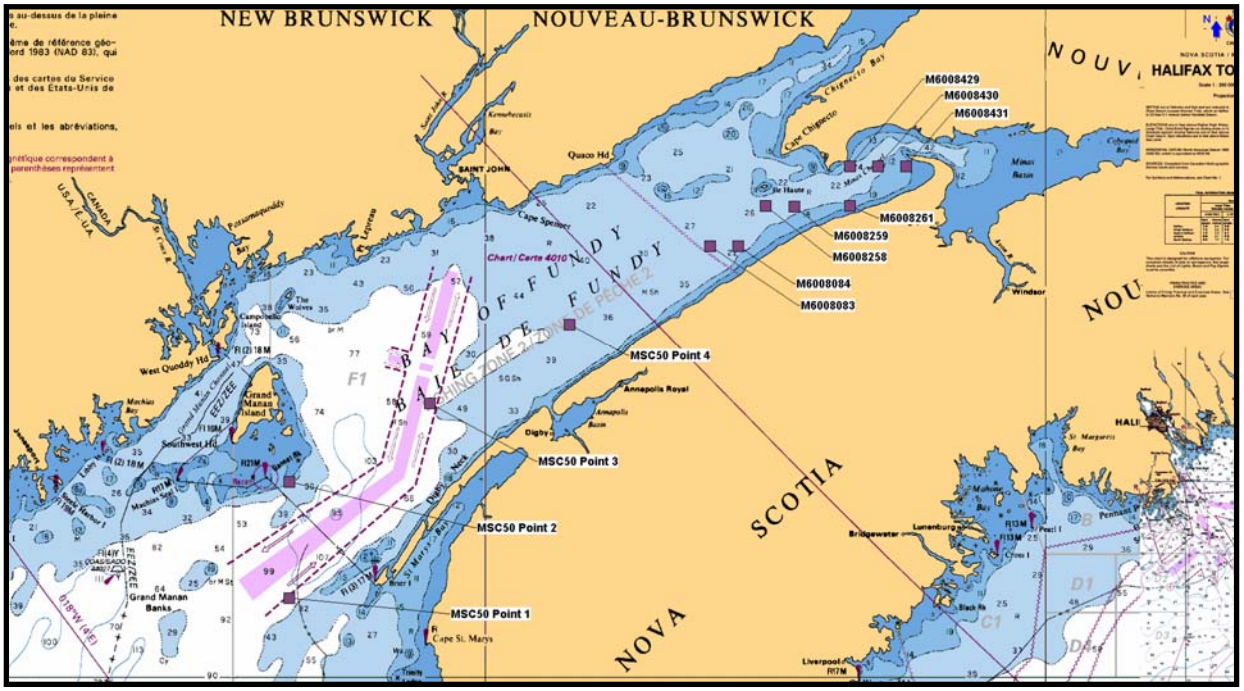

Figure 2-3: Selected Wave Hindcast Locations

Table 2-1: Wave Hindcast Locations and Water Depths

MSC50 Grid Point	Latitude (deg N)	Longitude (deg W)	Water Depth (m)
M6008261	45.2	64.7	40.2469
M6008429	45.3	64.7	42.2421
M6008430	45.3	64.6	N/A
M6008431	45.3	64.5	70.6013
M6008258	45.2	65.0	56.9263
M6008259	45.2	64.9	43.9586
M6008083	45.1	65.2	67.1576
M6008084	45.1	65.1	48.6007
M6006383	44.2	66.7	164.1991
M6006974	44.5	66.7	83.1367
M6007354	44.7	66.2	121.3621
M6007721	44.9	65.7	84.5464

3.0 RESULTS OF THE 1D ANALYSIS

3.1 SWANONE WAVE MODEL

A 1D Analysis has been carried out using the SwanOne wave model to calculate wave spectra changes that occur with an input spectrum on the outer boundary (no wind over the model grid) of a grid of tidal currents. The model is run from the outer boundary offshore of Cape Split through the Minas Channel to the Parrsboro shoreline.

Results of this 1D Analysis are presented in this section. The net effect on any portion of shorelines in the Bay of Fundy would become quantified in the more integrated 2-D modeling described in subsequent sections.

The 1D Analysis using the SwanOne wave model included computations for waves with no current, ebb currents of -1, -2, -4 m/s, and flood currents of +1, +2, +4 m/s. Resulting changes in significant wave height as the offshore waves propagate toward the shoreline are shown in Figure 3-1. The input significant wave height is plotted as a function of *Xp*, which is the distance from the offshore boundary of the grid. At the offshore boundary (*Xp* = 0), a significant wave height of 1.0 m and a peak period of 4.5 sec are chosen.

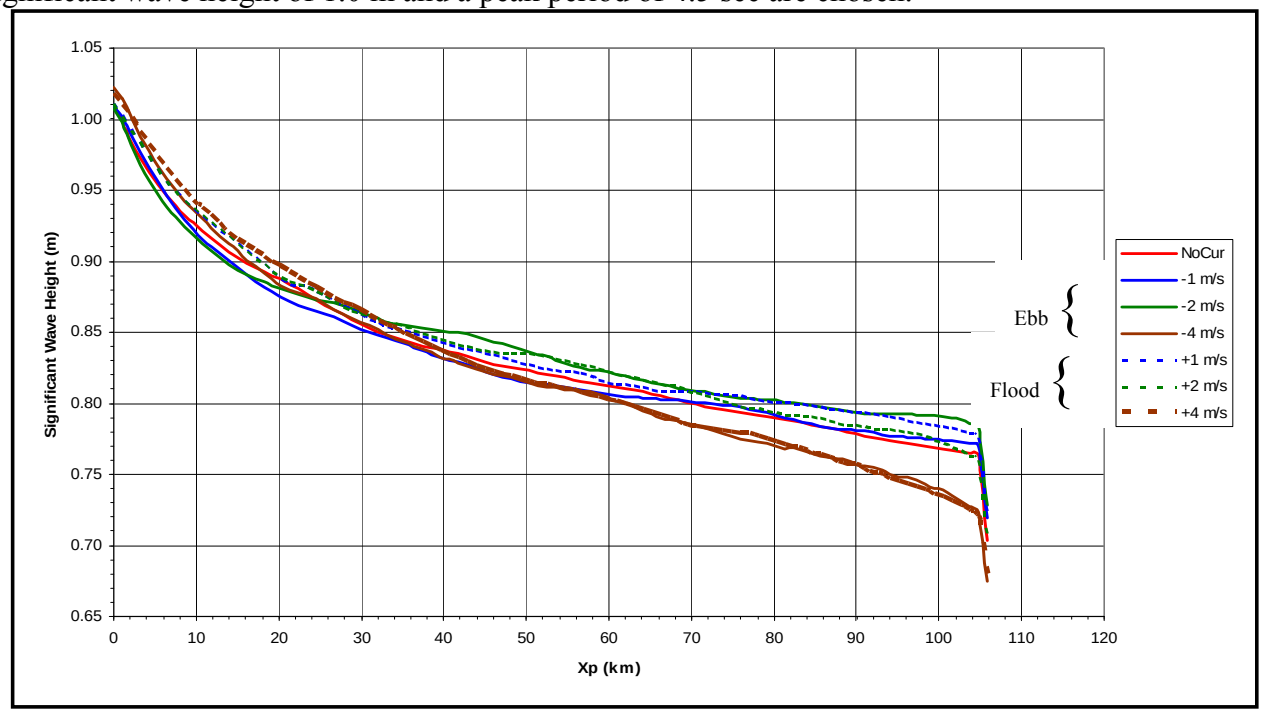

Figure 3-1: Changes in Significant Wave Height due to a Range of Tidal Currents (No Surface Wind)

Changes in the spectral shape of the waves and the redistribution of wave energy to different frequency bands are shown in Figure 3-2. These results show the resulting spectral energy

peak decreases with current interaction. The spectra also broaden over a wider frequency range as the peak shifts due to interaction of the waves and current. Hence, there is a net change in the characteristics of energy propagating through the model.

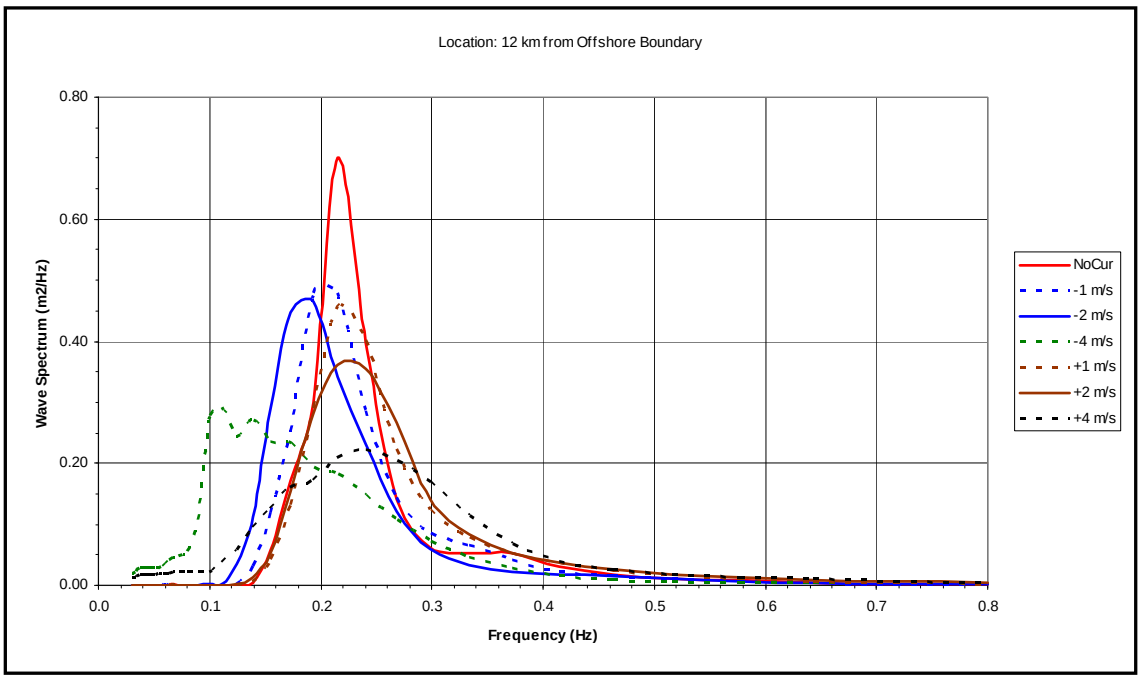

(a) Near Offshore Boundary

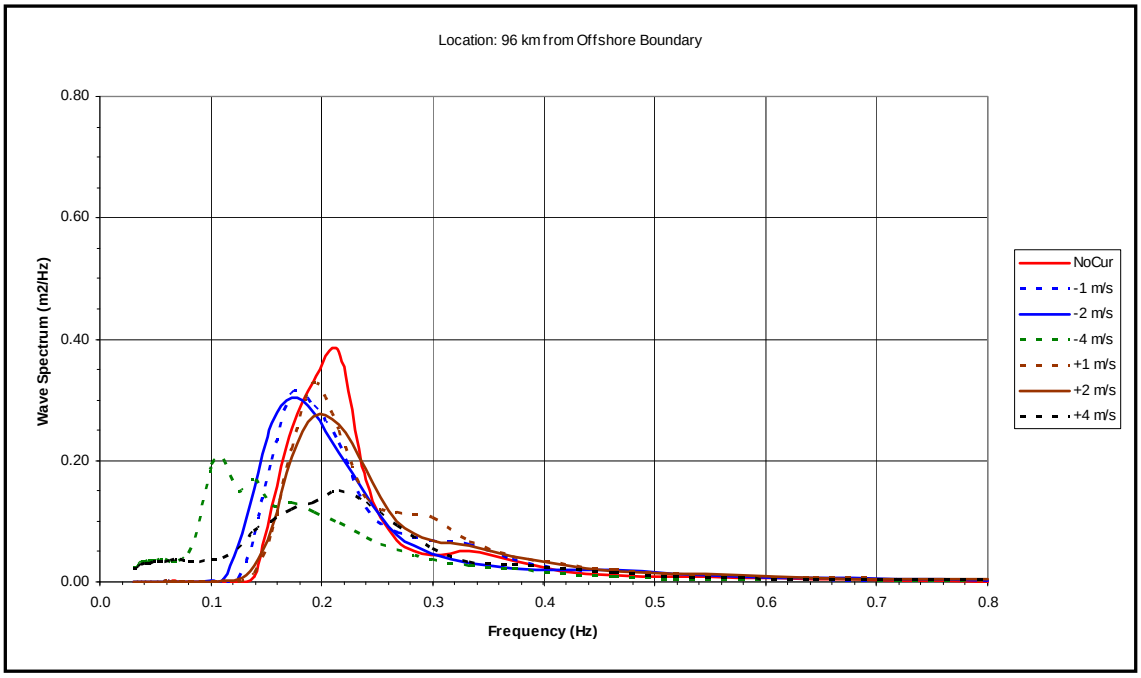

(b) Near Coastline

Figure 3-2: Changes in Wave Spectra due to Tidal Currents (No Surface Wind)

3.2 DATA SHARING BETWEEN TIDAL MODEL AND WAVE MODEL

In order to establish the effect of currents on the waves over the area of interest near Minas Channel, the current model and the wave model, each with its own grid and data formats, must share data developed by each. This requires one to automate repetitive user tasks for the control of data sharing between the circulation and the wave propagation models. In the Surface-water Modelling System (SMS) used by the U.S. Army Corps of Engineers, a coupled modeling system has been developed as a pre- and post-processor for operating various numerical hydrodynamic models (Zundel et al., 2002). The SMS software package allows users to create and edit meshes and grids, set up and save model input files, run numerical model simulations and view model solutions. In our case, we are using the BIO hydrodynamic tidal model for the inner Bay of Fundy that computes water surface elevations and current velocities at finite element grid locations. The wave field in our case is to be developed from selected AES MSC50 hindcast stations in the Bay of Fundy and refined with a detailed STWAVE steady state finite-difference model that calculates wave spectra at each cell in a rectangular grid over the same area of the Bay of Fundy as the hydrodynamic model.

In order to integrate the tidal current model with the STWAVE or Swan wave model through the SMS steering model (Zundel et al., 2002), a change in data format must be performed. The output files from BIO's tidal current model, a modified version of FVCOM (Chen et al., 2006) were used to create SMS files that use the format for an ADCIRC grid (SMS hydrodynamic model) grid and velocity time series (see Appendix A).

3.3 WAVE FREQUENCY OF OCCURRENCE TABLES

To quantify existing wave conditions (without tidal extraction devices) throughout the inner region of the Bay of Fundy, the MSC50 data sets were analyzed to generate frequency of occurrence tables for significant wave height, peak period and vector mean wave direction, which is the direction to which waves are travelling measured clockwise from North (see Appendix B).

3.4 SWANONE MODEL INCLUDING WIND INPUT

In order to investigate the wave growth due to wind, a 1D Analysis was also carried out using the SwanOne wave model described above without tidal currents, but with a range of wind speeds applied over the entire model grid. The objective of this analysis was to establish the changes in significant wave height and wave spectra that occur when local winds produce growth in the waves approaching the shoreline.

This analysis using the SwanOne wave model included computations for waves with no wind, and with wind speeds of 5, 10, 15, 20, 25, 30, and 35 m/s in the same direction as the waves. Changes in wave height as the offshore waves propagate toward the shoreline are shown in Figure 3-3. The significant wave height is plotted as a function of *Xp*, which is the distance

from the offshore boundary of the grid. At the offshore boundary (Xp = 0), the significant wave height is 1.0 m and the peak period is 4.5 sec. A wind speed of 5 m/s has very little effect on the nearshore wave conditions, but as the wind speed increases from 10 to 35 m/s, the additional energy causes a wind-wave growth that increases the significant wave height by a considerable amount as the waves propagate toward the coast.

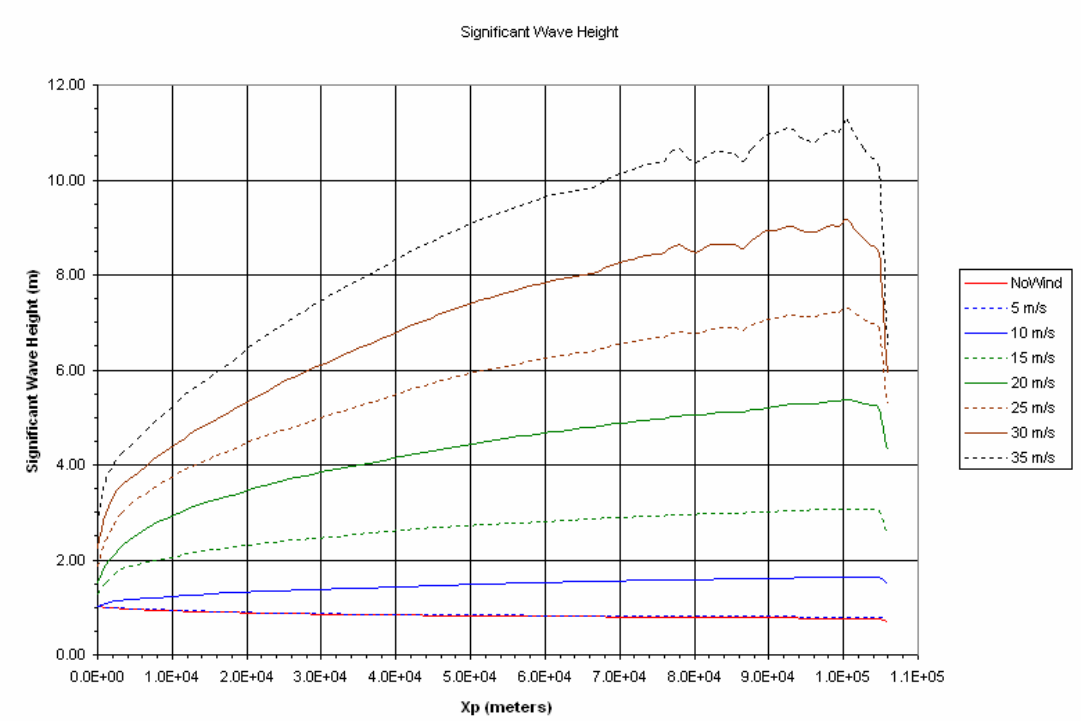

Figure 3-3: Changes in Significant Wave Height due to Wind (No Currents)

Changes in the shape of the wave spectra and the redistribution of wave energy to different frequency bands are shown in Figure 3-4. The results show the increase in the spectral energy peak as the wind speed and propagation distance increase.

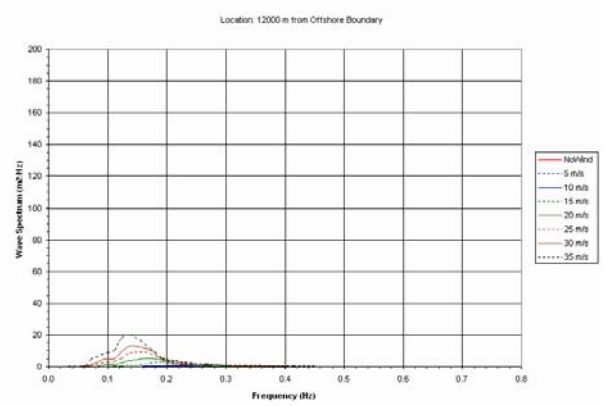

(a) 1200 m from Offshore Boundary

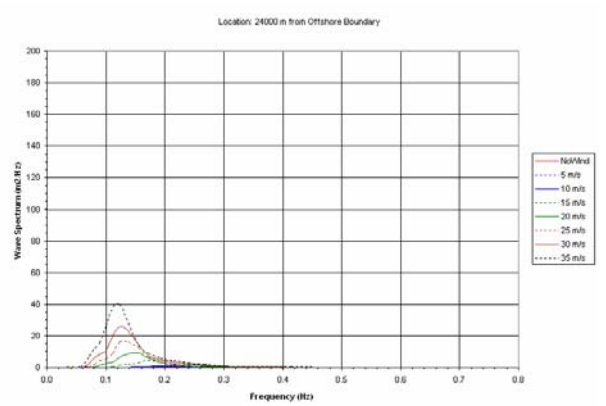

(b) 2400 m from Offshore Boundary

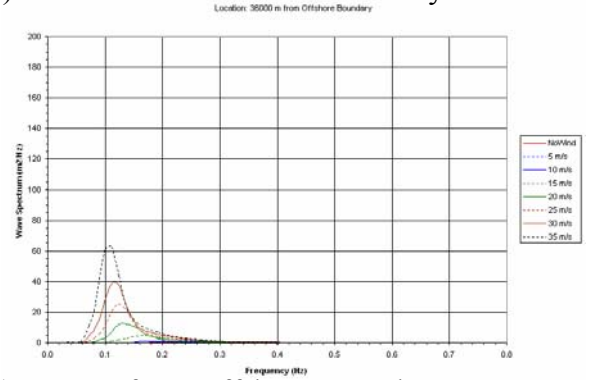

(c) 3600 m from Offshore Boundary

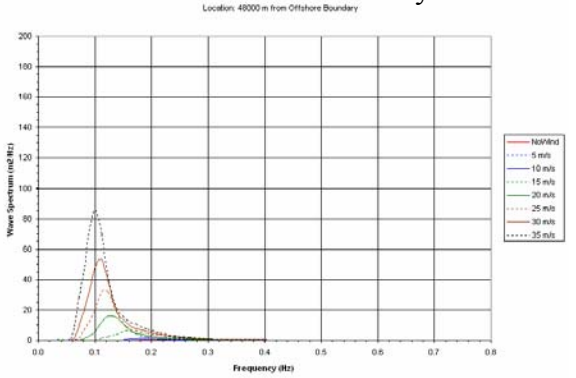

(d) 4800 m from Offshore Boundary

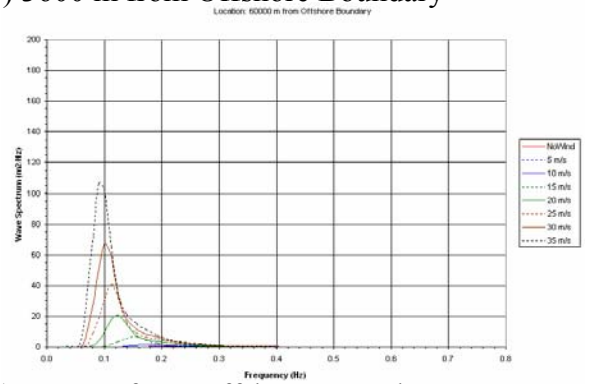

(e) 6000 m from Offshore Boundary

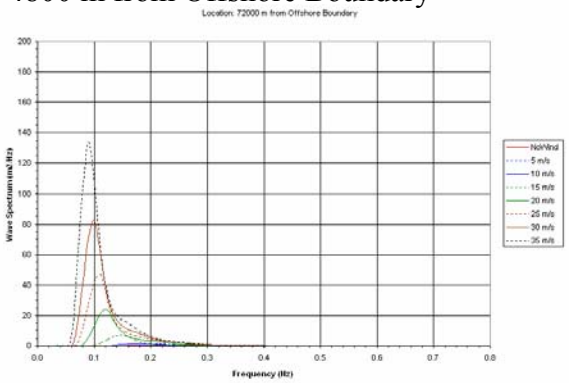

(f) 7200 m from Offshore Boundary

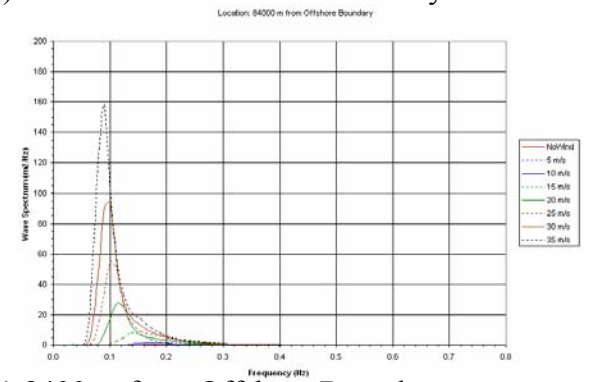

(g) 8400 m from Offshore Boundary

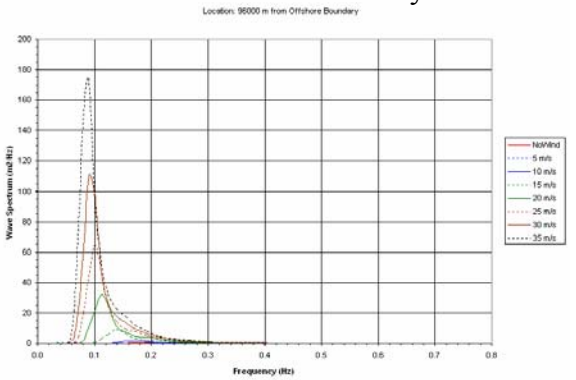

(h) 9600 m from Offshore Boundary

Figure 3-4: Changes in Wave Spectra due to Wind

3.5 SWANONE INCLUDING TIDAL CURRENTS AND STORM WAVES

In preparation for the work to be performed in Phase II, a 1D Analysis using SwanOne was also carried out to examine the effect of tidal currents on large waves generated by storms with a large wind speed. The objective of the analysis was to establish the changes that occur in storm waves due to wind and tidal currents. The model was run from the outer boundary offshore of Cape Split through the Minas Channel to the Parrsboro shoreline, with a constant wind speed and a range of tidal current conditions.

Results of this 1D Analysis are presented in this section. The net effect on shorelines in the Bay of Fundy is considered in the more integrated 2-D modeling carried out in subsequent stages of the work.

The 1D Analysis using the SwanOne wave model included computations for waves with no current, ebb currents of -1, -2, -4, -6 m/s, and flood currents of +1, +2, +4, +6 m/s. Changes in wave energy as the offshore waves propagate toward the shoreline are shown in Figure 3-5. The significant wave height is plotted as a function of *Xp*, which is the distance from the offshore boundary of the grid. At the offshore boundary (*Xp* = 0), the significant wave height is 4.0 m and the peak period is 9.0 sec. A constant wind speed of 14 m/s is applied in the same direction as the waves.

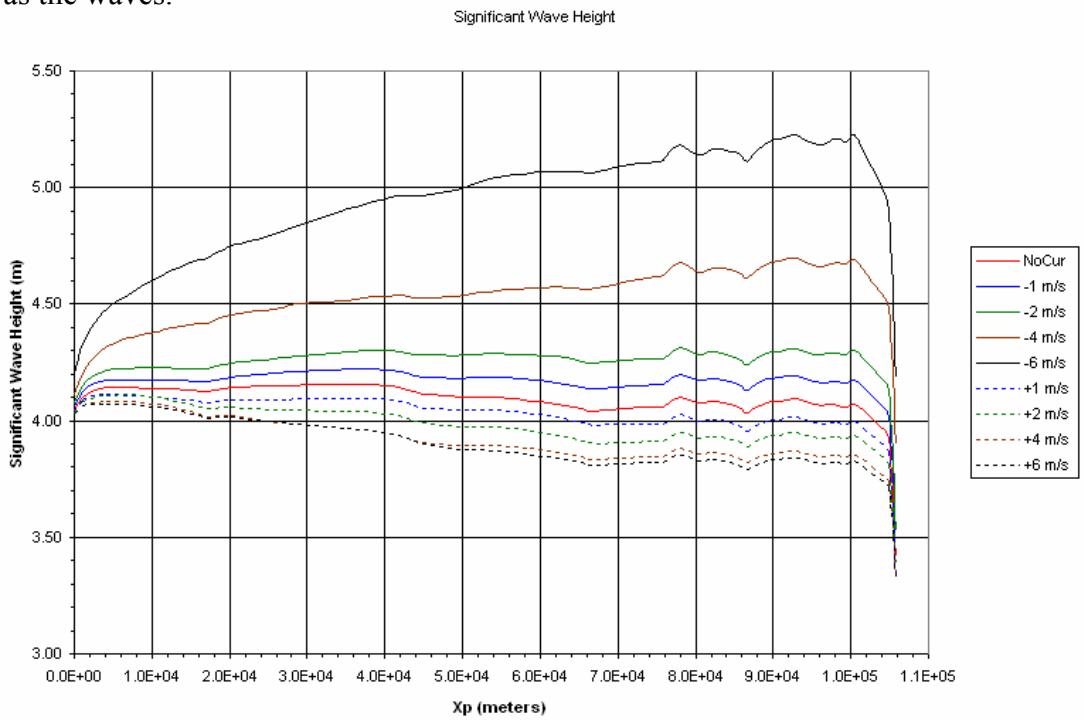

Figure 3-5: Changes in Significant Wave Height due to Wind and Tidal Current

Changes in the shape of the wave spectra and the redistribution of wave energy to different frequency bands are shown in Figure 3-6.

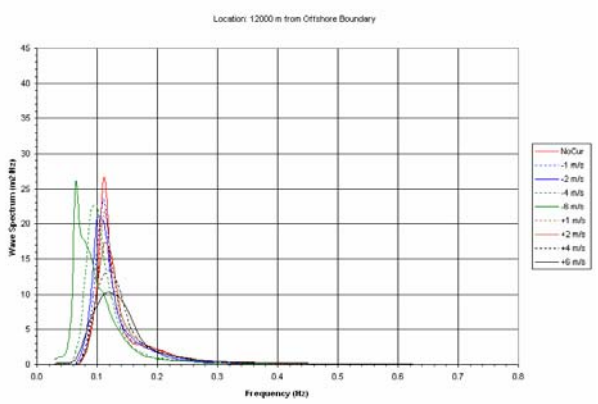

(a) 1200 m from Offshore Boundary

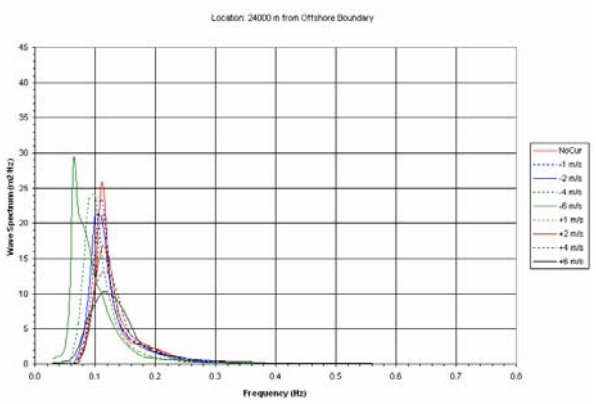

(b) 2400 m from Offshore Boundary

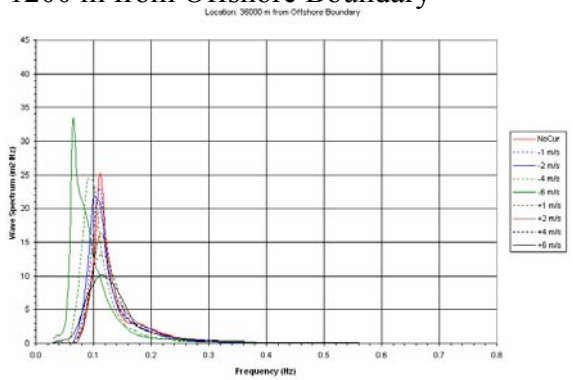

(c) 3600 m from Offshore Boundary

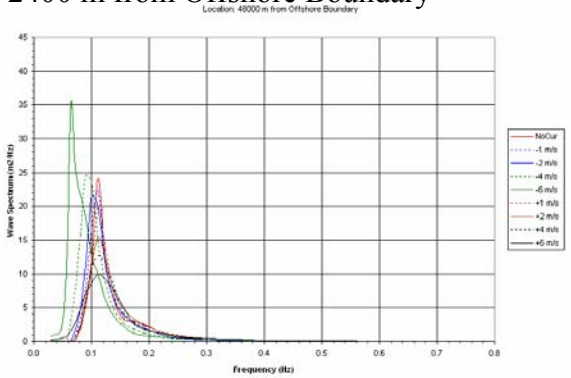

(d) 4800 m from Offshore Boundary

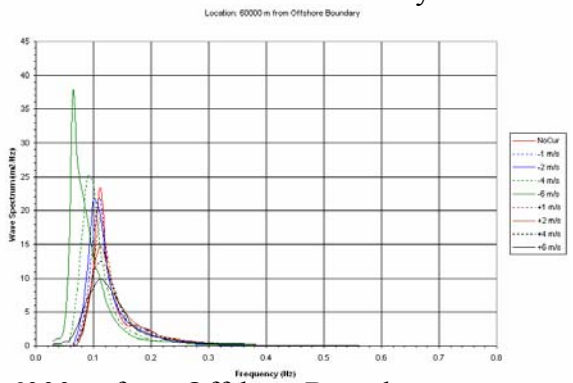

(e) 6000 m from Offshore Boundary

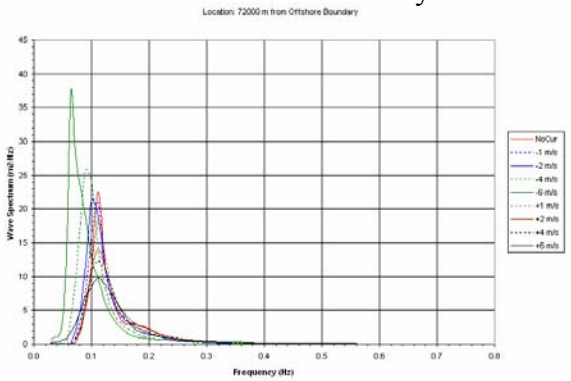

(f) 7200 m from Offshore Boundary

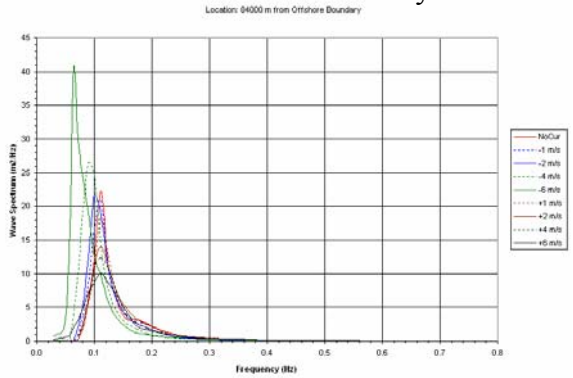

(g) 8400 m from Offshore Boundary

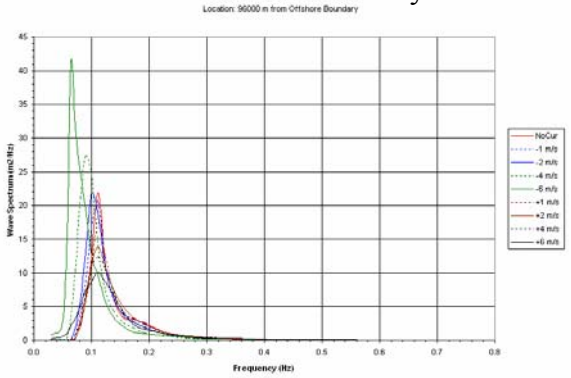

(h) 9600 m from Offshore Boundary

Figure 3-6: Changes in Wave Spectra due to Wind and Tidal Current

3.6 MODELLING THE INTERACTION OF WAVES AND CURRENTS

To establish the effect of the tidal currents on the waves in the Minas Channel region, very detailed grids of the current fields and wave fields are required. The detailed current field is available from the existing BIO tidal current model (see Appendix A). Evaluation has indicated that the STWAVE model for the wave modelling would be the preferred choice, giving the detail required and the computational speed necessary for development purposes.

Results from the testing of an integrated BIO current model with an STWAVE analysis over the Minas Channel and Basin is shown in Figure 3-7 and Figure 3-8. Figure 3-7 presents the results of the STWAVE model analysis for an input significant wave at the outer boundary of 4.5 m with a peak period of 9.5 seconds. Coupling the wave model to the tidal current model produces the wave field shown in Figure 3-8 for ebb currents out of Minas Basin. There are significant differences in the pattern of wave heights throughout the region due to the tidal current interaction with the incoming waves. Changes in the wave patterns nearshore are also evident in the results.

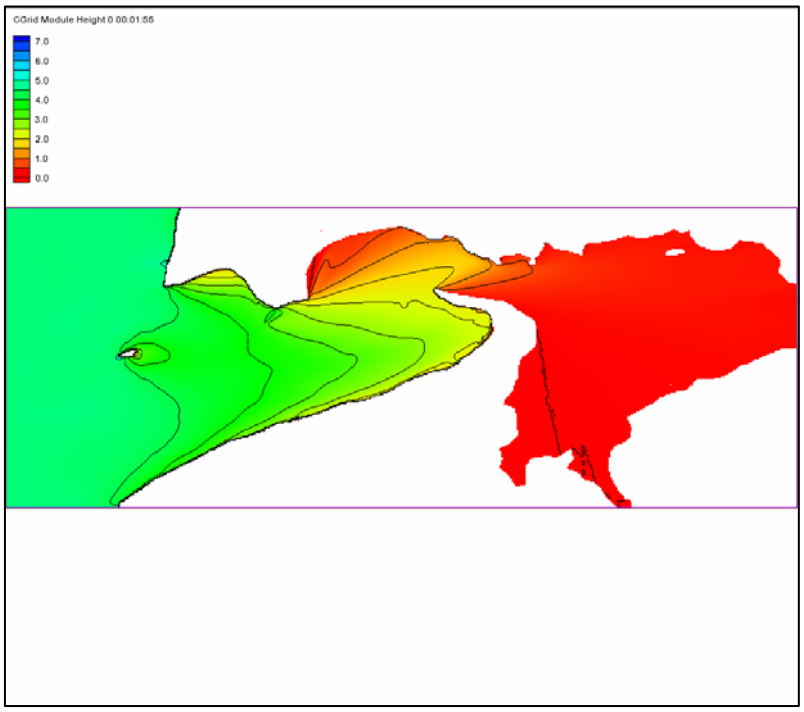

Figure 3-7: Modelling Results of STWAVE showing significant wave heights throughout the model domain with an Input Wave of H_s= 4.5m and T_p = 9.5s at the Outer Boundary with <u>no tidal current</u>

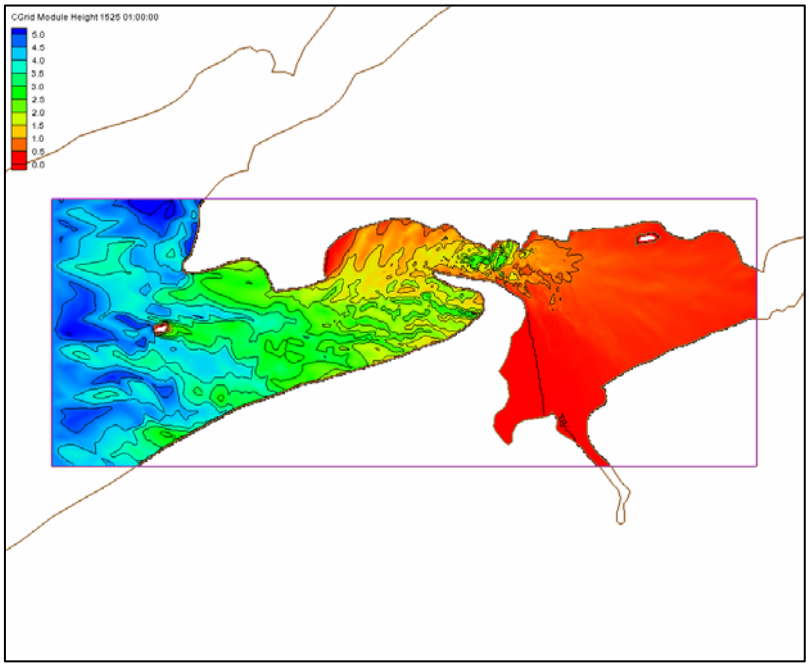

Figure 3-8: Modelling Results showing significant wave height throughout the model domain including the interaction of <u>an ebb tidal current</u> with the input wave

4.0 RESULTS OF THE 2D ANALYSIS

4.1 STWAVE WAVE MODEL

A 2D analysis has been carried out using the STWAVE wave model to determine the effect on wave spectra of changes in the tidal currents due to extraction of energy by turbines. Since STWAVE is a finite difference code, a regular Cartesian grid was generated to model an area extending from an outer boundary west of Cape Chignecto beyond Isle Haute in the main Bay of Fundy offshore of Cape Split (shown in Figure 4-2(a)), through the Minas Channel to the upper region of Minas Basin at the entrance to Cobequid Basin. The ADCIRC mesh derived from the centroids of the tidal current model and the boundaries of the STWAVE Cartesian grid are shown in Figure 4-1.

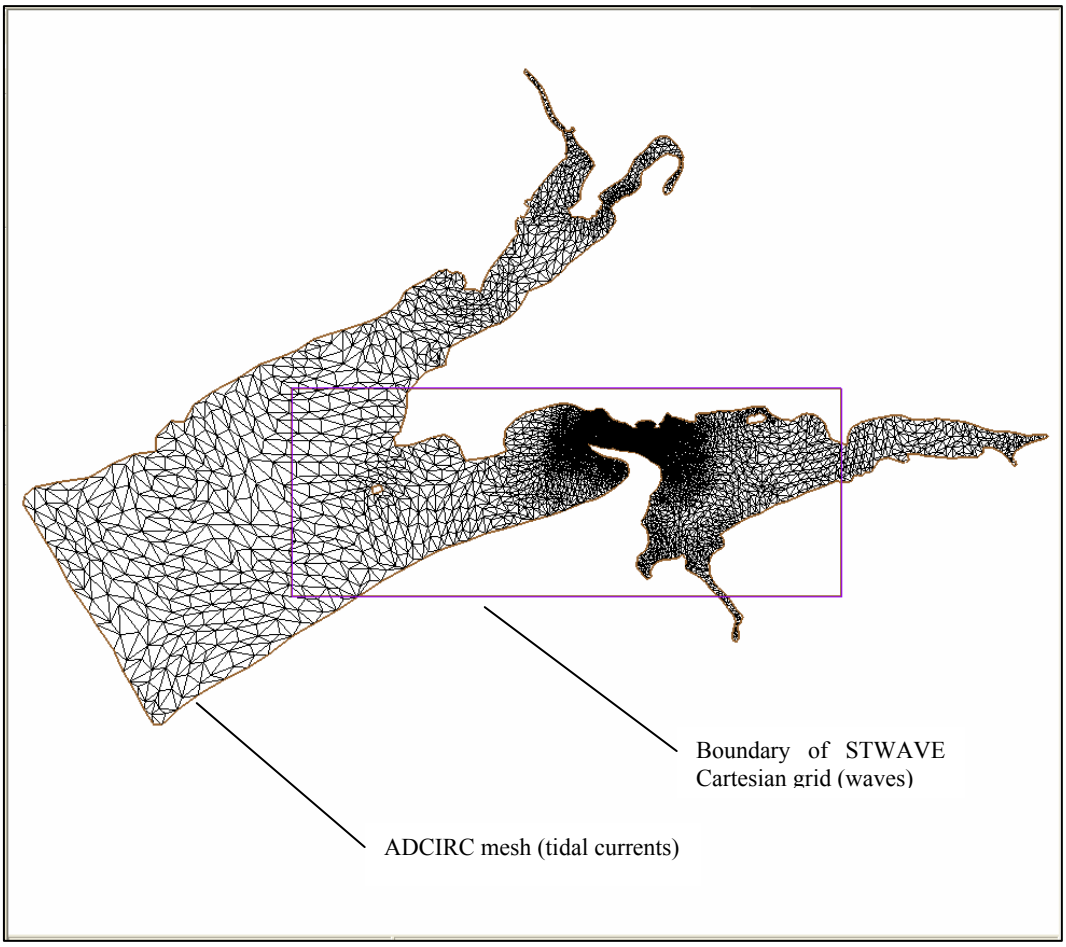

Figure 4-1: ADCIRC mesh (tidal currents) and boundary of STWAVE Cartesian grid (waves)

The STWAVE grid consists of 101,136 cells. The grid resolution is 200m x 200m, with a grid orientation of 0º counter-clockwise from east. The grid was 103,200 m (516 cells) in the east-west direction and 39,200 m (196 cells) at its widest section in the north-south) direction.

4.2 TIDAL CURRENTS

As discussed in Section 3.2, the output files from the BIO tidal model were converted to the SMS file format for an ADCIRC grid and velocity time series. This change in data format allows the STWAVE model to be integrated with the BIO tidal current model. The time series of tidal currents from the BIO model consists of 697 hourly timesteps from day 35 to day 64.

To set up an STWAVE analysis, the water depths and tidal current data for all timesteps in the data set were interpolated from the ADCIRC mesh to the STWAVE grid. This approach allows the water surface elevations and current velocities from the finite elements in the BIO model to be defined for the finite difference cells in the STWAVE model.

The current field throughout the Bay of Fundy is very complex, particularly through the Minas Passage region (see Figure 4-2 (a)). Tidal currents in the area of Minas Passage are displayed as a plot of current vectors on the STWAVE grid in Figure 4-2 (b).

The variability in the current's magnitude and direction over small horizontal distances is evident in this plot. These changes have a pronounced effect on wave behaviour in this region, as described in following sections.

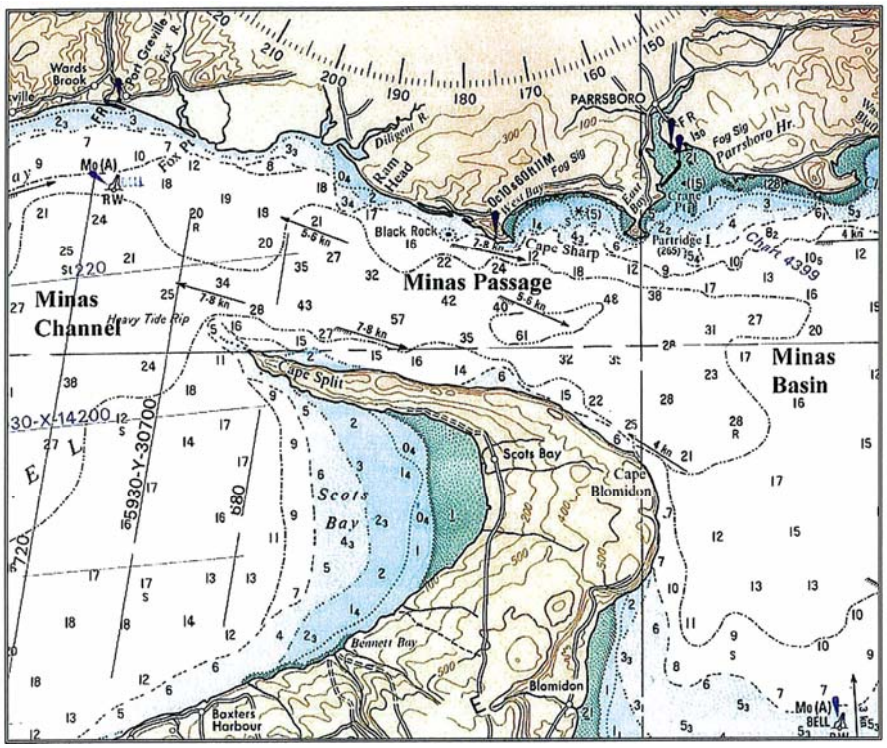

(a) The Canadian Hydrographic Chart for Minas Passage, NS (Chart #4010, depths in fathoms and feet)

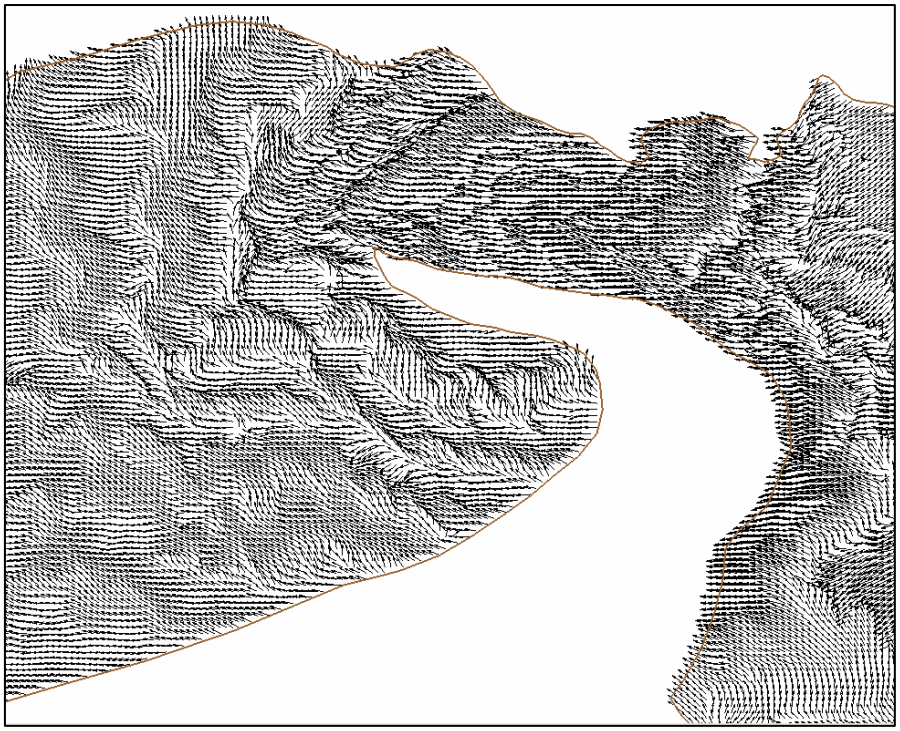

(b) Plot of current vectors in Minas Channel, Minas Passage and the entrance to Minas Basin

Figure 4-2: Tidal currents in the area of Minas Passage

To run the steady state STWAVE model in a dynamic simulation mode requires long execution times, and the time stepping must be coordinated with the tidal model output data. However, since the main objective is to assess the largest changes in wave conditions that may be caused by the extraction of energy from tidal currents, STWAVE was run in steady state mode using tidal currents at only two timesteps, which corresponded to large flood and ebb flows. Node 6299 in the BIO model was the node closest to MSC50 station M6008431, which was located near Minas Passage. The time series for this node was plotted (see Figure 4-3), and two timesteps were selected for use in the STWAVE analysis. The timing of minimum and maximum of the V component matches the timing of the minimum and maximum of the velocity magnitude at the location of this node. The timestep t=45.833 days was selected to represent flow conditions for an ebb current and the timestep t=46.125 days was selected to represent flow conditions for a flood current.

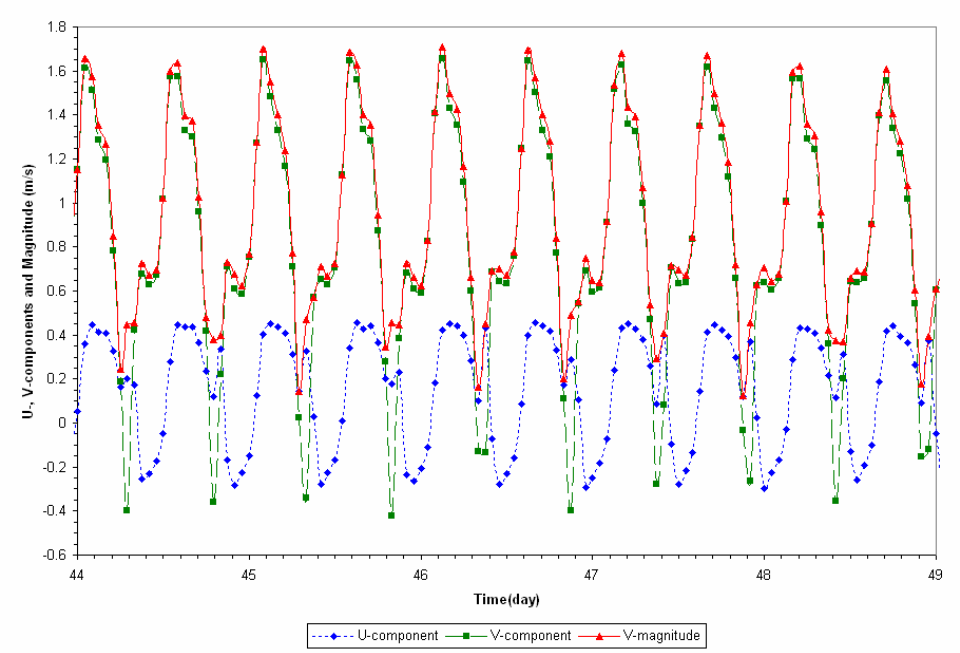

Figure 4-3: Time Series of Tidal Currents (Node 6299, days 44-49)

Since the tidal flow through the Minas Passage region includes a complex pattern of vortices and opposing flows, a check was made to verify that the interpolated tidal current data on the STWAVE Cartesian grid were consistent with the original tidal data on the ADCIRC finite element mesh. A vector plot of the BIO model's tidal currents on the ADCIRC mesh (blue vectors) and the tidal currents interpolated to the STWAVE grid (red vectors) is shown in Figure 4-4 (a) for flood currents and Figure 4-4 (b) for ebb currents. The vectors were displayed on a grid and the spacing was adjusted so that both datasets could be shown on the same plot.

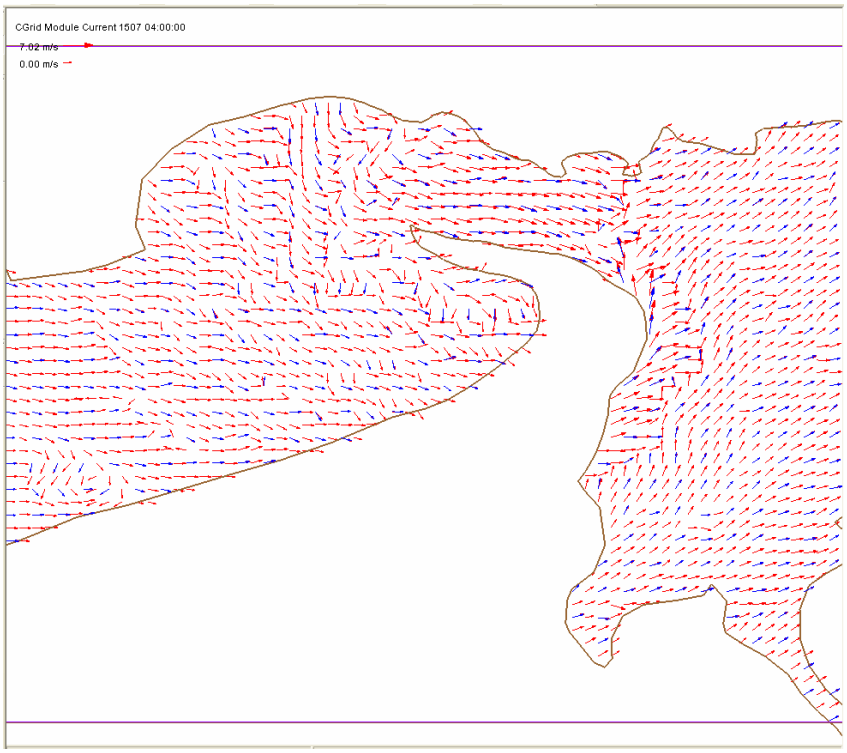

(a) Flood Currents (BIO – blue, STWAVE – red)

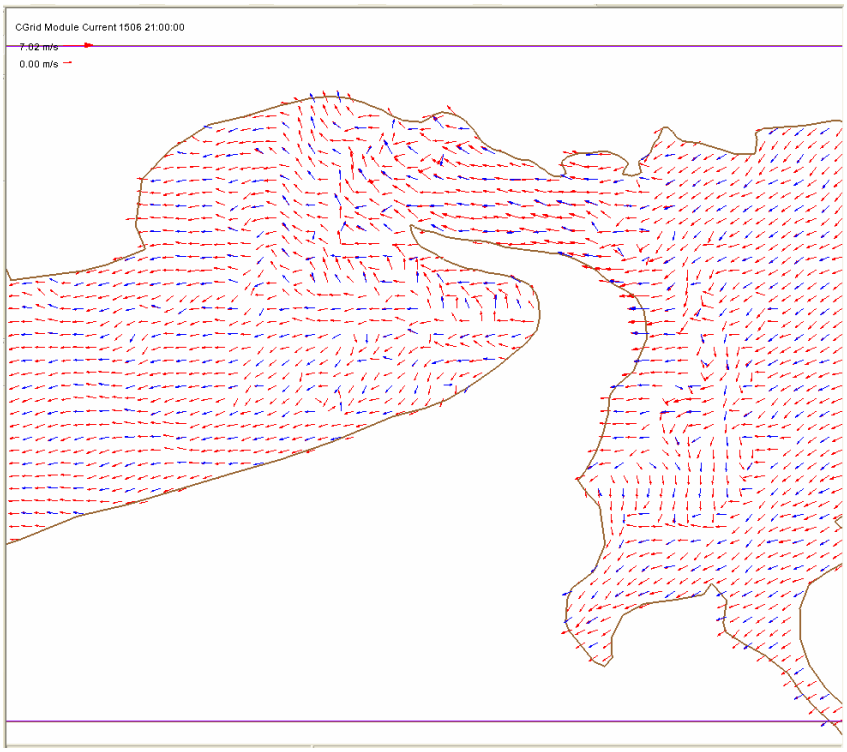

(b) Ebb Currents (BIO – blue, STWAVE – red)

Figure 4-4: Comparison of Tidal currents for BIO model and tidal currents interpolated from that data

4.3 WAVE CONDITIONS

As discussed in Section 3.3, the AES MSC50 hindcast data sets for the Bay of Fundy were analyzed to generate frequency of occurrence tables for significant wave height, peak period and vector mean wave direction. The significant wave height and peak period data in these tables were used to define existing wave conditions (without tidal extraction devices) in the Bay of Fundy.

The wave conditions at the offshore boundary of the STWAVE model were based on the AES MSC50 hindcast station in the Bay of Fundy that was closest to this boundary. Assuming that waves approach the offshore boundary of the STWAVE grid from a westerly direction, the wave data from from station M6008083 (see Figure 2-3) were used to generate TMA wave spectra to be applied as forcing conditions on this boundary.

All wave cases in the frequency of occurrence tables (see Appendix B) were run with the tidal currents for the selected ebb and flood flows. The results for several selected wave-current conditions are presented in the following section.

4.4 MODELLING OF WAVE – CURRENT INTERACTION

As discussed in Section 3.6, the STWAVE model with very detailed grids of the current fields and wave fields can be used to establish the effect of the tidal currents on waves in the Minas Channel region. The 1D Analysis indicated that there are significant differences in the pattern of wave heights throughout the region due to interaction of the tidal currents with incoming waves, particularly in the nearshore areas of Minas Passage and Minas Basin.

The tidal currents in this area are quite dynamic, and there are gyres and currents that flow in opposing directions throughout the tidal cycle. For ebb flows, there are situations where incoming waves may be blocked by a strong opposing current. When wave blocking occurs, the wave energy is dissipated through breaking of the wave. If the relative wave group celerity is smaller than the magnitude of the opposing current, then the wave energy cannot propagate against the current, and wave blocking occurs. In deep water, such as the channel through Minas Passage, blocking occurs for an opposing current that has a velocity magnitude greater than one-fourth the deepwater wave celerity without current (i.e., $|V| > 0.25 g T_a /(2\pi)$, where T_a is the absolute wave period).

For example, waves with a period of 9.5 sec will be blocked by ebb currents with a velocity magnitude greater than 3.70 m/sec. Similarly, waves with periods of 5.5 sec and 3.5 sec will be blocked by ebb currents with velocities exceeding 2.26 m/sec and 1.36 m/sec, respectively. Plots showing the location of ebb currents that can block waves with these periods are shown in Figure 4-5. The smaller waves with shorter periods are almost completely blocked by ebb currents through Minas Passage, but the larger storm waves with longer periods can enter Minas Basin.

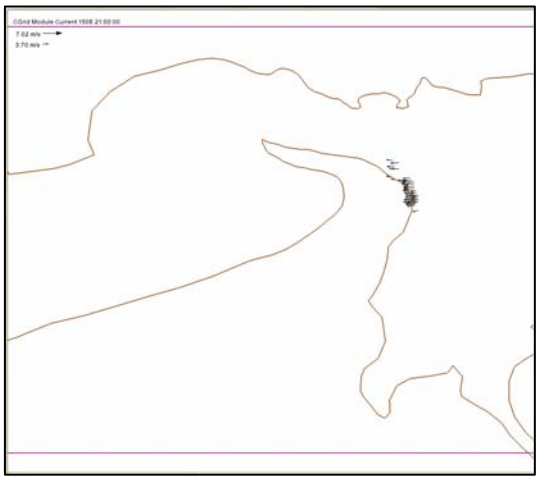

(a) Locations where waves with T=9.5 sec are blocked by currents > 3.70 m/sec

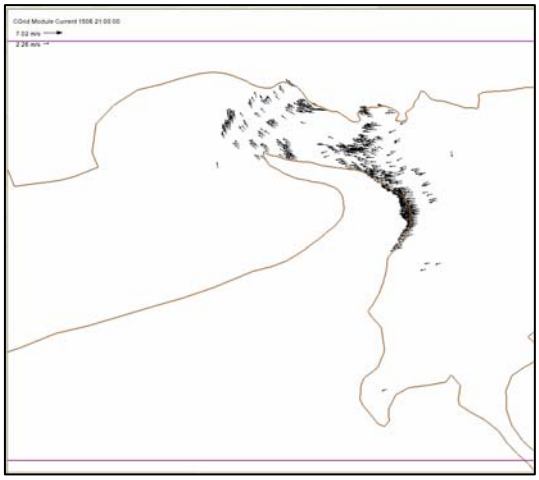

(b) Locations where waves with period T=5.5 sec are blocked by currents > 2.26 m/sec

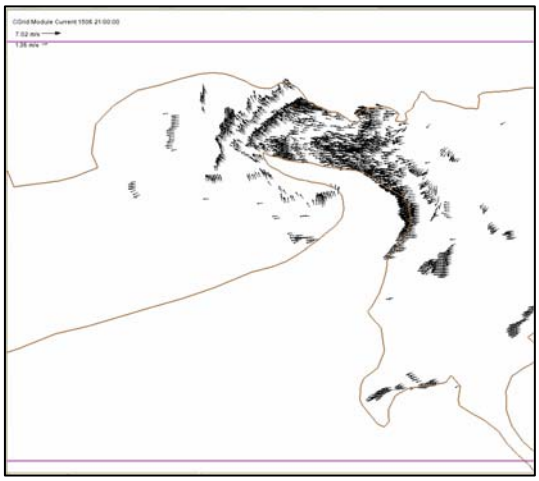

(c) Locations where waves with period T=3.5 sec are blocked by currents > 1.36 m/sec

Figure 4-5: Locations of Blocking Currents for Ebb Flows with incoming waves

The detailed wave - current modelling was carried out for three types of wave conditions.

- Non-Storm Wave Conditions – Initial implementation of the spectral wave model to numerically simulate wave transformation in detail for non-storm conditions with no tidal energy extraction to calibrate the model, followed by test cases to include energy extraction.
- Storm Wave Conditions – Incorporation of operation conditions from numerical tidal models produced by others (e.g., Dalhousie, BIO, Acadia) and the addition of 'storm' events to determine areas of increased wave intensity and sediment transport along the coastline.
- Extreme Wave Conditions – Establish extreme wave conditions at the energy extraction locations to establish overall effect of wave and current changes due to the operation of the tidal devices and the resultant effect of these changing fields on the integrity of the structures.

For the storm and extreme wave conditions, it was planned to investigate the effects of changes in water surface elevation due to storms and extreme high tides, by having researchers at BIO and Dalhousie University run their storm surge and tidal models. The storm surge model would be run to determine the storm surge for a series of storm wave conditions in the Bay of Fundy and the tidal model would be run to determine the Highest High Water level at this location over a 19 year period. However, because the Bay of Fundy has the largest tides in the world, it was felt that these changes in water surface elevation would be relatively small in comparison with the normal tidal range at this location. It is possible that a 100 year storm wave may occur at the same time as the 100 year storm surge and 19 year high tide, but the probability is relatively small. Consequently, it was decided that an extremal analysis of waves, surge and 19 year tides to assess their effect on the wave-current interaction results presented in this report should be postponed for investigation in future work.

The frequency of occurrence tables were used to select wave cases representative of seasonal, storm and extreme wave conditions for the purposes of a wave-current interaction analysis. The significant wave heights and peak periods selected for use in STWAVE simulations with ebb and flood currents are summarized in Table 4-1.

Table 4-1: Wave Conditions selected for Wave-Current Interaction Analysis

	Significant Wave Height Hs(m)	**Peak Wave Period Tp (sec)**
Non-Storm Wave Conditions	0.44	3.5
Storm Wave Conditions	2.25	6.5
Extreme Wave Conditions	4.50	9.5

4.4.1 Tidal Power Extraction by Turbines

Simulations were performed for the seasonal, storm and extreme wave conditions for both ebb and flood flows with no tidal extraction by turbines. The simulations were then repeated with

tidal extraction by turbines. A study by Acadia University researchers (Karsten et al., 2010) indicates that an extreme case, which involves the operation of an intense concentration of 225 turbines (20 m diameter) across Minas Passage to generate an average extracted power of 600 MW, would produce up to a 20% decrease in local velocity as shown in Figure 4-6.

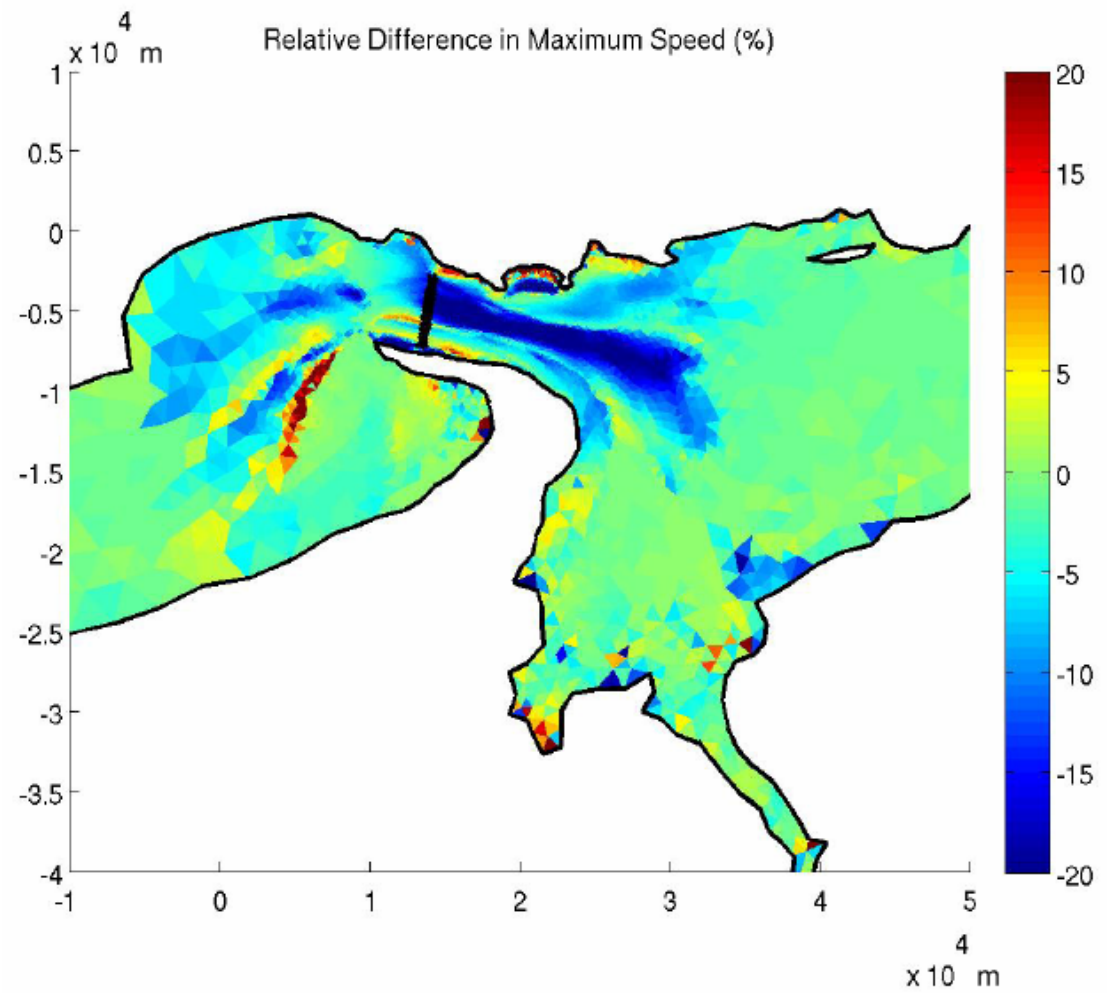

Figure 4-6: Relative Change in Maximum Speed due to Tidal Energy Extraction for an array of 225 turbines (each 20 m diameter) across Minas Passage (Karsten, et al., 2010)

The dark blue shading in this plot indicates the area in Minas Passage where the 20% reduction in speed occurs over a large area during flood flows. A similar reduction in flow region was used to estimate the area to the west of the 225 turbine array where a 20% reduction in speed may occur during ebb flows.

To establish the overall effect of a large portion of the reduction in currents due to the energy extraction turbines, the areas of the STWAVE grid where the tidal currents were assumed to be reduced by 20% are shown in Figure 4-7 (a) for flood currents and Figure 4-7 (b) for ebb currents.

Two other areas in the plot of Figure 4-6 where there are observable changes in current flow occurring are (a) the shoreline region in Minas Passage, east of Cape Split with a decrease in velocity, and (b) to the west of Cape Split showing increased current speed where sand waves were reported from the recent multi-beam surveys of the region. More detailed analysis of the changes expected in these regions and their effect on sediment transport should be studied further under a range of turbine device locations, sediment characteristics and environmental conditions.

Results of the wave-current interaction modelling for the non-storm and storm wave conditions are presented in the following sections including the tidal current reduction areas shown in Figure 4-7. Results of the wave-current interaction modelling for the extreme wave conditions are presented in Section 4.5.

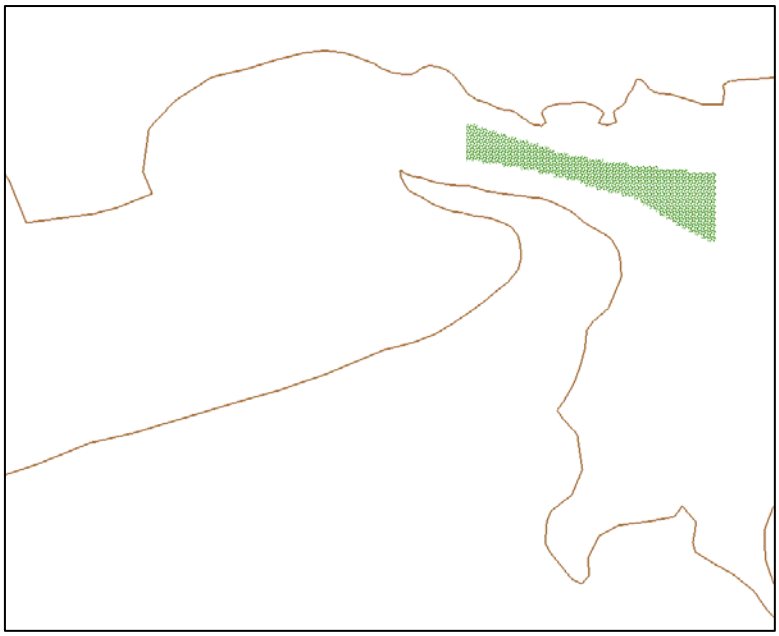

(a) Flood Currents

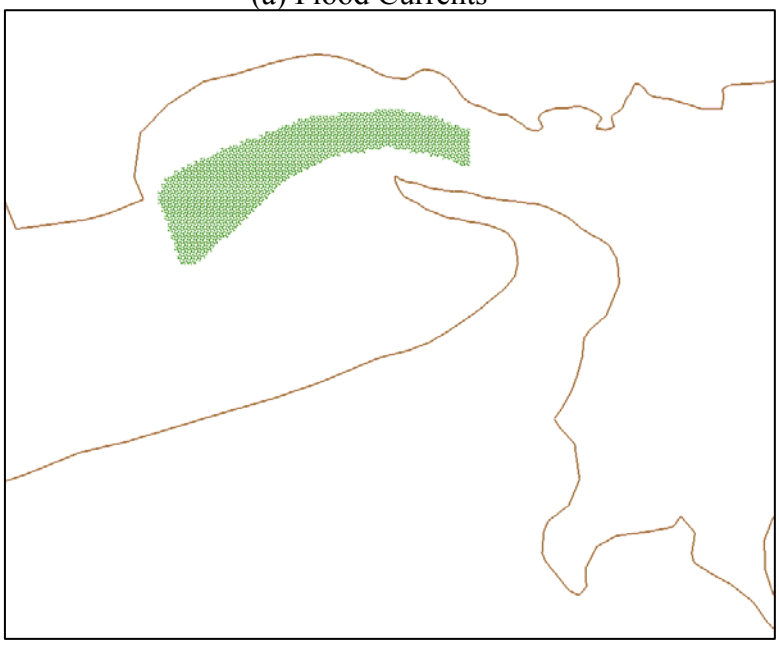

(b) Ebb Currents

Figure 4-7: Areas of STWAVE Grid where Tidal Currents are Reduced due to an Array of 225 Turbines in the Region of Minas Passage

4.4.2 Non-Storm Wave Conditions

Simulations were performed to investigate the interaction of tidal currents with non-storm wave boundary conditions (Hs = 0.44 m, Tp = 3.5 s) for existing flood and ebb flows, with no extraction of energy by turbines. These simulations were then repeated with the flow velocity reduced by 20% in the localized areas near the turbines (turbine location shown in Figure 4-6).

(a) Flood Flow

Contour plots of significant wave height are shown in Figure 4-8 (a) for flood flows with no turbines and in Figure 4-8 (b) for flood flows with 20% reduction in velocity due to energy extraction by turbines. Some minor differences in wave height contours are identified and shown within the dashed lines of each figure.

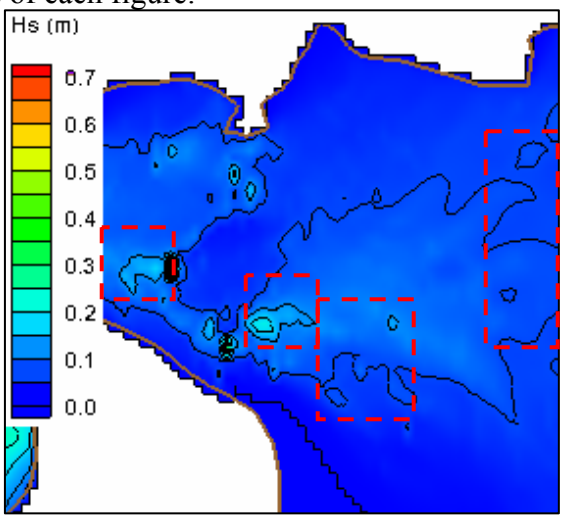

(a) Significant Wave Height for Flood Flows with No Turbines in Minas Passage

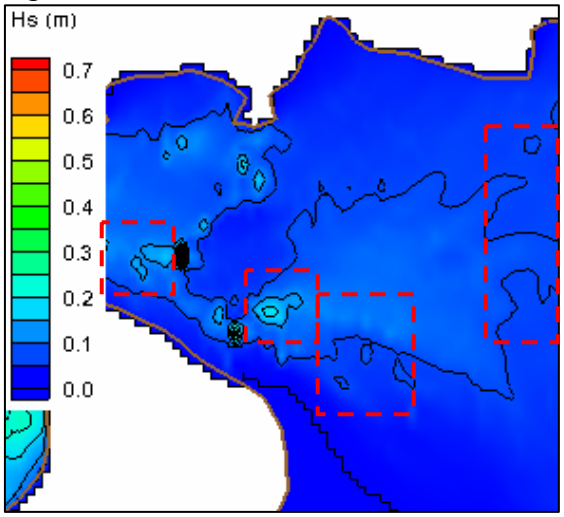

(b) Significant Wave Height for Flood Flows with an array of 225 Turbines in Minas Passage

Figure 4-8: Non-Storm Waves in Flood Currents, with and without Turbines

(b) Ebb Flow

Contour plots of significant wave height are shown in Figure 4-9 (a) for ebb flows with no turbines and in Figure 4-9 (b) for ebb flows with 20% reduction in velocity due to energy extraction by an array of 225 turbines across Minas Passage. Some minor differences in wave height contours are identified and shown within the dashed lines of each figure.

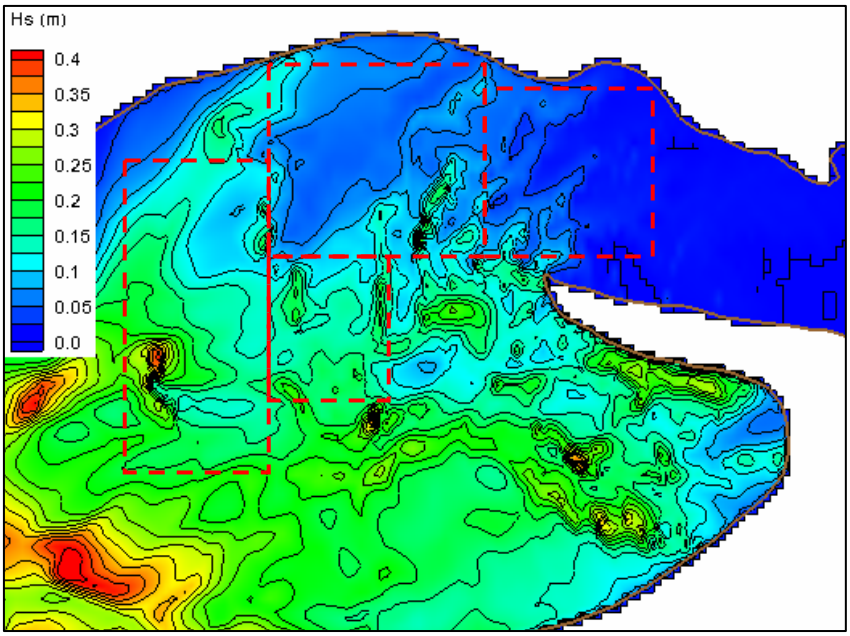

(a) Significant Wave Height for Ebb Flows with No Turbines in Minas Passage

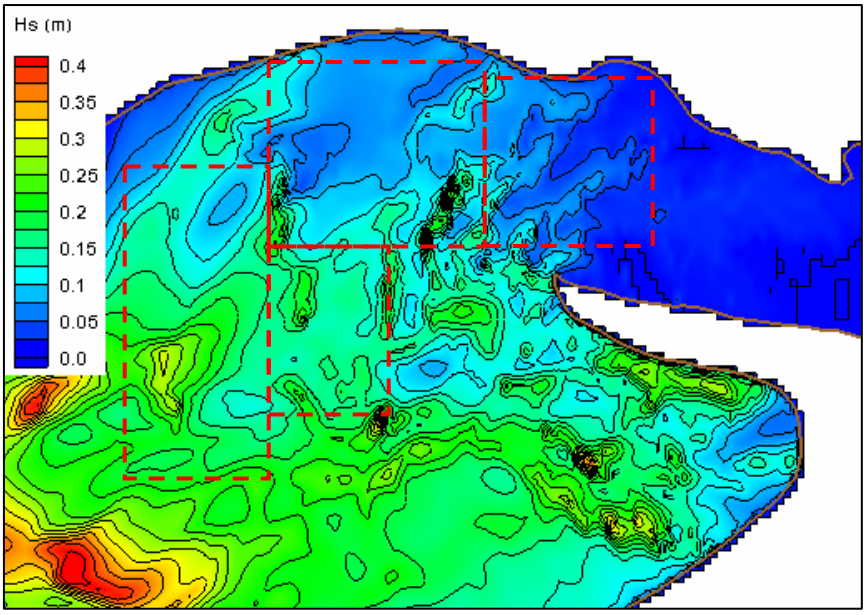

(b) Significant Wave Height for Ebb Flows with an array of 225 Turbines in Minas Passage

Figure 4-9: Non-storm Waves in Ebb Currents, with and without Turbines

4.4.3 Storm Wave Conditions

Simulations were performed to investigate the interaction of tidal currents with storm wave boundary conditions (Hs = 2.25 m, Tp = 6.5 s) for existing flood and ebb flows, with no extraction of energy by turbines. These simulations were then repeated with the flow velocity reduced by 20% in the localized areas near the turbines (turbine location shown in Figure 4-6).

(a) Flood Flow

Contour plots of significant wave height are shown in Figure 4-10 (a) for flood flows with no turbines and in Figure 4-10 (b) for flood flows with 20% reduction in velocity due to energy extraction by turbines. Some minor differences in wave height contours are identified and shown within the dashed lines of each figure.

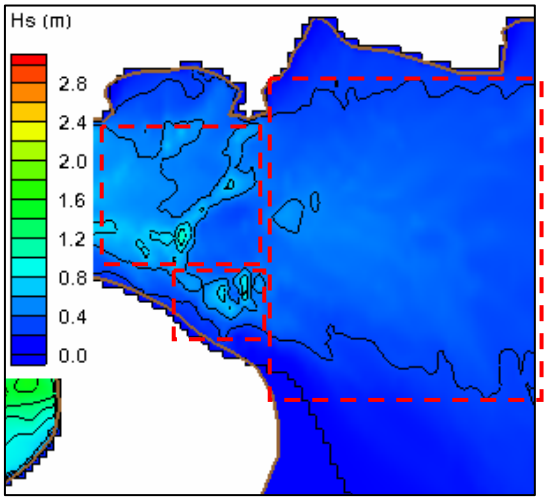

(a) Significant Wave Height for Flood Flows with No Turbines in Minas Passage

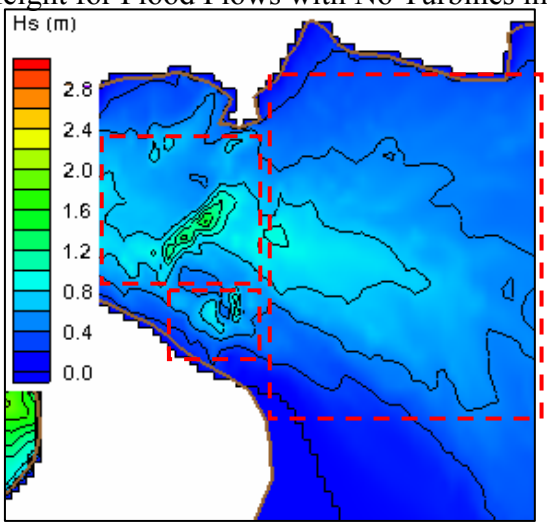

(b) Significant Wave Height for Flood Flows with an array of 225 Turbines in Minas Passage

Figure 4-10: Storm Waves in Flood Currents, with and without Turbines

(b) Ebb Flow

Contour plots of significant wave height are shown in Figure 4-11 (a) for ebb flows with no turbines and in Figure 4-11 (b) for ebb flows with 20% reduction in velocity due to energy extraction by turbines. Some minor differences in wave height contours are identified and shown within the dashed lines of each figure.

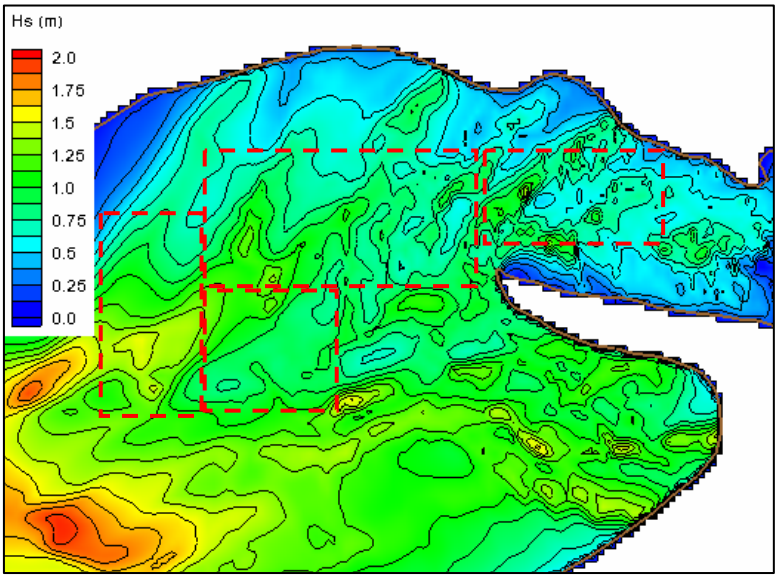

(a) Significant Wave Height for Ebb Flows with No Turbines in Minas Passage

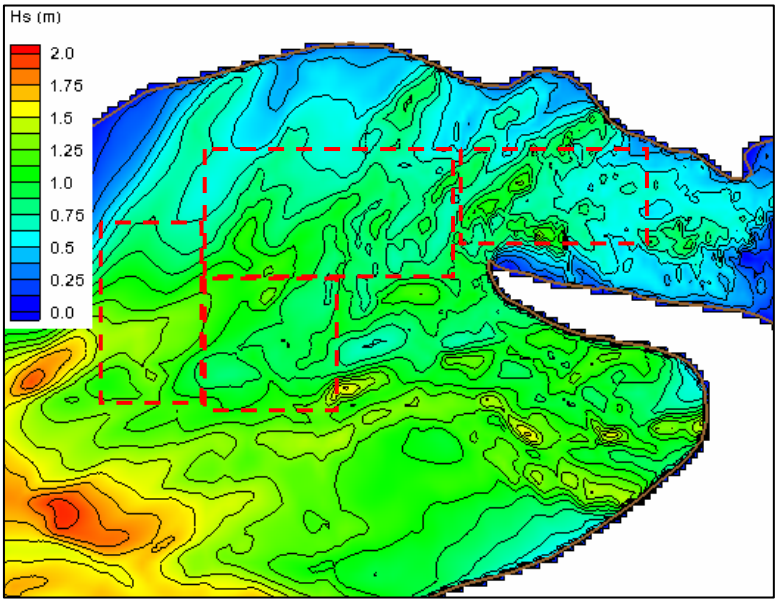

(b) Significant Wave Height for Ebb Flows with an array of 225 Turbines in Minas Passage

Figure 4-11: Storm Waves in Ebb Currents, with and without Turbines in Minas Passage

4.5 NEAR-FIELD EFFECTS OF TIDAL POWER EXTRACTION

4.5.1 Effects on Extreme Wave Conditions

Simulations were performed to investigate the interaction of tidal currents with extreme wave boundary conditions (Hs = 4.5 m, Tp = 9.5 s) for existing flood and ebb flows, with no extraction of energy by turbines. These simulations were then repeated with the flow velocity reduced by 20% in the localized areas near the turbines (turbine location shown in Figure 4-6).

(a) Flood Flow

Contour plots of significant wave height are shown in Figure 4-12 (a) for flood flows with no turbines and in Figure 4-12 (b) for flood flows with 20% reduction in velocity due to energy extraction by turbines. Some minor differences in contours are identified by dashed lines.

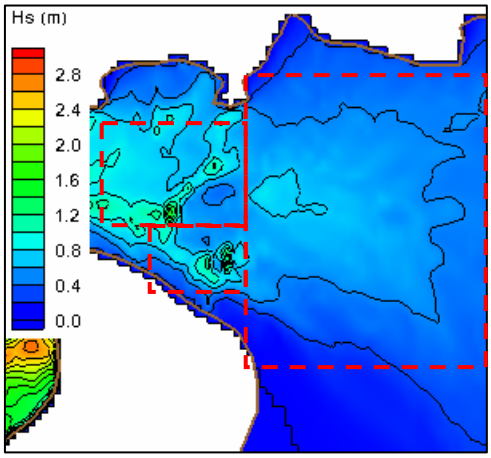

(a) Significant Wave Height for Flood Flows with No Turbines in Minas Passage

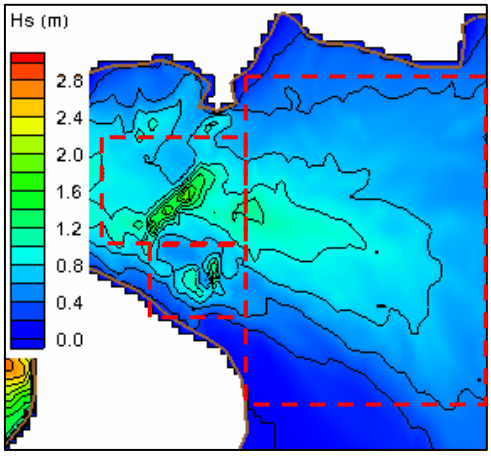

(b) Significant Wave Height for Flood Flows with an array of 225 Turbines in Minas Passage

Figure 4-12: Extreme Waves in Flood Currents, with and without Turbines

(b) Ebb Flow

Contour plots of significant wave height are shown in Figure 4-13 (a) for ebb flows with no turbines and in Figure 4-13 (b) for ebb flows with 20% reduction in velocity due to energy extraction by turbines. Some minor differences in contours are identified by dashed lines.

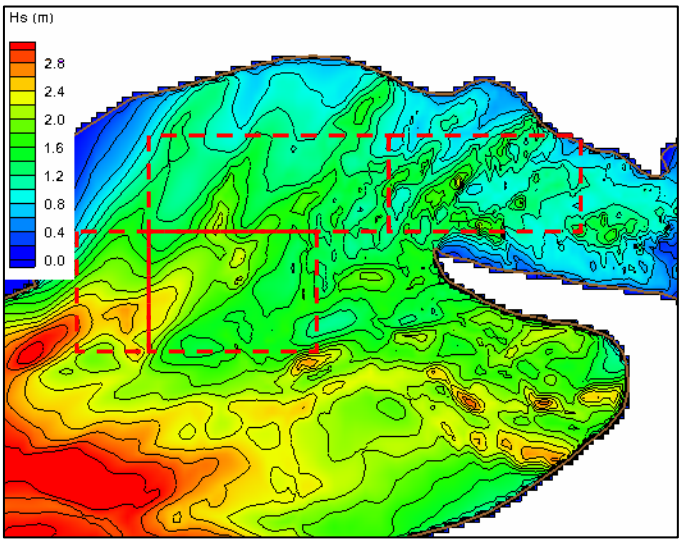

(a) Significant Wave Height for Ebb Flows with No Turbines in Minas Passage

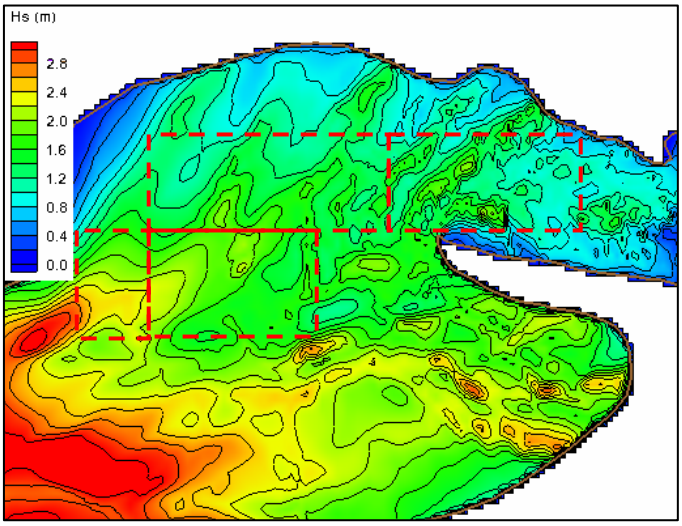

(b) Significant Wave Height for Ebb Flows with an array of 225 Turbines in Minas Passage

Figure 4-13: Extreme Waves in Ebb Currents, with and without Turbines

These figures demonstrate that only small changes occur in wave conditions throughout the Minas Passage region with the installation of 225 turbines as located in Figure 4-6. Difference plots of significant wave height in Figure 4-14 demonstrate that for the given flow conditions the changes are small and are very localized.

4.5.2 Effects on Coastline Integrity

One of the research objectives is to assess the effect of tidal power extraction on coastline integrity in the Bay of Fundy. In general, extreme storm wave events, such as hurricane-generated waves, have a more significant impact on sediment transport processes than the normal storm and non-storm wave conditions experienced during the rest of the year.

As storm waves increase in height, they have a larger effect along the coastline because of the increased intensity of breaking waves and the increased longshore transport of sediment. During extreme storm wave conditions, the wave heights can be further increased by nonlinear wave-current interactions that increase the steepness of the wave profile and alter the breaking wave characteristics. The focus of our research was to assess the effects of tidal power extraction on coastline integrity during extreme wave conditions.

The modification in extreme wave conditions due to tidal energy extraction by turbines was examined by computing changes in significant wave height over the model domain. To identify areas where there was an increase in significant wave height, the wave heights for the case of 'tidal currents with no turbines' were subtracted from the wave heights for the case of 'tidal currents with turbines'.

The differences in extreme waves for flood currents are shown in Figure 4-14 (a). A 20% reduction in velocity of the flood currents in Minas Passage increases the wave heights at the entrance to Minas Basin. The change in wave height occurs at a location where there are opposing currents in the complex circulation pattern of Minas Passage.

The differences in extreme waves for ebb currents are shown in Figure 4-14 (b). A 20% reduction in velocity of the ebb currents in Minas Passage decreases the wave heights in Minas Passage and the area to the west of the 225 turbine array, with the changes in wave height extending to the northern shore of these areas.

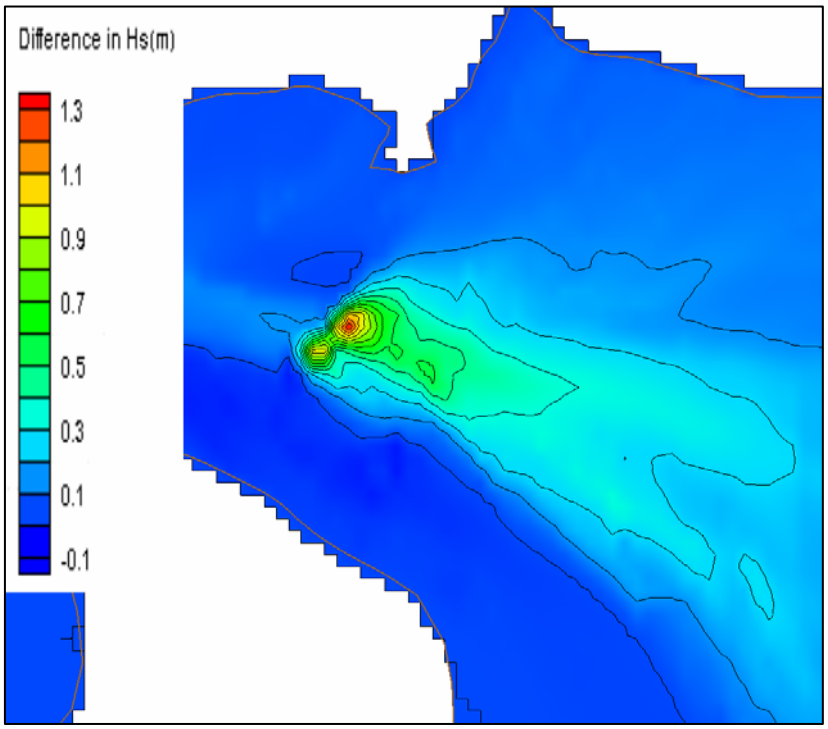

(a) Difference in Significant Wave Height for Extreme Wave Conditions for Flood Currents with and without an array of 225 Turbines in Minas Passage

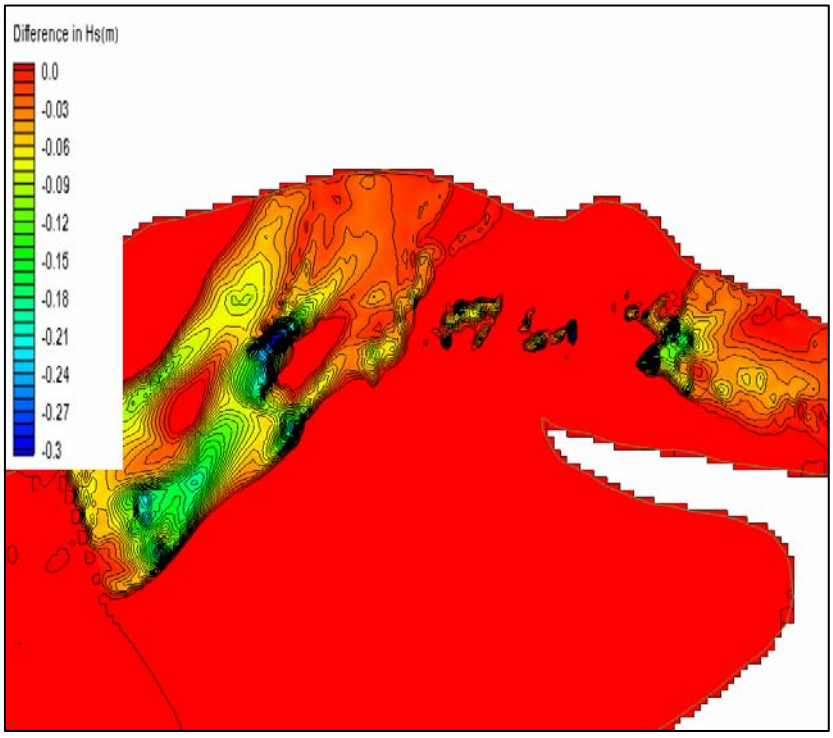

(b) Difference in Significant Wave Height for Extreme Wave Conditions for Ebb Currents with and without an array of 225 Turbines in Minas Passage

Figure 4-14: Differences in Wave Heights for Extreme Wave Conditions

For the conditions considered, the changes in significant wave height through the Minas Passage and Upper Minas Channel are small and localized. There is no change identified in the Cape Split region, with small changes on the shoreline on the north side of Minas Passage.

Longshore sediment transport is the movement of sediment parallel to a coastline under the action of waves and currents. This process may erode sand from beaches or cliffs and deposit it in mudflats or estuaries further along the shoreline. Estimates of the longshore transport rate are based on the sediment properties, the longshore component of wave energy flux entering the surf zone, and an empirical coefficient based on field measurements. Since the tasks for this study do not include interfacing a sediment transport model to the wave-current model and the analysis of measurements from a field survey, computations of longshore sediment transport based on the wave energy flux are outside the scope of work.

However, the wave energy flux is dependent on the wave energy density, which can be determined directly from the significant wave height:

$$E = \frac{\rho g H^2}{8}$$

where E = wave energy density [Nm/m^2],
ρ = mass density of water [kg/m^3],
g = acceleration of gravity [m/sec^2],
H = wave height [m]

To gain insight into the effects of tidal extraction by turbines on the coastline integrity in the Bay of Fundy, the wave energy density was computed using the refracted significant wave heights, Hs, from the STWAVE model. The wave energy densities for the case of 'tidal currents with no turbines' were subtracted from the wave energy densities for the case of 'tidal currents with turbines' case.

The differences in wave energy density of extreme waves for flood currents are shown in Figure 4-15 (a). The pattern of changes in wave energy density in Minas Passage is similar to that for significant wave height. The 20 % reduction in flood current produces the largest changes in wave energy density in mid-channel.

The differences in wave energy density of extreme waves for ebb currents are shown in Figure 4-15 (b). Once again, the pattern of changes in wave energy density in Minas Passage and the area to the west of the 225 turbine array is similar to that for significant wave height. The 20 % reduction in ebb current produces the largest changes in wave energy density in mid-channel of Minas Passage and the western side of the area to the west of the 225 turbine array. In the energy density plots, the wave height occurs as a squared term and the changes in wave height are amplified and very small changes are shown near the shoreline.

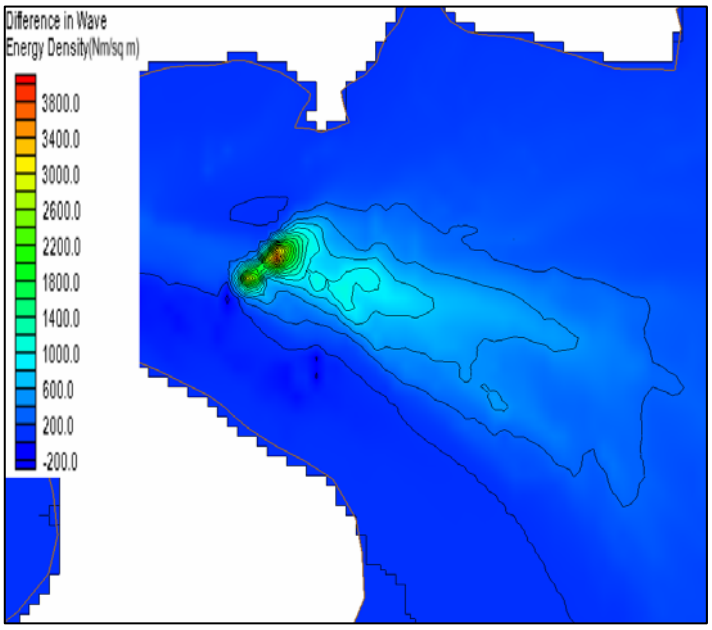

(a) Difference in Wave Energy Density for Flood Currents with and without an array of 225 Turbines in Minas Passage

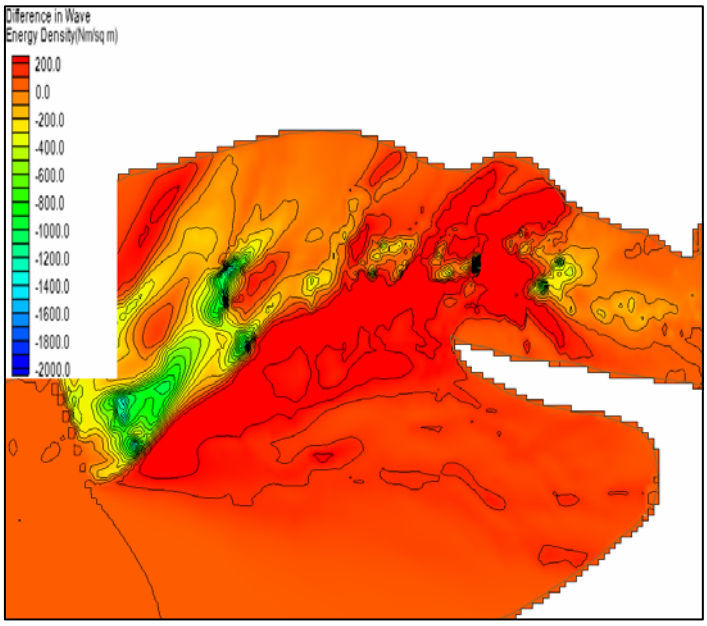

(b) Difference in Wave Energy Density for Ebb Currents with and without an array of 225 Turbines in Minas Passage

Figure 4-15: Differences in Wave Energy Density for Extreme Wave Conditions

Small changes in wave energy density also extend to the southern shore of Minas Passage and may affect the coastline integrity in that region. The rock cliffs in this region are predominantly basalt and are not easily erodable. Some local shoreline sediment may be

subject to transport, however, details on the shore-attached sediment would be necessary to assess this possibility. The basalt cliffs are affected by freeze-thaw cycles within the rock face fissures. These areas erode under storm conditions affecting the rock face, and deposit on the nearshore areas of the Blomidon shoreline.

The most recent assessment of the source of fine-grained sediment material in suspension in Minas Passage is: (a) the inner part of the Bay of Fundy, (b) the adjacent Minas Channel to the west, (c) from the entrance to Minas Basin in the east, and (d) the northern part of Minas Channel where slumped deposits occur (Fader, 2009).

The recent multi-beam survey has identified large sandwave fields to the west of Cape Split and near Cape D'Or, a promontory in the western end of Minas Channel. Ongoing detailed evaluation of the multi-beam survey will define these features in more detail and subsequent surveys will assist in assessing potential movement of the features.

Thus, the existing floor of Minas Passage is presently being kept clear of recent sediment deposition processes, but close examination is required to ensure that current velocity changes due to tidal extraction devices do not induce undesirable changes in sediment behaviour over the long term.

The resulting nearshore effects observed in the model due to wave-current interaction were small decreases in wave energy levels at the adjacent shoreline. Therefore, it can be expected that under the conditions analyzed, the energy extraction could involve increased deposition of suspended sediment in some near-field regions of the Minas Basin channel and Passage.

5.0 CONCLUSIONS AND RECOMMENDATIONS

- The results of the analysis carried out using the SwanOne wave model (a one-dimensional model) show that changes in the current affect the spectral shape of the waves and redistribute wave energy to different frequency bands. As expected, changes in the current produce a net change in the characteristics of energy propagating through the model. More detailed analysis of the transformations occurring, particularly the redistribution of energy to the various frequency bands, was carried out using two-dimensional models.

- The modelling of the wave-current interaction using the 2-dimensional STWAVE model with the BIO tidal current model is shown to be a powerful tool to quantify expected changes in wave energy throughout the model domain.

- The modelling and refinement of the wave-current model was carried out to help define areas of interest in regards to shoreline response to changing conditions.

- Some of the modelling results from the on-going BIO/Acadia research were integrated into our analysis to incorporate any expected changes in the flow field with the introduction of tidal energy extraction devices.

- In particular, the extreme case of an intense concentration of 225 turbines installed across Minas Passage had shown a decrease of up to 20% in current magnitude in close proximity to the turbines. Using this value of change in the current field in a portion of Minas Passage and combining with a series of wave conditions, nearshore effects produced only small localized changes in wave energy levels at the adjacent shoreline.

- Based on the analysis carried out on potential changes in wave patterns as a result of current changes caused by a set of 225 tidal turbines positioned offshore from Cape Split across a portion of Minas Passage, the resulting nearshore effects observed in the model were small decreases in wave energy levels at the adjacent shoreline. Therefore, it can be expected that under the conditions analyzed, the energy extraction could cause increased deposition of suspended sediment in some near-field regions of the Minas Basin channel and Passage. Far field effects of tidal changes were not considered as part of this study.

- Small changes shown in the analysis carried out could still represent more significant changes in sedimentation or erosion as a cumulative effect over the longer term. More detailed information on flow and sediment properties are required.

- Details of the flow field surrounding the individual turbines and the resultant details of flow around an array require further characterization.

- Sediment properties in the regions of flow changes should be better quantified for predictive effects of deposition or scour due to flow changes.

6.0 REFERENCES

Chen, C., R.C. Beardsley, and G. Cowles. 2006. *An Unstructured Grid, Finite-Volume Coastal Ocean Model: FVCOM User Manual.* SMAST/UMASSD-06-0602, Second Edition, July 2006. Marine Ecosystem Dynamics Modeling Laboratory, Woods Hole Oceanographic Institution, Woods Hole, MA.

Fader, G.B.J.. 2009. *Appendix 3 Geology, Bathymetry, Ice and Seismic Conditions*, In: Environmental Assessment Registration Document - Fundy Tidal Energy Demonstration Project, Volume 2: Appendices, June 2009.

Karsten, R., D. Greenberg, M. Tarbotton, R. Walters, J. Culina, and M. O'Flaherty-Sproul. 2010. *Assessment of the Potential of Tidal Power from Minas Passage and Minas Basin.* OEER/FORCE Tidal Energy Workshop. Wolfville, NS. October 13-14, 2010.

Smith, J.M., A.R. Sherlock, and D.T. Resio. 2001. *Steady-State Spectral Wave Model: User's Manual for STWAVE, Version 3.0.* Supplemental Report ERDC/CHL SR-01-1. US Army Engineer Research and Development Center, Vicksburg, MS.

TU Delft. 2009. *SwanOne User Manual.* Version 10-3-2009. Delft University of Technology. Delft, Netherlands.

Zundel, A.K., M.A. Cialone, and T.J. Moreland. 2002. *Steady-State SMS Steering Module for Coupling Waves and Currents 1. ADCIRC and STWAVE.* Coastal and Hydraulics Engineering Technical Note ERDC/CHL CHWRN-IV-41. US Army Engineer Research and Development Center, Vicksburg, MS.

APPENDIX A

DEVELOPMENT OF ADCIRC DATA FILES

APPENDIX A. DEVELOPMENT OF ADCIRC DATA FILES

The Surface-water Modeling System (SMS) developed by the U.S. Army Corps of Engineers (USACE) includes a 'Steering Module' that provides coupling of waves and currents, by automating the sharing of data between STWAVE and the circulation model ADCIRC (hydrodynamic model in SMS modelling system) or M2D. However, hydrodynamic modeling of tidal currents in the Bay of Fundy is presently being carried out with other software developed by Fisheries and Oceans Canada (Dr. David Greenberg). Translators are being developed to read output files from the Bay of Fundy circulation models and write the data into new files in the ADCIRC format. This will allow circulation models of the Bay of Fundy to be coupled to STWAVE using the SMS Steering Module, and will also allow the use of mesh generation and post-processing features in SMS.

It is proposed that the wave - current modeling analysis be organized into three phases.

- Phase I Seasonal (Non-Storm) Wave Conditions - Initial implementation of the spectral wave model to numerically simulate wave transformation in detail for non-storm conditions with no tidal energy extraction to calibrate the model, followed by test cases to include energy extraction.
- Phase II Storm Wave Conditions - Incorporation of operational conditions from numerical tidal models produced by others (eg. Dalhousie, BIO, Acadia) and the addition of 'storm' events to determine areas of increased wave intensity and sediment transport along the coastline.
- Phase III Extreme Wave Conditions –Establish extreme wave conditions at the energy extraction locations to establish overall effect of wave and current changes due to the operation of the tidal devices and the resultant effect of these changing fields on the integrity of the structures.

To date, the output files from BIO's model for tidal currents with no tidal energy extraction have been used to create SMS files for an ADCIRC grid and velocity time series.

The tidal current model is based on a grid of triangular elements in which the water depths and free surface elevations are specified at the nodes of the triangle and the (u,v) velocity components are specified at the triangle centroids. However, in the ADCIRC model the depths, elevations and (u,v) velocity components are all specified at the nodes of the triangle. The data transformation was carried out by interpolating the water depths to the triangle centroids. The centroids of the tidal current model were then defined as the nodes of an ADCIRC grid of triangular elements (see Figure A-1), which has increased resolution in the area of interest in Minas Channel. The depth contours for this ADCIRC grid are shown in Figure A-2. The node coordinates and depths were written to an ADCIRC *fort.14* data file.

Since the (u,v) velocity components from the tidal current model for a 29 day run are written to a binary file in NetCDF format, a Matlab script was created to read the surface currents from this file and write a time series of the (u,v) velocity components at each node to an ADCIRC *fort.64* file. Sample results from the tidal current model were used to generate vector plots as a check that the grid data and binary file were read correctly. A vector plot of the surface currents in the Bay of Fundy is shown in Figure A-3, and a detailed view showing the complex circulation pattern near Cape Split is presented in Figure A-4.

The Matlab script was modified to read the surface currents from the NetCDF binary file and write a time series of the (u,v) velocity components at each node to an ASCII vector dataset file in SMS format. The SMS software was then used to open the ADCIRC grid file, import (u,v) velocity components from the dataset file, and generate vector plots of the tidal currents in the Bay of Fundy (see Figure A-5) and in Minas Channel (see Figure A-6).

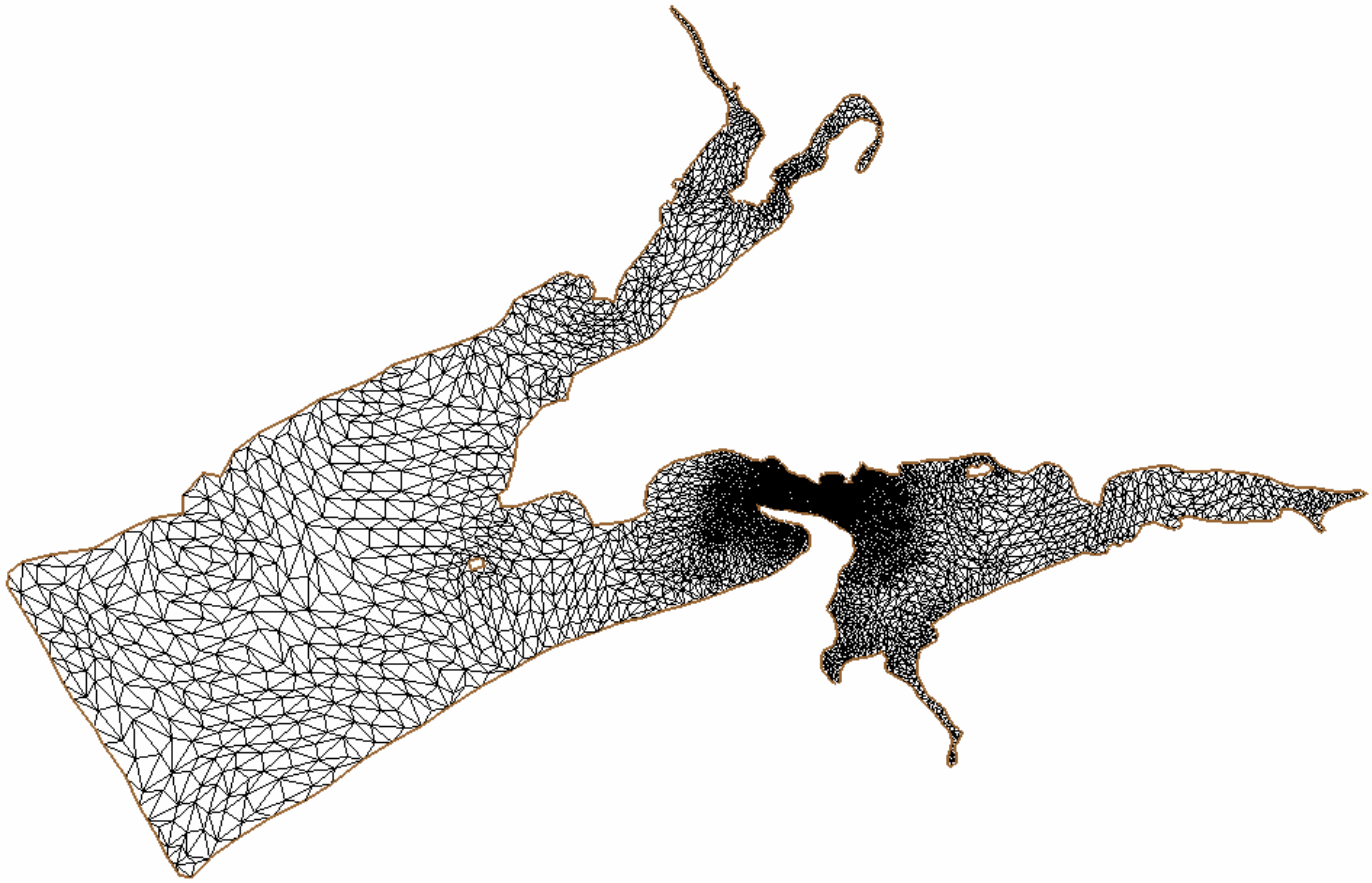

Figure A-1: Mesh derived from centroids of tidal current model

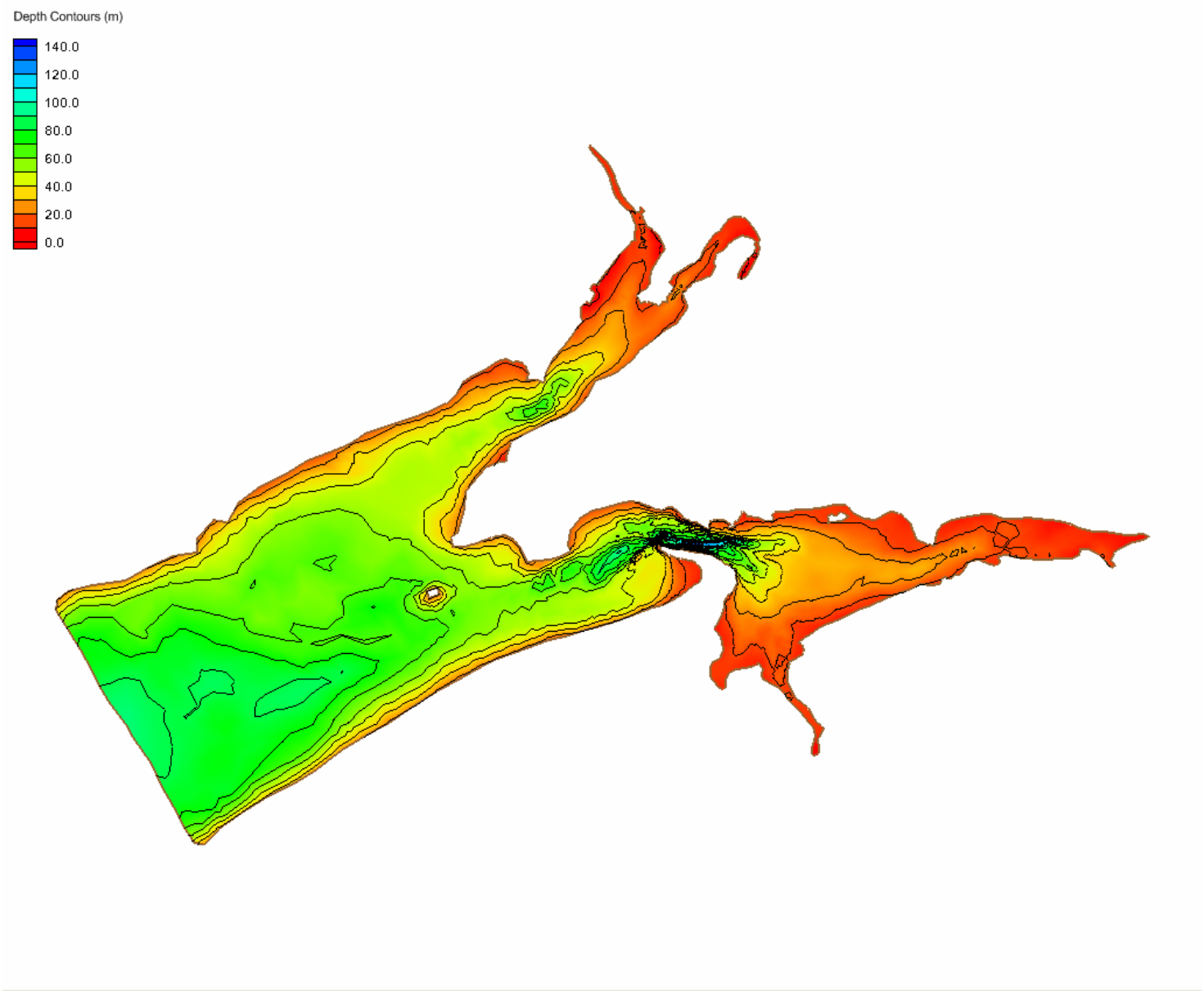

Figure A-2: Depth Contours derived from tidal current model

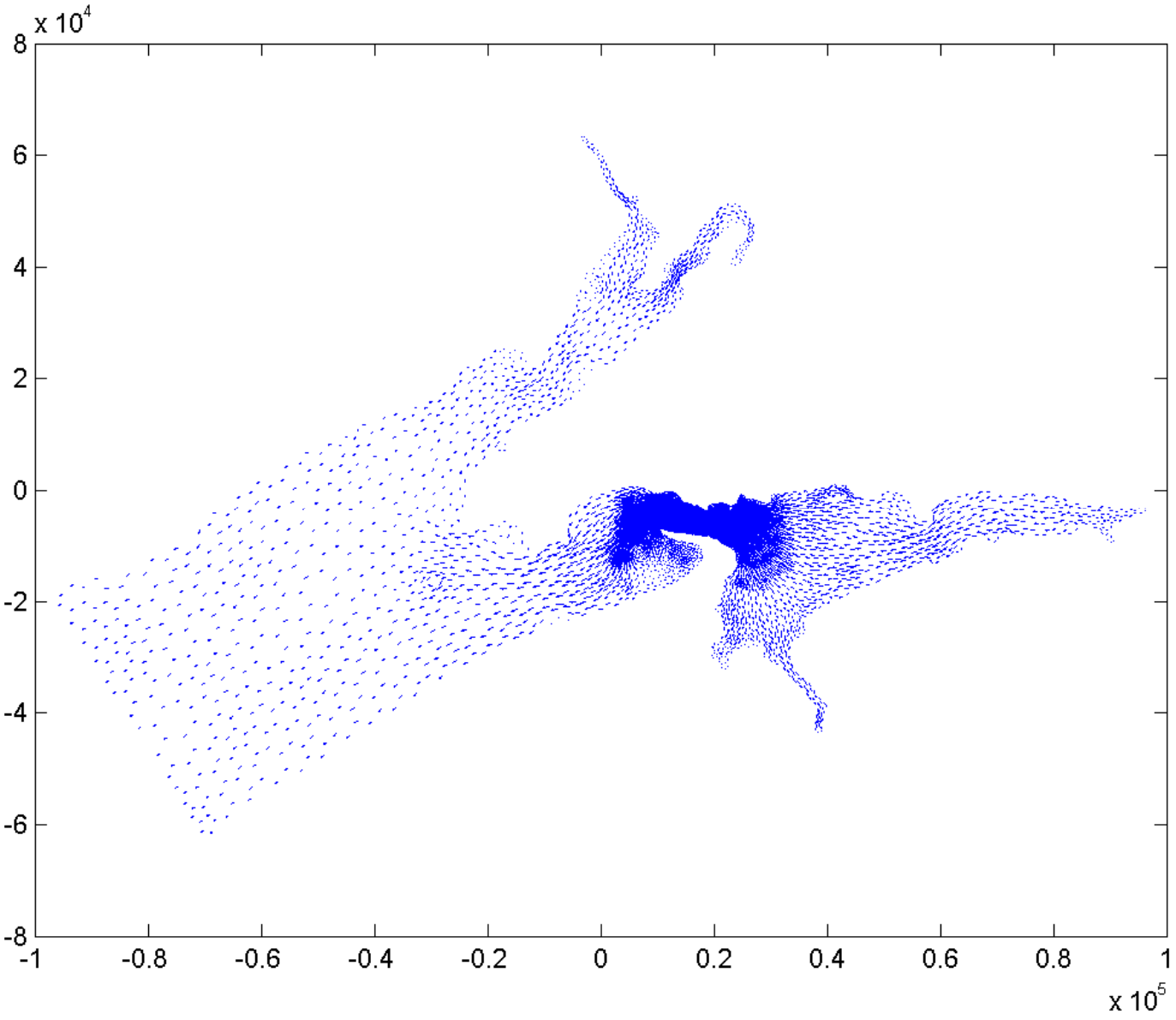

Figure A-3: Sample tidal model results showing surface currents in the Bay of Fundy

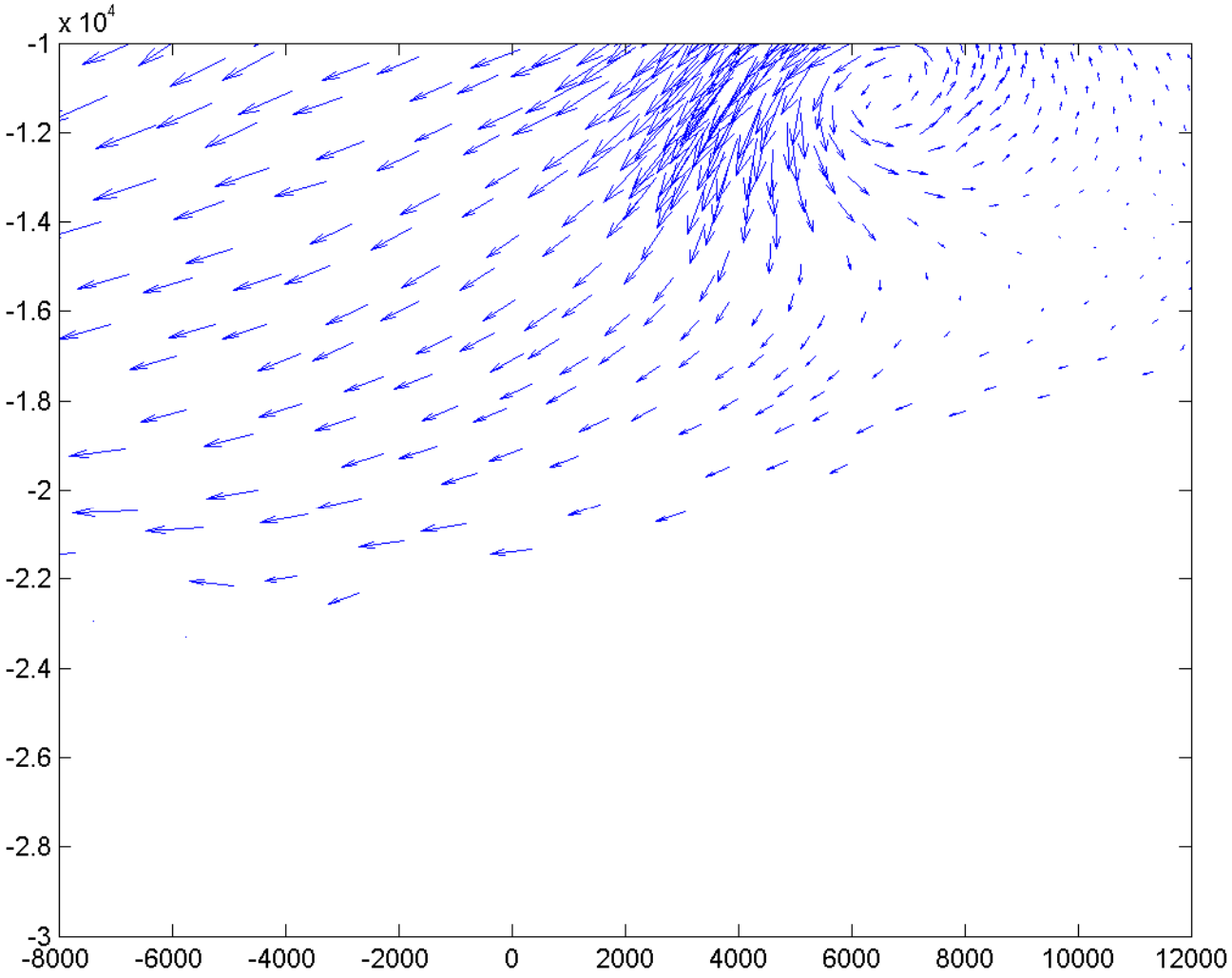

Figure A-4: Sample tidal model results showing circulation pattern near Cape Split

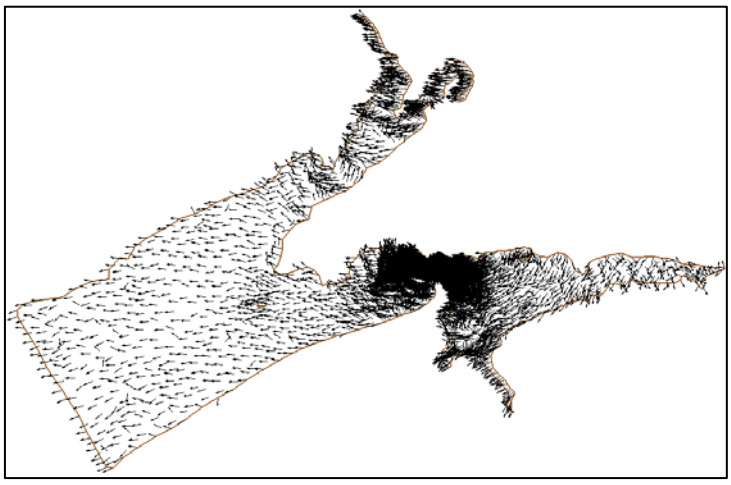

(a) Timestep 1

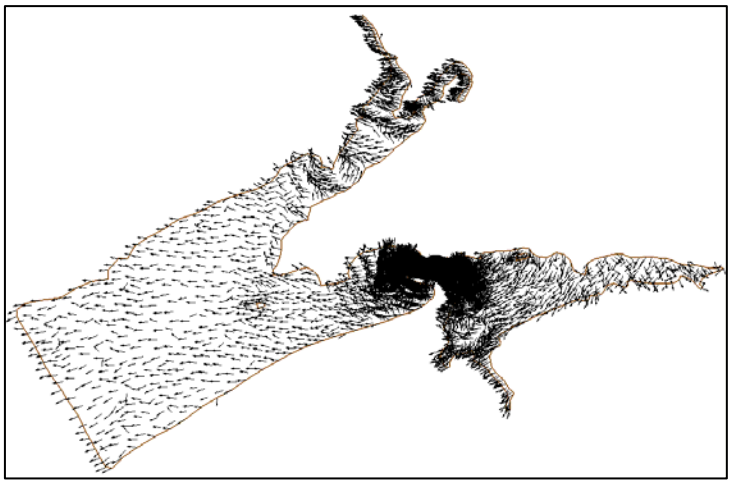

(b) Timestep 2

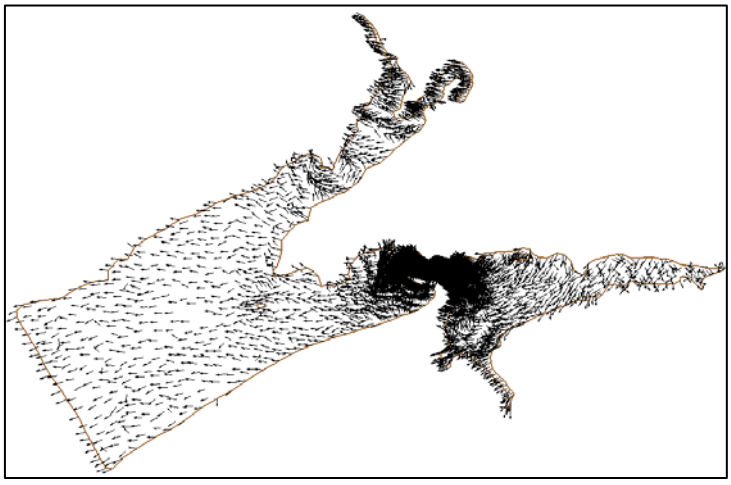

(c) Timestep 3

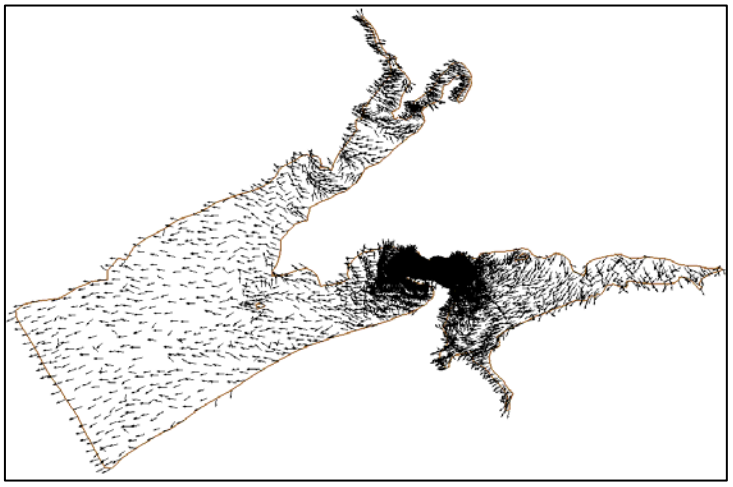

(d) Timestep 4

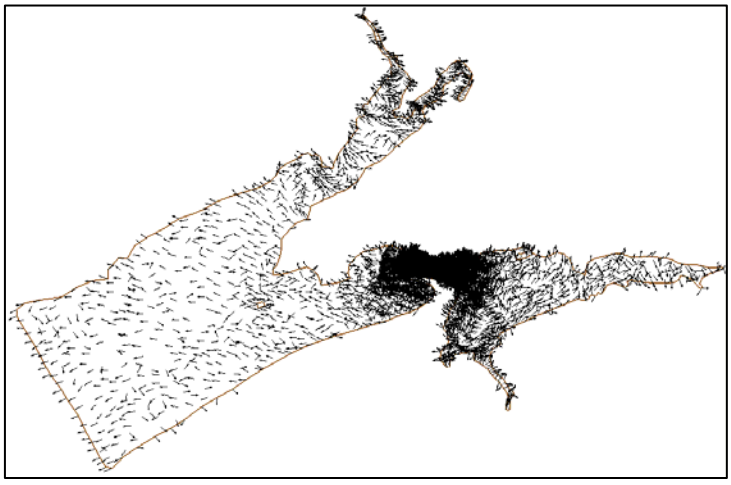

(e) Timestep 5

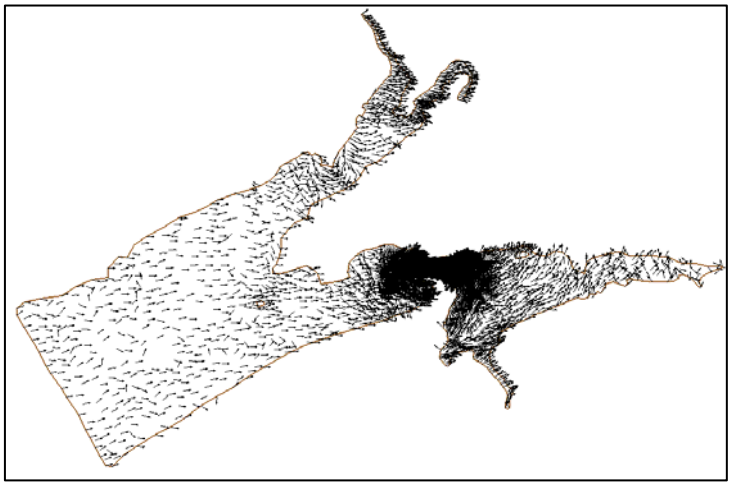

(f) Timestep 6

Figure A-5: SMS vector plots of tidal currents in the Bay of Fundy

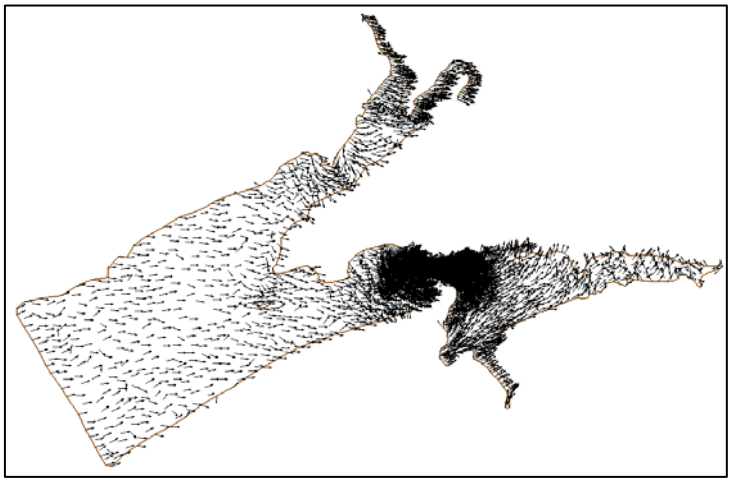

(g) Timestep 7

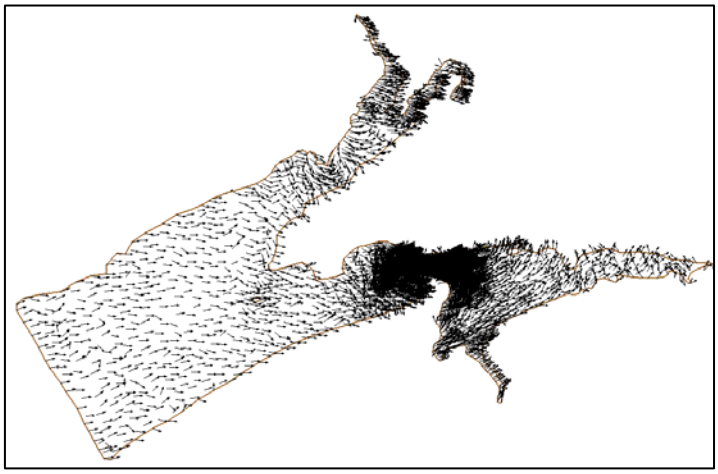

(h) Timestep 8

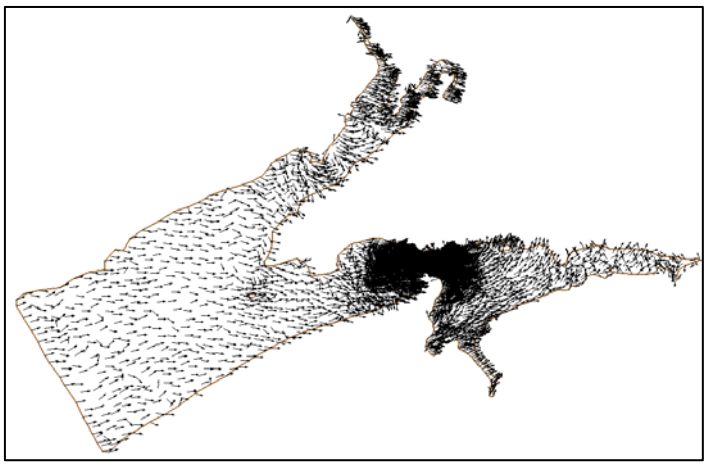

(i) Timestep 9

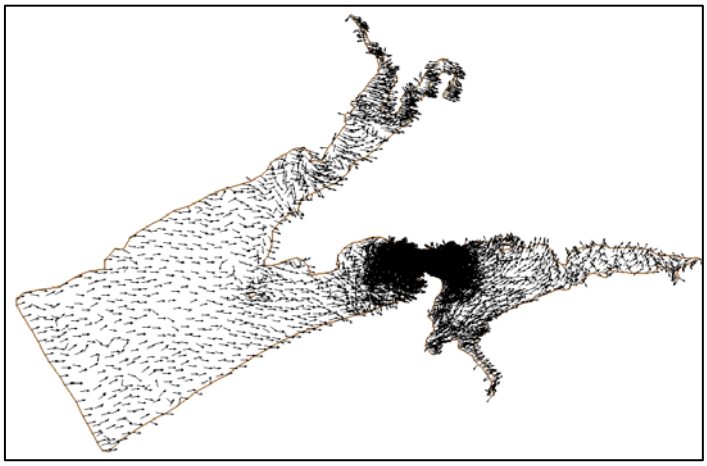

(j) Timestep 10

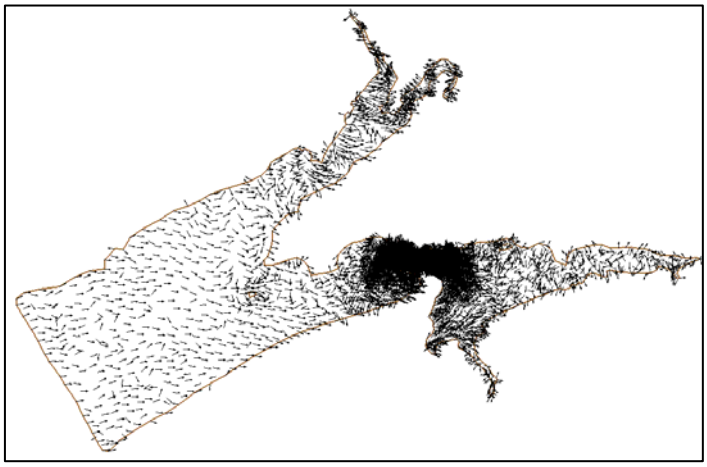

(k) Timestep 11

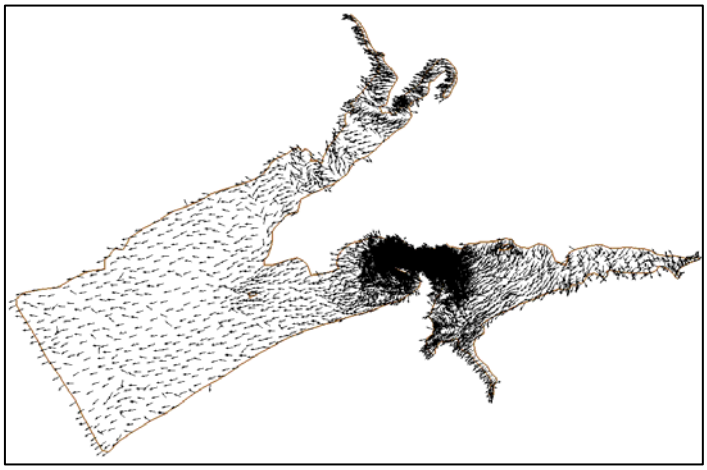

(l) Timestep 12

Figure A-5 (continued): SMS vector plots of tidal currents in the Bay of Fundy

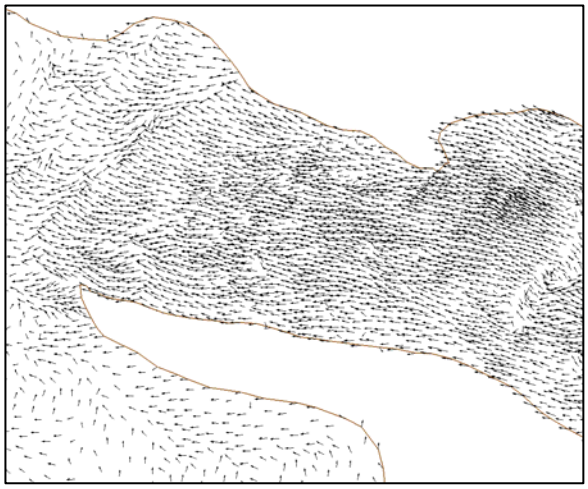

(a) Timestep 1

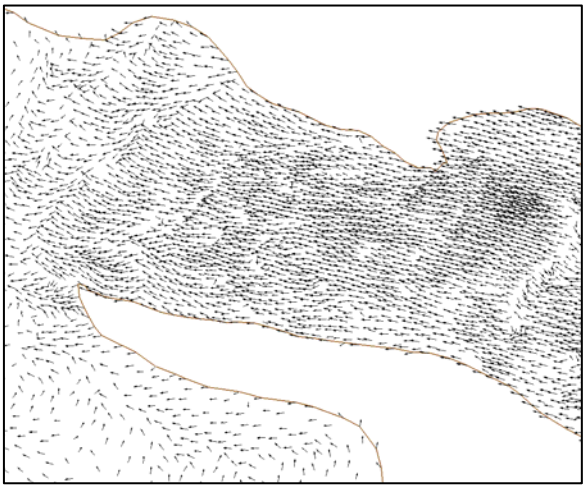

(b) Timestep 2

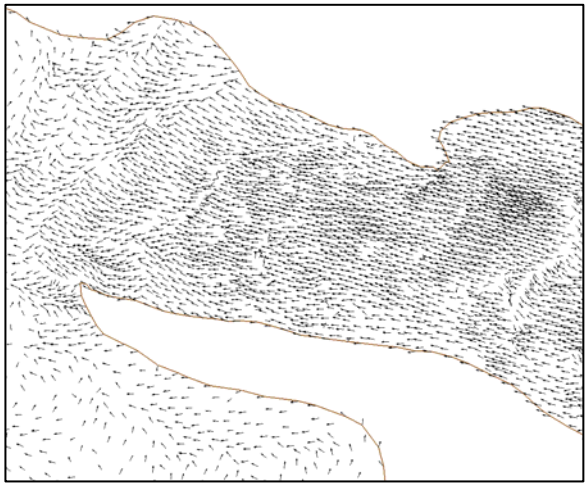

(c) Timestep 3

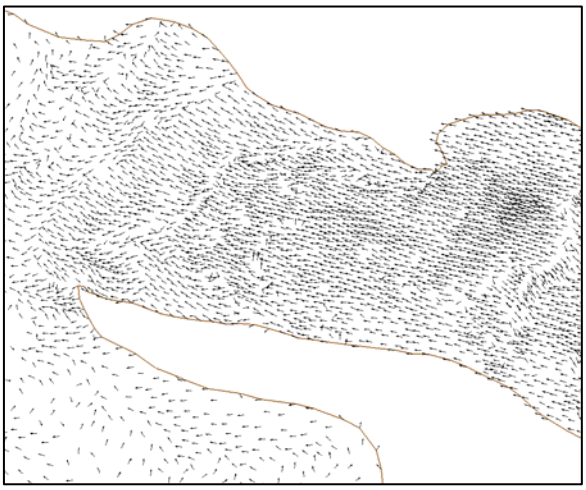

(d) Timestep 4

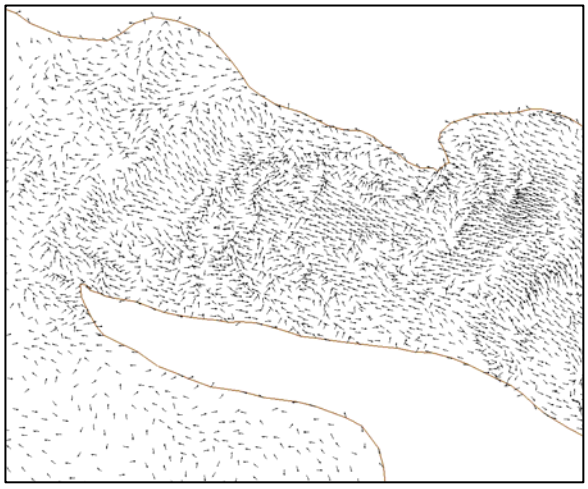

(e) Timestep 5

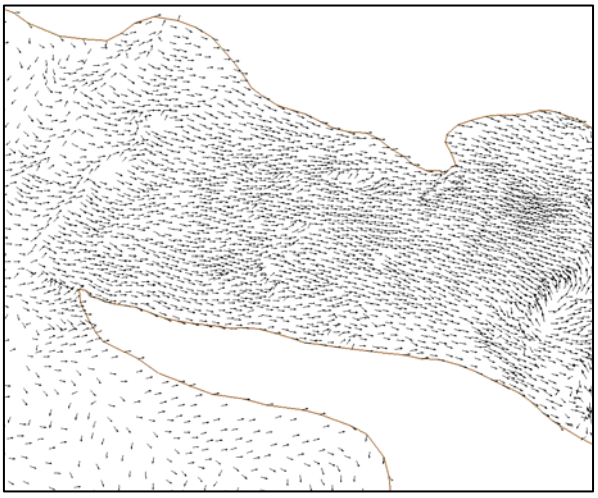

(f) Timestep 6

Figure A-6: SMS vector plots of tidal currents in Minas Channel

(g) Timestep 7

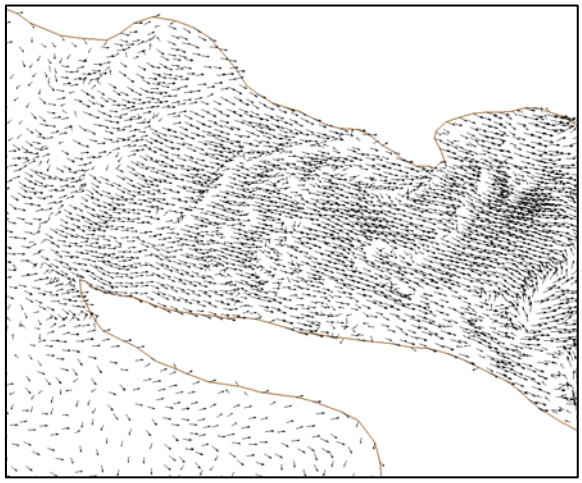

(h) Timestep 8

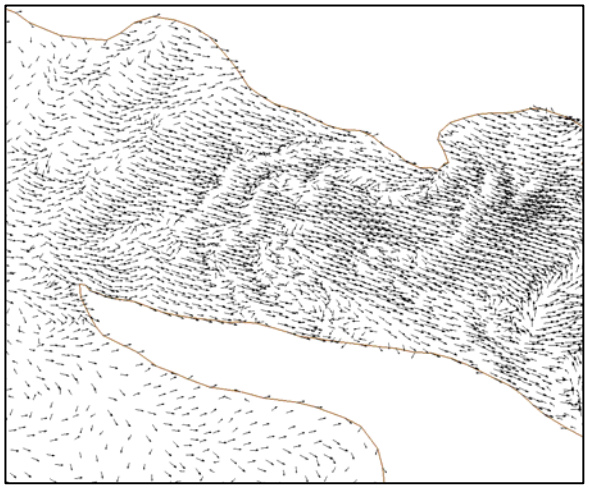

(i) Timestep 9

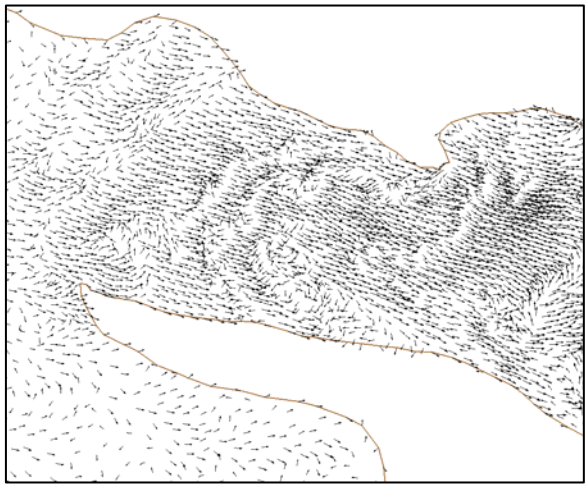

(j) Timestep 10

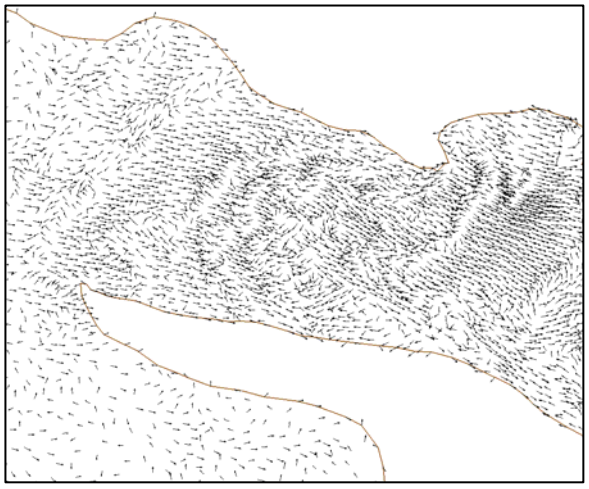

(k) Timestep 11

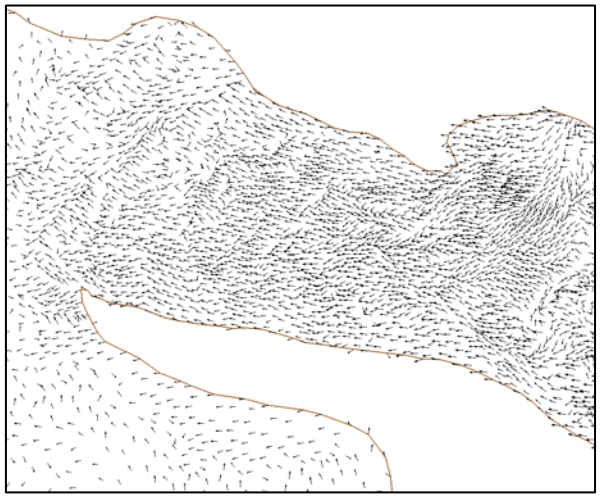

(l) Timestep 12

Figure A-6 (continued): SMS vector plots of tidal currents in Minas Channel

APPENDIX B

FREQUENCY OF OCCURRENCE TABLES FOR WAVE DATA

APPENDIX B. FREQUENCY OF OCCURRENCE TABLES FOR WAVE DATA

MSC grid points M6008430 and M6008431 were excluded from analysis, because the data were considered unreliable. Normalized frequency of occurrence tables for the other selected wave hindcast locations are presented in the following tables.

B.1 MSC Grid Point M6008261

Table B-1: Wave Conditions at Location M6008261

Significant Wave Height (cm) Versus Peak Period (sec)

	0-3	3-4	4-5	5-6	6-7	7-8	8-9	9-10	10-11	11-12	12-13	13-14	14-16	16-18	18-20	20-40	Subtotal
1-25	0.150955	0.011155	0.063561	0.016833	0.119114	0.029438	0.00129	0.010487	0.000129	0.000131	0.000041	0.000023	0.000002	0	0	0	0.403158
25-38	0.049615	0.089734	0.013204	0.001338	0.002562	0.008757	0.000977	0.000207	0	0	0	0	0	0	0	0	0.166393
38-50	0	0.112925	0.008888	0.003659	0.000071	0.001143	0.000786	0.000153	0	0	0	0	0	0	0	0	0.127624
50-62	0	0.081514	0.010319	0.005266	0.000046	0.00005	0.000245	0.000104	0	0	0	0	0	0	0	0	0.097543
62-75	0	0.054014	0.017275	0.00548	0.000097	0.00001	0.000023	0.000039	0	0	0	0	0	0	0	0	0.076939
75-88	0	0.017481	0.027924	0.004196	0.000214	0	0	0	0	0	0	0	0	0	0	0	0.049814
88-100	0	0.002493	0.022266	0.004011	0.000282	0.00001	0	0	0	0	0	0	0	0	0	0	0.029062
100-125	0	0.000396	0.015633	0.013382	0.000504	0.000046	0	0	0	0	0	0	0	0	0	0	0.02996
125-150	0	0.00001	0.001527	0.008682	0.000487	0.000054	0	0	0	0	0	0	0	0	0	0	0.01076
150-175	0	0	0.000114	0.003335	0.001547	0.000062	0	0	0	0	0	0	0	0	0	0	0.005059
175-200	0	0	0.000004	0.000508	0.001354	0.000133	0	0	0	0	0	0	0	0	0	0	0.001999
200-250	0	0	0	0.000106	0.000697	0.000369	0.00001	0	0	0	0	0	0	0	0	0	0.001182
250-300	0	0	0	0	0.000095	0.000263	0.000006	0	0	0	0	0	0	0	0	0	0.000365
300-400	0	0	0	0	0.000002	0.000064	0.000068	0	0	0	0	0	0	0	0	0	0.000135
400-500	0	0	0	0	0	0	0.000006	0	0	0	0	0	0	0	0	0	0.000006
500-600	0	0	0	0	0	0	0	0	0	0	0	0	0	0	0	0	0
600-700	0	0	0	0	0	0	0	0	0	0	0	0	0	0	0	0	0
Subtotal	0.20057	0.369721	0.180712	0.066796	0.127072	0.040399	0.003412	0.010991	0.000129	0.000131	0.000041	0.000023	0.000002	0	0	0	

Significant Wave Height (cm) Versus Vector Mean Direction (to which waves are travelling, clockwise from North)

	22.5	45	67.5	90	112.5	135	157.5	180	202.5	225	247.5	270	292.5	315	337.5	360	Subtotal
1-25	0.006453	0.007064	0.033656	0.249811	0.044763	0.010935	0.010259	0.010752	0.007768	0.002686	0.002155	0.002864	0.004764	0.002904	0.00158	0.003039	0.401453
25-38	0.005005	0.008786	0.016153	0.057071	0.029952	0.008477	0.006979	0.009773	0.006857	0.002277	0.001962	0.002927	0.005445	0.001778	0.000693	0.001599	0.165733
38-50	0.003368	0.009087	0.01729	0.03141	0.023462	0.008025	0.006102	0.008892	0.007288	0.001977	0.001475	0.001719	0.004441	0.001122	0.000624	0.000786	0.127068
50-62	0.002259	0.005521	0.011719	0.02178	0.019828	0.007456	0.004658	0.006853	0.00805	0.001834	0.000962	0.001348	0.003111	0.000705	0.000537	0.000489	0.097112
62-75	0.001058	0.004038	0.008655	0.015724	0.01534	0.006772	0.00382	0.006631	0.007942	0.001238	0.000956	0.001143	0.002143	0.000467	0.000342	0.000342	0.076611
75-88	0.000436	0.001663	0.005409	0.009738	0.009991	0.006129	0.003128	0.004592	0.005086	0.000755	0.000568	0.000577	0.000896	0.000239	0.000158	0.000245	0.049608
88-100	0.000185	0.000635	0.00331	0.005938	0.005845	0.004244	0.002211	0.002871	0.002362	0.000452	0.000245	0.000158	0.000257	0.000066	0.000058	0.000106	0.028942
100-125	0.000151	0.000508	0.002808	0.007098	0.00699	0.004941	0.002338	0.001867	0.001906	0.000523	0.000261	0.000114	0.000141	0.000037	0.000048	0.0001	0.02983
125-150	0.000039	0.000112	0.000813	0.002669	0.003694	0.001771	0.000639	0.000359	0.00039	0.000114	0.000048	0.000031	0.000017	0.000002	0.000006	0.00001	0.010715
150-175	0.000008	0.000037	0.000307	0.001589	0.001946	0.000612	0.000183	0.000143	0.000131	0.000077	0	0	0.000002	0.000002	0	0.000002	0.005038
175-200	0	0.000017	0.000122	0.000896	0.000556	0.000176	0.000085	0.000075	0.000058	0.000008	0	0	0	0	0	0	0.001993
200-250	0	0.000002	0.000066	0.000502	0.000386	0.000114	0.000041	0.000027	0.000039	0	0	0	0	0	0	0	0.001178
250-300	0	0	0.000008	0.000129	0.000172	0.000056	0	0	0	0	0	0	0	0	0	0	0.000365
300-400	0	0	0	0.000097	0.000035	0.000002	0	0	0	0	0	0	0	0	0	0	0.000135
400-500	0	0	0	0.000002	0.000004	0	0	0	0	0	0	0	0	0	0	0	0.000006
500-600	0	0	0	0	0	0	0	0	0	0	0	0	0	0	0	0	0
600-700	0	0	0	0	0	0	0	0	0	0	0	0	0	0	0	0	0
Subtotal	0.018961	0.037471	0.100318	0.404454	0.162964	0.059709	0.040443	0.052834	0.047877	0.011941	0.008632	0.010881	0.021216	0.007322	0.004047	0.006718	

Peak Period (sec) Versus Vector Mean Direction (to which waves are travelling, clockwise from North)

	22.5	45	67.5	90	112.5	135	157.5	180	202.5	225	247.5	270	292.5	315	337.5	360	Subtotal
1-3	0.007025	0.006403	0.012088	0.061132	0.043616	0.010507	0.011202	0.013426	0.009947	0.003229	0.002732	0.004001	0.006463	0.003175	0.001352	0.003126	0.199425
3-4	0.010151	0.024734	0.038636	0.07764	0.067332	0.023468	0.018926	0.032495	0.033016	0.007251	0.005279	0.006486	0.014224	0.00365	0.002134	0.002767	0.368189
4-5	0.000734	0.00354	0.018831	0.091138	0.027364	0.017298	0.008174	0.005946	0.004397	0.001178	0.000479	0.000297	0.000338	0.000075	0.000118	0.000265	0.180173
5-6	0.000023	0.000209	0.00638	0.038553	0.014616	0.005393	0.000778	0.000286	0.000234	0.000062	0	0	0	0.000002	0.000008	0.000006	0.066552
6-7	0.000666	0.001659	0.015861	0.098269	0.005484	0.00167	0.000782	0.000431	0.000185	0.000149	0.000093	0.000079	0.000127	0.000321	0.000332	0.000396	0.126504
7-8	0.000153	0.000475	0.00532	0.029786	0.003088	0.000782	0.000274	0.000102	0.000035	0.000027	0.000012	0.000004	0.000027	0.000048	0.000058	0.000073	0.040265
8-9	0.000044	0.000093	0.000506	0.001883	0.000589	0.000129	0.000046	0.000021	0.000015	0.000015	0.000012	0.000004	0.000008	0.00001	0.000006	0.000017	0.003397
9-10	0.00016	0.000355	0.002669	0.005876	0.00085	0.000427	0.000232	0.000112	0.000039	0.000029	0.000025	0.00001	0.000027	0.000039	0.000037	0.000068	0.010957
10-11	0.000004	0.000002	0.000012	0.000066	0.000015	0.000017	0.000006	0.000004	0	0	0	0	0.000002	0	0	0	0.000129
11-12	0	0	0	0.000073	0.000006	0.000012	0.000021	0.00001	0.000008	0	0	0	0	0	0	0	0.000131
12-13	0.000002	0	0.000004	0.000023	0.000004	0.000006	0.000002	0	0	0	0	0	0	0	0	0	0.000041
13-14	0	0	0.000008	0.000015	0	0	0	0	0	0	0	0	0	0	0	0	0.000023
14-16	0	0	0.000002	0	0	0	0	0	0	0	0	0	0	0	0	0	0.000002
16-18	0	0	0	0	0	0	0	0	0	0	0	0	0	0	0	0	0
18-20	0	0	0	0	0	0	0	0	0	0	0	0	0	0	0	0	0
20-40	0	0	0	0	0	0	0	0	0	0	0	0	0	0	0	0	0
Subtotal	0.018961	0.037471	0.100318	0.404454	0.162964	0.059709	0.040443	0.052834	0.047877	0.011941	0.008632	0.010881	0.021216	0.007322	0.004047	0.006718	

B.2 MSC Grid Point M6008429

Table B-2: Wave Conditions at Location M6008429

Significant Wave Height (cm) Versus Peak Period (sec)

	0-3	3-4	4-5	5-6	6-7	7-8	8-9	9-10	10-11	11-12	12-13	13-14	14-16	16-18	18-20	20-40	Subtotal
1-25	0.266555	0.005017	0.033779	0.038848	0.110002	0.069242	0.003885	0.007992	0.000079	0.00027	0.000158	0.000031	0.00023	0	0	0	0.536087
25-38	0.06556	0.107403	0.00001	0.000135	0.000085	0.000124	0.000075	0.000012	0	0	0	0	0	0	0	0	0.173405
38-50	0	0.11207	0.000004	0.000012	0.000033	0.000054	0	0	0	0	0	0	0	0	0	0	0.112174
50-62	0	0.075956	0.000064	0.000012	0.000019	0.000056	0	0	0	0	0	0	0	0	0	0	0.076107
62-75	0	0.050307	0.002255	0.000012	0.000033	0.000056	0	0	0	0	0	0	0	0	0	0	0.052664
75-88	0	0.018947	0.00665	0.000025	0.000044	0.00005	0	0	0	0	0	0	0	0	0	0	0.025715
88-100	0	0.005538	0.006158	0.000035	0.00005	0.000048	0	0	0	0	0	0	0	0	0	0	0.011829
100-125	0	0.001135	0.007037	0.000131	0.000301	0.00027	0	0	0	0	0	0	0	0	0	0	0.008873
125-150	0	0.000008	0.00151	0.000265	0.000137	0.00033	0.000008	0	0	0	0	0	0	0	0	0	0.002259
150-175	0	0	0.000249	0.000249	0.000033	0.000102	0.000025	0	0	0	0	0	0	0	0	0	0.000657
175-200	0	0	0.000008	0.000077	0.000004	0.000035	0.000056	0	0	0	0	0	0	0	0	0	0.00018
200-250	0	0	0	0.000021	0.000002	0.000006	0.000021	0	0	0	0	0	0	0	0	0	0.00005
250-300	0	0	0	0	0	0	0	0	0	0	0	0	0	0	0	0	0
300-400	0	0	0	0	0	0	0	0	0	0	0	0	0	0	0	0	0
400-500	0	0	0	0	0	0	0	0	0	0	0	0	0	0	0	0	0
500-600	0	0	0	0	0	0	0	0	0	0	0	0	0	0	0	0	0
600-700	0	0	0	0	0	0	0	0	0	0	0	0	0	0	0	0	0
Subtotal	0.332116	0.376381	0.057724	0.039823	0.110743	0.070372	0.004069	0.008004	0.000079	0.00027	0.000158	0.000031	0.00023	0	0	0	

Significant Wave Height (cm) Versus Vector Mean Direction (to which waves are travelling, clockwise from North)

	22.5	45	67.5	90	112.5	135	157.5	180	202.5	225	247.5	270	292.5	315	337.5	360	Subtotal
1-25	0.016182	0.031943	0.204467	0.151831	0.026298	0.008767	0.008139	0.016012	0.021322	0.011291	0.005167	0.004631	0.007687	0.004447	0.005299	0.009997	0.53348
25-38	0.011488	0.023168	0.026648	0.02912	0.018555	0.008637	0.005583	0.011723	0.01634	0.003839	0.002296	0.00369	0.003561	0.001705	0.001464	0.004764	0.172582
38-50	0.008634	0.014846	0.016485	0.015485	0.012716	0.006345	0.004557	0.004231	0.012625	0.002806	0.001427	0.002205	0.003275	0.001466	0.001004	0.00358	0.111688
50-62	0.006822	0.009755	0.009483	0.009143	0.007129	0.003623	0.002566	0.003072	0.010601	0.002512	0.00111	0.001429	0.003375	0.001211	0.001062	0.002906	0.075796
62-75	0.00548	0.007185	0.00583	0.005662	0.004009	0.00275	0.001755	0.002035	0.004731	0.002385	0.000732	0.001327	0.004179	0.001242	0.001016	0.002114	0.052433
75-88	0.0024	0.003688	0.00274	0.002481	0.001892	0.000944	0.000711	0.000568	0.000993	0.00139	0.000583	0.000989	0.002916	0.001226	0.000813	0.001286	0.025619
88-100	0.001025	0.001475	0.001099	0.001462	0.000618	0.000247	0.000259	0.000176	0.000234	0.000728	0.000338	0.000429	0.00161	0.001025	0.000537	0.000529	0.011791
100-125	0.000655	0.000942	0.001305	0.001025	0.000278	0.000112	0.000118	0.000137	0.000203	0.000541	0.000396	0.000394	0.00056	0.001112	0.000589	0.000477	0.008844
125-150	0.000185	0.000222	0.000373	0.000214	0.000066	0.000052	0.000039	0.000012	0.000071	0.000141	0.000085	0.000087	0.00006	0.000303	0.000164	0.000174	0.002248
150-175	0.000062	0.000066	0.000102	0.000077	0.000008	0.000002	0	0	0.000004	0.000058	0.000046	0.00001	0.000035	0.000068	0.000052	0.000066	0.000657
175-200	0.000029	0.000023	0.000052	0.000044	0	0	0	0	0	0.000008	0	0	0	0.00001	0.000004	0.00001	0.00018
200-250	0.000002	0.000004	0.00001	0.000019	0	0	0	0	0	0	0	0	0	0.000004	0.000008	0.000002	0.00005
250-300	0	0	0	0	0	0	0	0	0	0	0	0	0	0	0	0	0
300-400	0	0	0	0	0	0	0	0	0	0	0	0	0	0	0	0	0
400-500	0	0	0	0	0	0	0	0	0	0	0	0	0	0	0	0	0
500-600	0	0	0	0	0	0	0	0	0	0	0	0	0	0	0	0	0
600-700	0	0	0	0	0	0	0	0	0	0	0	0	0	0	0	0	0
Subtotal	0.052964	0.093316	0.268594	0.216561	0.071569	0.031479	0.023728	0.037966	0.067124	0.0257	0.012179	0.015193	0.027258	0.01382	0.012013	0.025906	

Peak Period (sec) Versus Vector Mean Direction (to which waves are travelling, clockwise from North)

	22.5	45	67.5	90	112.5	135	157.5	180	202.5	225	247.5	270	292.5	315	337.5	360	Subtotal
1-3	0.017337	0.031238	0.052043	0.083192	0.0295	0.009555	0.008867	0.020691	0.02632	0.012254	0.005859	0.005588	0.008522	0.004376	0.00499	0.01029	0.330625
3-4	0.029307	0.046713	0.052025	0.053692	0.037784	0.019911	0.013339	0.015776	0.037738	0.010696	0.005339	0.008877	0.017962	0.007481	0.005125	0.012974	0.374739
4-5	0.003368	0.006805	0.018974	0.016931	0.000566	0.000253	0.000303	0.000543	0.002246	0.00234	0.000763	0.000465	0.000367	0.00133	0.001037	0.001149	0.05744
5-6	0.000353	0.001047	0.019476	0.017184	0.000662	0.000224	0.000104	0.00006	0.000046	0.000064	0.000002	0.000004	0.000012	0.000044	0.000048	0.000147	0.039476
6-7	0.001466	0.004138	0.07339	0.025729	0.001348	0.00072	0.000514	0.000456	0.000367	0.000149	0.000095	0.000137	0.000224	0.000309	0.00045	0.000753	0.110247
7-8	0.000713	0.002282	0.046178	0.016966	0.001298	0.00062	0.000465	0.000278	0.000226	0.000122	0.00005	0.000062	0.000075	0.000156	0.000214	0.000344	0.070049
8-9	0.000197	0.000373	0.001599	0.001226	0.000147	0.00006	0.000044	0.000033	0.000012	0.000029	0.000023	0.000015	0.000044	0.000066	0.000064	0.00012	0.004053
9-10	0.000191	0.000682	0.004542	0.001475	0.000236	0.000112	0.000089	0.000116	0.000141	0.000025	0.000037	0.000044	0.000046	0.000054	0.000083	0.00011	0.007983
10-11	0.000002	0.000002	0.000035	0.000019	0	0.000006	0	0.000004	0.000004	0	0	0	0	0.000002	0.000002	0	0.000077
11-12	0	0.000004	0.000156	0.000056	0.00001	0.000002	0.000002	0.000002	0.000012	0.000015	0.000008	0	0	0	0	0	0.000268
12-13	0	0.000002	0.000108	0.000017	0.000006	0.000006	0	0	0.000006	0.000002	0.000002	0.000002	0.000004	0.000002	0	0	0.000158
13-14	0.000002	0.000004	0.000019	0.000002	0.000002	0.000002	0	0	0	0	0	0	0	0	0	0	0.000031
14-16	0.000027	0.000025	0.00005	0.000073	0.000008	0.000006	0.000002	0.000006	0.000004	0.000004	0	0	0.000002	0	0	0.000019	0.000226
16-18	0	0	0	0	0	0	0	0	0	0	0	0	0	0	0	0	0
18-20	0	0	0	0	0	0	0	0	0	0	0	0	0	0	0	0	0
20-40	0	0	0	0	0	0	0	0	0	0	0	0	0	0	0	0	0
Subtotal	0.052964	0.093316	0.268594	0.216561	0.071569	0.031479	0.023728	0.037966	0.067124	0.0257	0.012179	0.015193	0.027258	0.01382	0.012013	0.025906	

B.3 MSC Grid Point M6008258

Table B-3: Wave Conditions at Location M6008258

Significant Wave Height (cm) Versus Peak Period (sec)

	0-3	3-4	4-5	5-6	6-7	7-8	8-9	9-10	10-11	11-12	12-13	13-14	14-16	16-18	18-20	20-40	Subtotal
1-25	0.079899	0.009763	0.035982	0.029359	0.098126	0.037014	0.003437	0.016641	0.000324	0.000236	0.000436	0.000423	0.001273	0.000058	0	0	0.31297
25-38	0.030819	0.065278	0.006592	0.010997	0.015606	0.019158	0.000307	0.001475	0	0.000002	0.000002	0.000023	0	0	0	0	0.150258
38-50	0	0.095515	0.008118	0.003269	0.002559	0.011742	0.000929	0.000492	0	0	0.000008	0.000004	0	0	0	0	0.122636
50-62	0	0.086343	0.010312	0.003972	0.000353	0.006629	0.001386	0.000452	0	0	0	0	0	0	0	0	0.109446
62-75	0	0.070644	0.014975	0.005826	0.000075	0.003341	0.001715	0.000548	0.000004	0	0	0	0	0	0	0	0.097128
75-88	0	0.035115	0.024983	0.006141	0.000054	0.000836	0.001269	0.000614	0.000023	0.000004	0	0	0	0	0	0	0.069039
88-100	0	0.011013	0.027411	0.004704	0.000097	0.000116	0.000444	0.000541	0.00001	0.000002	0	0	0	0	0	0	0.04434
100-125	0	0.003804	0.037346	0.010105	0.000415	0.000085	0.000131	0.000367	0.000029	0.000004	0	0	0	0	0	0	0.052286
125-150	0	0.000164	0.009719	0.011659	0.00074	0.000176	0.000002	0.000017	0.000012	0.000008	0	0	0	0	0	0	0.022498
150-175	0	0.000002	0.000884	0.00788	0.000958	0.000212	0	0.000004	0	0	0	0	0	0	0	0	0.009939
175-200	0	0	0.000066	0.00281	0.001699	0.000251	0	0	0	0	0	0	0	0	0	0	0.004826
200-250	0	0	0.000006	0.000952	0.001394	0.000933	0.000019	0	0	0	0	0	0	0	0	0	0.003304
250-300	0	0	0	0.000039	0.000377	0.000458	0.000035	0	0	0	0	0	0	0	0	0	0.000911
300-400	0	0	0	0	0.00006	0.000172	0.000131	0	0	0	0	0	0	0	0	0	0.000363
400-500	0	0	0	0	0	0.000004	0.00005	0.000002	0	0	0	0	0	0	0	0	0.000056
500-600	0	0	0	0	0	0	0	0	0	0	0	0	0	0	0	0	0
600-700	0	0	0	0	0	0	0	0	0	0	0	0	0	0	0	0	0
Subtotal	0.110718	0.37764	0.176394	0.097713	0.122513	0.081129	0.009854	0.021152	0.000402	0.000257	0.000446	0.00045	0.001273	0.000058	0	0	

Significant Wave Height (cm) Versus Vector Mean Direction (to which waves are travelling, clockwise from North)

	22.5	45	67.5	90	112.5	135	157.5	180	202.5	225	247.5	270	292.5	315	337.5	360	Subtotal
1-25	0.004822	0.008033	0.126095	0.116679	0.013318	0.004997	0.004839	0.009657	0.007156	0.001332	0.001284	0.00191	0.004088	0.002889	0.001807	0.002522	0.311427
25-38	0.002707	0.004285	0.018003	0.063889	0.017937	0.007112	0.00521	0.009568	0.007261	0.001724	0.001135	0.001856	0.004449	0.002269	0.000977	0.001209	0.149591
38-50	0.002084	0.006523	0.01612	0.034507	0.018198	0.008962	0.006005	0.008861	0.00884	0.001707	0.001215	0.001757	0.004076	0.001713	0.000707	0.000788	0.122063
50-62	0.00151	0.006772	0.016568	0.023242	0.016286	0.008477	0.005569	0.009707	0.010352	0.001641	0.00102	0.001383	0.003912	0.001452	0.000496	0.000568	0.108955
62-75	0.001236	0.005575	0.013488	0.017997	0.014179	0.007884	0.005559	0.009674	0.010466	0.001674	0.001049	0.001363	0.004287	0.001319	0.000502	0.000504	0.096755
75-88	0.000884	0.003499	0.009682	0.012308	0.009481	0.006309	0.004831	0.006834	0.005698	0.001873	0.00072	0.001114	0.003337	0.00128	0.000458	0.000421	0.068727
88-100	0.00061	0.002111	0.006426	0.007869	0.005413	0.004945	0.003808	0.003617	0.002951	0.001367	0.000463	0.00084	0.002138	0.000987	0.000342	0.000245	0.044133
100-125	0.000761	0.001985	0.007618	0.009329	0.00582	0.007481	0.00537	0.002916	0.002835	0.002089	0.000662	0.000915	0.002134	0.001404	0.00038	0.000369	0.052068
125-150	0.000189	0.000614	0.003358	0.00476	0.002945	0.003812	0.001906	0.000687	0.000881	0.001074	0.000336	0.00033	0.0005	0.000624	0.000218	0.000156	0.02239
150-175	0.000062	0.000274	0.00145	0.002045	0.001798	0.001616	0.000767	0.00027	0.000371	0.000533	0.000257	0.000108	0.000085	0.000141	0.000058	0.000073	0.009908
175-200	0.000033	0.000083	0.000631	0.001164	0.001182	0.000628	0.000253	0.000114	0.000166	0.000166	0.000127	0.00005	0.000062	0.000071	0.000039	0.000031	0.004799
200-250	0.000021	0.000048	0.000489	0.00123	0.000429	0.000257	0.000158	0.000133	0.000151	0.000145	0.000058	0.000062	0.000054	0.000031	0.000012	0.000008	0.003287
250-300	0.000002	0.000017	0.000131	0.000303	0.000174	0.00011	0.000048	0.000017	0.000048	0.000041	0.000006	0	0.000006	0	0.000002	0.000002	0.000906
300-400	0	0.000002	0.000056	0.000156	0.000089	0.000035	0.000008	0	0.000017	0	0	0	0	0	0	0	0.000363
400-500	0	0	0.000002	0.000037	0.000017	0	0	0	0	0	0	0	0	0	0	0	0.000056
500-600	0	0	0	0	0	0	0	0	0	0	0	0	0	0	0	0	0
600-700	0	0	0	0	0	0	0	0	0	0	0	0	0	0	0	0	0
Subtotal	0.014921	0.039821	0.220116	0.295514	0.107266	0.062625	0.04433	0.062053	0.057193	0.015365	0.008332	0.011688	0.029129	0.014181	0.005998	0.006896	

Peak Period (sec) Versus Vector Mean Direction (to which waves are travelling, clockwise from North)

	22.5	45	67.5	90	112.5	135	157.5	180	202.5	225	247.5	270	292.5	315	337.5	360	Subtotal
1-3	0.003843	0.003677	0.00723	0.033275	0.013822	0.004685	0.004741	0.012088	0.00934	0.001775	0.001527	0.002394	0.005343	0.003063	0.001404	0.002033	0.110241
3-4	0.007857	0.025966	0.040698	0.061124	0.050874	0.029517	0.022251	0.042169	0.042115	0.006365	0.004694	0.007544	0.021301	0.007761	0.002732	0.002974	0.37594
4-5	0.001035	0.003742	0.030784	0.059224	0.021181	0.020424	0.013382	0.006002	0.00431	0.006187	0.00169	0.001408	0.001993	0.002528	0.000884	0.000743	0.175517
5-6	0.000209	0.000973	0.025561	0.053101	0.007857	0.004219	0.001707	0.000631	0.001056	0.000881	0.000321	0.000176	0.000207	0.000153	0.000093	0.000095	0.097242
6-7	0.000981	0.002466	0.065973	0.044494	0.003572	0.001226	0.000875	0.000448	0.000212	0.000083	0.000056	0.000097	0.000139	0.000348	0.000504	0.000498	0.121972
7-8	0.00051	0.001354	0.03448	0.034326	0.006378	0.001626	0.000823	0.000382	0.000068	0.000019	0.000015	0.000035	0.000081	0.000166	0.000207	0.00029	0.080761
8-9	0.000129	0.000516	0.002325	0.003798	0.00235	0.000336	0.000124	0.000039	0.000019	0.000017	0.00001	0.000012	0.000019	0.000025	0.000031	0.000054	0.009804
9-10	0.000336	0.001014	0.011592	0.005295	0.001083	0.000512	0.000382	0.000255	0.000064	0.000031	0.000019	0.000019	0.000041	0.000122	0.000114	0.000191	0.021071
10-11	0.000006	0.00001	0.00018	0.000118	0.000041	0.000015	0.00001	0.000006	0	0.000002	0	0	0	0.000002	0.000004	0.000006	0.000402
11-12	0.000002	0.000031	0.000145	0.000041	0.00001	0.000015	0	0.000002	0	0	0	0	0	0.000002	0.000008	0	0.000257
12-13	0.000004	0.000008	0.000253	0.00012	0.000017	0.000019	0.000006	0.000006	0.000002	0	0	0	0	0	0.000002	0.000004	0.000442
13-14	0.000002	0.000012	0.000247	0.000127	0.000019	0.00001	0.000008	0.000006	0	0	0	0	0.000004	0.000002	0.000004	0.000008	0.00045
14-16	0.000006	0.000048	0.000606	0.000463	0.000062	0.000023	0.000017	0.000019	0.000006	0.000004	0	0.000002	0	0.000006	0.00001	0	0.001271
16-18	0	0.000002	0.000041	0.000008	0.000002	0	0.000002	0	0.000002	0	0	0	0	0	0	0	0.000058
18-20	0	0	0	0	0	0	0	0	0	0	0	0	0	0	0	0	0
20-40	0	0	0	0	0	0	0	0	0	0	0	0	0	0	0	0	0
Subtotal	0.014921	0.039821	0.220116	0.295514	0.107266	0.062625	0.04433	0.062053	0.057193	0.015365	0.008332	0.011688	0.029129	0.014181	0.005998	0.006896	

B.4 MSC Grid Point M6008259

Table B-4: Wave Conditions at Location M6008259

Significant Wave Height (cm) Versus Peak Period (sec)

	0-3	3-4	4-5	5-6	6-7	7-8	8-9	9-10	10-11	11-12	12-13	13-14	14-16	16-18	18-20	20-40	Subtotal
1-25	0.105147	0.007187	0.03918	0.031201	0.108685	0.033567	0.002255	0.013164	0.000382	0.000309	0.000272	0.000168	0.000801	0.000048	0	0	0.342364
25-38	0.041254	0.079617	0.007185	0.006361	0.009699	0.014977	0.000394	0.000353	0	0	0	0	0	0	0	0	0.159839
38-50	0	0.108907	0.009344	0.004026	0.000933	0.00749	0.001091	0.00033	0	0	0	0	0	0	0	0	0.13212
50-62	0	0.084505	0.014075	0.00587	0.000077	0.0028	0.001124	0.00027	0.000004	0	0	0	0	0	0	0	0.108725
62-75	0	0.055586	0.023703	0.006977	0.000068	0.000595	0.000811	0.000365	0.000015	0	0	0	0	0	0	0	0.08812
75-88	0	0.019849	0.033213	0.005727	0.000097	0.000056	0.000174	0.000212	0.000017	0	0	0	0	0	0	0	0.059344
88-100	0	0.004766	0.027279	0.004387	0.000178	0.000017	0.000025	0.000029	0.000008	0	0	0	0	0	0	0	0.036689
100-125	0	0.001327	0.029635	0.010719	0.000604	0.000058	0	0.000008	0	0	0	0	0	0	0	0	0.042351
125-150	0	0.000027	0.00443	0.011435	0.000724	0.000102	0	0	0	0	0	0	0	0	0	0	0.016717
150-175	0	0.000002	0.000481	0.005283	0.001226	0.000174	0	0	0	0	0	0	0	0	0	0	0.007166
175-200	0	0	0.000027	0.001773	0.001543	0.000212	0	0	0	0	0	0	0	0	0	0	0.003555
200-250	0	0	0.000002	0.000423	0.00106	0.000641	0.00001	0	0	0	0	0	0	0	0	0	0.002136
250-300	0	0	0	0.000004	0.00029	0.000301	0.000021	0	0	0	0	0	0	0	0	0	0.000616
300-400	0	0	0	0	0.000017	0.000112	0.000106	0	0	0	0	0	0	0	0	0	0.000234
400-500	0	0	0	0	0	0.000002	0.000021	0	0	0	0	0	0	0	0	0	0.000023
500-600	0	0	0	0	0	0	0	0	0	0	0	0	0	0	0	0	0
600-700	0	0	0	0	0	0	0	0	0	0	0	0	0	0	0	0	0
Subtotal	0.146401	0.361773	0.188553	0.094185	0.125201	0.061103	0.006031	0.01473	0.000425	0.000309	0.000272	0.000168	0.000801	0.000048	0	0	

Significant Wave Height (cm) Versus Vector Mean Direction (to which waves are travelling, clockwise from North)

	22.5	45	67.5	90	112.5	135	157.5	180	202.5	225	247.5	270	292.5	315	337.5	360	Subtotal
1-25	0.004414	0.006664	0.084976	0.163049	0.026463	0.008516	0.007784	0.015102	0.004733	0.002149	0.002931	0.003806	0.003215	0.002352	0.00201	0.002574	0.340738
25-38	0.002622	0.004824	0.011279	0.054024	0.033092	0.012069	0.008093	0.012611	0.004623	0.002134	0.001757	0.004009	0.003034	0.002031	0.001249	0.001748	0.1592
38-50	0.002064	0.006031	0.015373	0.031439	0.024647	0.012542	0.008564	0.012824	0.005252	0.001695	0.001468	0.003066	0.00269	0.001674	0.001074	0.001176	0.131579
50-62	0.001506	0.00486	0.013229	0.022141	0.019364	0.010953	0.008226	0.012163	0.005042	0.001427	0.001265	0.00207	0.002786	0.001448	0.000834	0.000894	0.108206
62-75	0.001062	0.003082	0.009914	0.016657	0.014979	0.009481	0.007467	0.010008	0.004681	0.001487	0.000863	0.001834	0.003258	0.001359	0.00085	0.000738	0.08772
75-88	0.000533	0.001775	0.006737	0.010848	0.009207	0.007763	0.006519	0.005026	0.002622	0.001238	0.000523	0.001217	0.00273	0.001217	0.000628	0.000479	0.059062
88-100	0.000415	0.000852	0.003874	0.006637	0.005077	0.006038	0.004513	0.002524	0.001386	0.000935	0.000388	0.000786	0.001636	0.000888	0.000348	0.000253	0.036552
100-125	0.000265	0.000684	0.004103	0.008367	0.006104	0.009392	0.004895	0.001661	0.001309	0.001137	0.000527	0.000765	0.001489	0.000964	0.000288	0.000207	0.042158
125-150	0.000071	0.000251	0.001583	0.00358	0.003092	0.004227	0.001168	0.000398	0.000498	0.000429	0.000326	0.000247	0.000377	0.000222	0.000087	0.000077	0.016632
150-175	0.000037	0.000071	0.000521	0.001558	0.00208	0.001522	0.000446	0.000145	0.000164	0.000131	0.000156	0.000068	0.000116	0.000052	0.000023	0.000039	0.007129
175-200	0.000012	0.000029	0.000259	0.000981	0.001147	0.000537	0.000197	0.000102	0.000081	0.000058	0.000037	0.000035	0.000044	0.000012	0.000002	0	0.003534
200-250	0.000002	0.000027	0.000151	0.000869	0.000431	0.000247	0.000116	0.00006	0.000066	0.000073	0.000023	0.000035	0.000015	0.000006	0.000004	0.000002	0.002128
250-300	0	0	0.000046	0.00018	0.000205	0.00012	0.000031	0.000004	0.000025	0	0	0	0.000002	0	0	0	0.000614
300-400	0	0	0.000004	0.000124	0.000087	0.000019	0	0	0	0	0	0	0	0	0	0	0.000234
400-500	0	0	0	0.000006	0.000017	0	0	0	0	0	0	0	0	0	0	0	0.000023
500-600	0	0	0	0	0	0	0	0	0	0	0	0	0	0	0	0	0
600-700	0	0	0	0	0	0	0	0	0	0	0	0	0	0	0	0	0
Subtotal	0.013003	0.029152	0.152048	0.320461	0.145994	0.083427	0.058019	0.072627	0.030481	0.012893	0.010263	0.017939	0.021392	0.012225	0.007398	0.008189	

Peak Period (sec) Versus Vector Mean Direction (to which waves are travelling, clockwise from North)

	22.5	45	67.5	90	112.5	135	157.5	180	202.5	225	247.5	270	292.5	315	337.5	360	Subtotal
1-3	0.003806	0.004094	0.008041	0.036015	0.029554	0.009296	0.008522	0.018854	0.005973	0.002626	0.003294	0.004922	0.003995	0.002572	0.001809	0.002396	0.145768
3-4	0.006923	0.017541	0.034312	0.053304	0.059402	0.036398	0.029485	0.048275	0.020668	0.006797	0.005393	0.010893	0.014641	0.007444	0.004269	0.004441	0.360187
4-5	0.000707	0.003275	0.020559	0.069576	0.031031	0.028	0.016458	0.004136	0.002893	0.003055	0.001234	0.001701	0.002315	0.00168	0.000651	0.000514	0.187785
5-6	0.000151	0.000639	0.014666	0.057776	0.011316	0.005957	0.001437	0.000585	0.000624	0.000183	0.000081	0.000127	0.000141	0.000037	0.000023	0.000058	0.093801
6-7	0.000782	0.001977	0.047623	0.063465	0.005546	0.001624	0.000993	0.000417	0.000205	0.000149	0.000162	0.000153	0.00018	0.000301	0.000411	0.000458	0.124448
7-8	0.000315	0.000784	0.018596	0.031871	0.006347	0.001386	0.000672	0.000178	0.000056	0.000037	0.000046	0.000071	0.000058	0.000089	0.000139	0.000185	0.060829
8-9	0.000091	0.000263	0.001257	0.002308	0.001632	0.000203	0.000062	0.000015	0.000019	0.000015	0.00001	0.000027	0.000015	0.000019	0.000023	0.000041	0.006
9-10	0.000189	0.000527	0.006471	0.005129	0.001002	0.000471	0.000328	0.000143	0.000033	0.000029	0.000044	0.000039	0.000046	0.000073	0.000066	0.000091	0.014681
10-11	0.00001	0.000004	0.000153	0.000133	0.00005	0.000025	0.000021	0.000006	0.000002	0	0	0	0	0.000006	0.000006	0.000004	0.000421
11-12	0.000021	0.000017	0.000081	0.000141	0.000027	0.000008	0.000006	0.000002	0	0	0	0.000002	0.000002	0.000002	0	0	0.000309
12-13	0.000002	0	0.00005	0.000151	0.000033	0.000021	0.000012	0.000002	0	0	0	0	0	0	0	0	0.000272
13-14	0.000002	0.000006	0.000052	0.000073	0.000019	0.000004	0.000004	0	0	0.000002	0	0	0	0	0.000002	0	0.000164
14-16	0.000002	0.000025	0.000183	0.000481	0.000035	0.000033	0.000015	0.000012	0.000004	0	0	0.000004	0	0.000002	0	0	0.000796
16-18	0	0	0.000004	0.000037	0	0	0.000002	0.000002	0.000002	0	0	0	0	0	0	0	0.000048
18-20	0	0	0	0	0	0	0	0	0	0	0	0	0	0	0	0	0
20-40	0	0	0	0	0	0	0	0	0	0	0	0	0	0	0	0	0
Subtotal	0.013003	0.029152	0.152048	0.320461	0.145994	0.083427	0.058019	0.072627	0.030481	0.012893	0.010263	0.017939	0.021392	0.012225	0.007398	0.008189	

B.5 MSC Grid Point M6008083

Table B-5: Wave Conditions at Location M6008083

Significant Wave Height (cm) Versus Peak Period (sec)

	0-3	3-4	4-5	5-6	6-7	7-8	8-9	9-10	10-11	11-12	12-13	13-14	14-16	16-18	18-20	20-40	Subtotal
1-25	0.080033	0.014102	0.025536	0.018159	0.118664	0.036125	0.003377	0.020023	0.000539	0.000504	0.000672	0.000645	0.001672	0.000112	0	0	0.320163
25-38	0.032234	0.066521	0.006415	0.009392	0.024381	0.020449	0.000328	0.002844	0	0	0.000019	0.000035	0.000017	0	0	0	0.162633
38-50	0	0.092171	0.011941	0.002999	0.005803	0.014446	0.001197	0.001089	0	0.000002	0.000015	0.000012	0	0	0	0	0.129675
50-62	0	0.071677	0.017375	0.004851	0.001365	0.008977	0.001686	0.000825	0	0.000002	0.000006	0	0	0	0	0	0.106764
62-75	0	0.04814	0.022809	0.008962	0.000265	0.004034	0.002211	0.000772	0.00001	0.000004	0	0	0	0	0	0	0.087208
75-88	0	0.020888	0.026463	0.01147	0.000079	0.000583	0.001537	0.000716	0.000008	0.000012	0	0	0	0	0	0	0.061756
88-100	0	0.006641	0.021089	0.010572	0.000102	0.000071	0.000456	0.00061	0.000029	0	0	0	0	0	0	0	0.03957
100-125	0	0.002676	0.02537	0.019959	0.000129	0.000052	0.000162	0.00038	0.000068	0	0	0	0	0	0	0	0.048795
125-150	0	0.000203	0.006963	0.015332	0.000183	0.000106	0.000002	0.000037	0.000037	0.000021	0	0	0	0	0	0	0.022884
150-175	0	0.000006	0.000796	0.0089	0.000454	0.000236	0	0.00001	0.000012	0	0	0	0	0	0	0	0.010416
175-200	0	0	0.000052	0.003729	0.000991	0.000392	0	0.000002	0	0	0	0	0	0	0	0	0.005167
200-250	0	0	0	0.000911	0.001375	0.001101	0.00001	0	0.000008	0	0	0	0	0	0	0	0.003406
250-300	0	0	0	0.000002	0.000502	0.000452	0.00006	0	0	0	0	0	0	0	0	0	0.001016
300-400	0	0	0	0	0.000106	0.000205	0.000178	0.000004	0	0	0	0	0	0	0	0	0.000494
400-500	0	0	0	0	0	0.000002	0.000048	0.000004	0	0	0	0	0	0	0	0	0.000054
500-600	0	0	0	0	0	0	0	0	0	0	0	0	0	0	0	0	0
600-700	0	0	0	0	0	0	0	0	0	0	0	0	0	0	0	0	0
Subtotal	0.112267	0.323025	0.16481	0.115237	0.154398	0.087231	0.011252	0.027316	0.000713	0.000545	0.000711	0.000693	0.001688	0.000112	0	0	

Significant Wave Height (cm) Versus Vector Mean Direction (to which waves are travelling, clockwise from North)

	22.5	45	67.5	90	112.5	135	157.5	180	202.5	225	247.5	270	292.5	315	337.5	360	Subtotal
1-25	0.002694	0.006739	0.134875	0.113186	0.016466	0.004536	0.003922	0.005374	0.013967	0.0029	0.002035	0.003422	0.003603	0.001987	0.001298	0.001782	0.318786
25-38	0.001877	0.004115	0.016821	0.074973	0.022759	0.005911	0.003964	0.004526	0.012947	0.002902	0.0014	0.002972	0.003673	0.001672	0.00067	0.000805	0.161985
38-50	0.001215	0.004818	0.016632	0.042189	0.022093	0.007301	0.004505	0.004437	0.012976	0.003335	0.001276	0.002483	0.003613	0.001261	0.000496	0.000448	0.129078
50-62	0.000655	0.00375	0.015294	0.027424	0.019461	0.00683	0.003874	0.004028	0.012374	0.00392	0.00128	0.002138	0.003605	0.000892	0.000396	0.000357	0.106279
62-75	0.000516	0.002481	0.010132	0.020272	0.015506	0.006581	0.003377	0.00369	0.01119	0.00493	0.00124	0.002078	0.003337	0.000755	0.000392	0.000305	0.086783
75-88	0.000425	0.001255	0.007042	0.013984	0.009721	0.005337	0.002752	0.003221	0.006687	0.004762	0.001135	0.001605	0.002354	0.000724	0.000317	0.000191	0.061512
88-100	0.000247	0.000651	0.004015	0.008549	0.005834	0.004096	0.002375	0.002213	0.003379	0.003615	0.000786	0.001166	0.001734	0.00045	0.000124	0.000174	0.03941
100-125	0.000274	0.000562	0.004078	0.01075	0.006886	0.006058	0.003443	0.002651	0.003752	0.004932	0.001222	0.001178	0.001821	0.000616	0.000209	0.000147	0.04858
125-150	0.000071	0.000193	0.001541	0.005326	0.004161	0.003509	0.001514	0.000799	0.001114	0.002626	0.00083	0.000413	0.000423	0.000149	0.000046	0.000056	0.02277
150-175	0.000035	0.000085	0.000687	0.002412	0.002259	0.001591	0.000728	0.000377	0.000299	0.001155	0.000442	0.000091	0.0001	0.00005	0.000037	0.000029	0.010377
175-200	0.00001	0.000021	0.000274	0.001276	0.00135	0.000701	0.000319	0.000127	0.000131	0.000566	0.000272	0.000039	0.00005	0.00001	0.000004	0.000004	0.005154
200-250	0.000004	0.000029	0.000193	0.001265	0.000529	0.000334	0.00017	0.000114	0.000151	0.000326	0.000205	0.000039	0.000012	0.000004	0.000004	0.000002	0.003383
250-300	0	0.000006	0.000075	0.000315	0.000185	0.000122	0.000058	0.000019	0.000027	0.000158	0.000046	0.000004	0	0	0	0	0.001014
300-400	0	0	0.000025	0.000156	0.000139	0.000054	0.000027	0	0.00001	0.000079	0	0	0	0	0	0	0.000489
400-500	0	0	0.000002	0.000025	0.000021	0.000002	0	0	0	0	0	0	0	0	0	0	0.00005
500-600	0	0	0	0	0	0	0	0	0	0	0	0	0	0	0	0	0
600-700	0	0	0	0	0	0	0	0	0	0	0	0	0	0	0	0	0
Subtotal	0.008025	0.024705	0.211685	0.322102	0.127371	0.052964	0.031029	0.031574	0.079003	0.036206	0.012167	0.01763	0.024325	0.00857	0.003995	0.0043	

Peak Period (sec) Versus Vector Mean Direction (to which waves are travelling, clockwise from North)

	22.5	45	67.5	90	112.5	135	157.5	180	202.5	225	247.5	270	292.5	315	337.5	360	Subtotal
1-3	0.001836	0.003358	0.006625	0.032225	0.018752	0.004003	0.003484	0.005519	0.017576	0.00363	0.002282	0.00421	0.00436	0.001831	0.000855	0.001263	0.111809
3-4	0.003893	0.014135	0.034747	0.058844	0.050959	0.020903	0.013928	0.016871	0.052104	0.013272	0.005098	0.01097	0.017761	0.004671	0.001827	0.001626	0.321608
4-5	0.000498	0.001406	0.022114	0.053522	0.022448	0.015886	0.009226	0.00649	0.007604	0.016107	0.00335	0.001887	0.001558	0.001116	0.000417	0.000336	0.163964
5-6	0.000062	0.000359	0.016935	0.062968	0.019592	0.008108	0.001881	0.000564	0.000419	0.002437	0.001018	0.000228	0.000112	0.000012	0.000015	0.000019	0.114729
6-7	0.000964	0.002862	0.078843	0.060089	0.00415	0.001551	0.001025	0.000807	0.000512	0.000566	0.000276	0.00018	0.000307	0.000564	0.000496	0.000595	0.153789
7-8	0.000355	0.000977	0.032877	0.041268	0.007042	0.001539	0.000813	0.000687	0.000373	0.000106	0.000052	0.000075	0.000093	0.000193	0.000193	0.000232	0.086874
8-9	0.000052	0.000442	0.002377	0.00476	0.002783	0.000363	0.000158	0.000089	0.000056	0.000019	0.000008	0.000019	0.00001	0.000019	0.000008	0.000031	0.011194
9-10	0.000317	0.00106	0.014855	0.007046	0.001423	0.000514	0.000446	0.000463	0.000311	0.000062	0.000075	0.000056	0.000118	0.000139	0.00017	0.000178	0.027233
10-11	0.000006	0.00001	0.000328	0.000245	0.000046	0.000025	0.000012	0.000023	0.000012	0	0	0	0	0.000002	0.000002	0.000002	0.000713
11-12	0.000012	0.000044	0.00033	0.000097	0.000019	0.000021	0.000004	0.00001	0	0	0	0	0.000002	0.000004	0	0.000002	0.000545
12-13	0.000008	0.000012	0.000429	0.000168	0.000037	0.000008	0.000017	0.00001	0.000004	0	0	0	0.000004	0.000004	0.000004	0.000004	0.000711
13-14	0.000004	0.000012	0.000411	0.000172	0.000035	0.000012	0.000008	0.000012	0.000004	0.000002	0.000006	0	0	0.000004	0.000004	0.000004	0.000693
14-16	0.000015	0.000023	0.000743	0.000676	0.000081	0.000031	0.000023	0.000029	0.000025	0.000004	0.000002	0.000004	0	0.00001	0.000002	0.000006	0.001674
16-18	0.000002	0.000004	0.000073	0.000021	0.000004	0	0.000004	0	0.000002	0	0	0	0	0	0.000002	0	0.000112
18-20	0	0	0	0	0	0	0	0	0	0	0	0	0	0	0	0	0
20-40	0	0	0	0	0	0	0	0	0	0	0	0	0	0	0	0	0
Subtotal	0.008025	0.024705	0.211685	0.322102	0.127371	0.052964	0.031029	0.031574	0.079003	0.036206	0.012167	0.01763	0.024325	0.00857	0.003995	0.0043	

B.6 MSC Grid Point M6008084

Table B-6: Wave Conditions at Location M6008084

Significant Wave Height (cm) Versus Peak Period (sec)

	0-3	3-4	4-5	5-6	6-7	7-8	8-9	9-10	10-11	11-12	12-13	13-14	14-16	16-18	18-20	20-40	Subtotal
1-25	0.105049	0.013042	0.021527	0.018428	0.135702	0.031271	0.002138	0.017958	0.000504	0.000577	0.000485	0.000398	0.00117	0.000046	0	0	0.348296
25-38	0.039557	0.077109	0.004088	0.004758	0.017296	0.015419	0.000359	0.001475	0	0.000004	0.000017	0.000023	0	0	0	0	0.160104
38-50	0	0.104813	0.007402	0.003441	0.003095	0.00863	0.001118	0.000601	0	0.000002	0	0	0	0	0	0	0.129103
50-62	0	0.078658	0.011499	0.007911	0.000417	0.00397	0.001352	0.000523	0.000015	0	0	0	0	0	0	0	0.104344
62-75	0	0.050847	0.018934	0.012606	0.000137	0.00085	0.001244	0.000487	0.000015	0	0	0	0	0	0	0	0.085121
75-88	0	0.020189	0.024105	0.012246	0.00012	0.000044	0.000429	0.000377	0.000029	0	0	0	0	0	0	0	0.05754
88-100	0	0.005391	0.019957	0.010296	0.000044	0.000031	0.000066	0.000162	0.000008	0	0	0	0	0	0	0	0.035955
100-125	0	0.00189	0.023108	0.017466	0.000139	0.000035	0.00001	0.000048	0.000025	0.000002	0	0	0	0	0	0	0.042722
125-150	0	0.000095	0.004499	0.014498	0.000303	0.000085	0	0.000006	0.000002	0.000008	0	0	0	0	0	0	0.019497
150-175	0	0.000002	0.000303	0.007626	0.000691	0.000187	0	0	0	0	0	0	0	0	0	0	0.008809
175-200	0	0	0.000021	0.002931	0.001249	0.000307	0	0	0	0	0	0	0	0	0	0	0.004507
200-250	0	0	0	0.000556	0.001466	0.000722	0.000025	0	0	0	0	0	0	0	0	0	0.002769
250-300	0	0	0	0	0.000423	0.000336	0.000044	0	0	0	0	0	0	0	0	0	0.000803
300-400	0	0	0	0	0.000066	0.000209	0.000127	0.000004	0	0	0	0	0	0	0	0	0.000407
400-500	0	0	0	0	0	0.000002	0.000023	0	0	0	0	0	0	0	0	0	0.000025
500-600	0	0	0	0	0	0	0	0	0	0	0	0	0	0	0	0	0
600-700	0	0	0	0	0	0	0	0	0	0	0	0	0	0	0	0	0
Subtotal	0.144607	0.352035	0.135443	0.112763	0.161148	0.062099	0.006936	0.021641	0.000597	0.000593	0.000502	0.000421	0.00117	0.000046	0	0	

Significant Wave Height (cm) Versus Vector Mean Direction (to which waves are travelling, clockwise from North)

	22.5	45	67.5	90	112.5	135	157.5	180	202.5	225	247.5	270	292.5	315	337.5	360	Subtotal
1-25	0.002721	0.005863	0.093443	0.161127	0.02889	0.006666	0.005301	0.008475	0.014759	0.003246	0.003474	0.005071	0.002912	0.001591	0.001348	0.001663	0.346552
25-38	0.002199	0.004729	0.011281	0.057243	0.033528	0.009811	0.005758	0.007297	0.013276	0.002257	0.00178	0.004298	0.002721	0.001259	0.000838	0.001155	0.159428
38-50	0.001647	0.005783	0.014822	0.029927	0.025995	0.011733	0.006042	0.006672	0.013716	0.001958	0.001556	0.003893	0.002443	0.001006	0.00055	0.000852	0.128594
50-62	0.001315	0.004063	0.010725	0.02015	0.020938	0.010497	0.005507	0.006764	0.014013	0.001705	0.00112	0.003053	0.00236	0.000689	0.000529	0.000543	0.103971
62-75	0.001097	0.002483	0.007378	0.014849	0.016348	0.009058	0.005048	0.006635	0.012841	0.001869	0.001004	0.002537	0.002097	0.000587	0.000477	0.000415	0.084721
75-88	0.000514	0.001354	0.004638	0.0099	0.010055	0.007019	0.004188	0.00521	0.00711	0.002255	0.000784	0.001746	0.001711	0.000328	0.000222	0.000268	0.057301
88-100	0.000274	0.000595	0.002676	0.005986	0.005747	0.005138	0.003294	0.003308	0.00363	0.002037	0.000668	0.000929	0.000983	0.000268	0.000143	0.000114	0.035789
100-125	0.000162	0.000427	0.002394	0.00745	0.007189	0.007616	0.004719	0.003018	0.004086	0.002769	0.000967	0.000653	0.000637	0.000234	0.000104	0.000118	0.042542
125-150	0.00005	0.000162	0.000857	0.003354	0.004269	0.004443	0.001782	0.000879	0.001327	0.001487	0.000409	0.000102	0.00011	0.000077	0.000035	0.000046	0.019387
150-175	0.000023	0.000035	0.000278	0.001452	0.002317	0.002014	0.000788	0.000334	0.000504	0.000732	0.000201	0.000025	0.000062	0.000008	0.000002	0.00001	0.008786
175-200	0.000006	0.000017	0.00012	0.000809	0.001468	0.000881	0.00029	0.000131	0.000255	0.000365	0.000106	0.000017	0.000008	0.000004	0.000004	0.000002	0.004484
200-250	0	0.000017	0.000073	0.000788	0.000699	0.000377	0.000187	0.000143	0.000218	0.000183	0.000056	0.000015	0.000002	0	0	0	0.002756
250-300	0	0.000002	0.000019	0.000178	0.000239	0.000118	0.000054	0.000035	0.000073	0.000081	0	0	0	0	0	0	0.000799
300-400	0	0	0.000006	0.000087	0.000162	0.000073	0.000019	0	0.000056	0.000002	0	0	0	0	0	0	0.000404
400-500	0	0	0	0	0.000023	0.000002	0	0	0	0	0	0	0	0	0	0	0.000025
500-600	0	0	0	0	0	0	0	0	0	0	0	0	0	0	0	0	0
600-700	0	0	0	0	0	0	0	0	0	0	0	0	0	0	0	0	0
Subtotal	0.010008	0.02553	0.148707	0.3133	0.157866	0.075446	0.042975	0.048901	0.085864	0.020944	0.012123	0.022338	0.016047	0.00605	0.004252	0.005187	

Peak Period (sec) Versus Vector Mean Direction (to which waves are travelling, clockwise from North)

	22.5	45	67.5	90	112.5	135	157.5	180	202.5	225	247.5	270	292.5	315	337.5	360	Subtotal
1-3	0.0023	0.003833	0.007546	0.037678	0.032375	0.0066	0.005001	0.009259	0.018576	0.003646	0.00381	0.006007	0.003281	0.001468	0.001116	0.001487	0.143982
3-4	0.005949	0.016018	0.031974	0.053981	0.057853	0.033246	0.020276	0.029096	0.055646	0.006822	0.005059	0.014703	0.011482	0.003491	0.002246	0.002794	0.350636
4-5	0.000371	0.00161	0.009701	0.038549	0.021419	0.020737	0.012787	0.007803	0.009188	0.007917	0.00235	0.001039	0.000535	0.00045	0.000226	0.000207	0.134889
5-6	0.000037	0.000377	0.011316	0.056239	0.026791	0.010518	0.002238	0.000684	0.001439	0.001997	0.000452	0.000073	0.0001	0.000004	0.000008	0.000008	0.112284
6-7	0.000884	0.002257	0.058513	0.083348	0.007577	0.001883	0.001276	0.001052	0.000649	0.000429	0.000292	0.00034	0.000433	0.000413	0.000392	0.000429	0.160166
7-8	0.000218	0.000643	0.017493	0.032308	0.007691	0.001417	0.000761	0.00046	0.000166	0.000048	0.000091	0.000071	0.000102	0.000108	0.000133	0.000106	0.061815
8-9	0.000039	0.000191	0.001305	0.002304	0.002427	0.000346	0.000112	0.000075	0.000029	0.00001	0.000015	0.000017	0.00001	0.000008	0.000017	0.000015	0.006919
9-10	0.000191	0.000568	0.009761	0.007301	0.001483	0.000593	0.000454	0.000404	0.000147	0.000068	0.000054	0.000081	0.000095	0.000093	0.000106	0.000131	0.021531
10-11	0.000012	0.000012	0.000272	0.00016	0.00006	0.000027	0.000021	0.000015	0.000008	0	0	0	0.000002	0.000002	0.000002	0.000004	0.000597
11-12	0.000002	0.000004	0.000326	0.000156	0.000054	0.000019	0.000008	0.000006	0.000004	0	0	0.000004	0.000002	0.000002	0.000002	0	0.000589
12-13	0.000002	0.000004	0.000129	0.00028	0.000027	0.000017	0.000019	0.000012	0.000002	0	0	0	0.000004	0.000002	0	0.000004	0.000502
13-14	0	0.000004	0.00016	0.000189	0.000039	0.000006	0.000004	0.000006	0.000002	0.000002	0	0	0	0.000002	0.000002	0.000002	0.000419
14-16	0.000002	0.000008	0.000209	0.000772	0.000068	0.000035	0.000019	0.000027	0.000006	0.000004	0	0.000004	0	0.000006	0.000002	0	0.001164
16-18	0	0	0.000004	0.000035	0.000002	0.000002	0	0.000002	0	0	0	0	0	0	0	0	0.000046
18-20	0	0	0	0	0	0	0	0	0	0	0	0	0	0	0	0	0
20-40	0	0	0	0	0	0	0	0	0	0	0	0	0	0	0	0	0
Subtotal	0.010008	0.02553	0.148707	0.3133	0.157866	0.075446	0.042975	0.048901	0.085864	0.020944	0.012123	0.022338	0.016047	0.00605	0.004252	0.005187	

B.7 MSC Grid Point M6006383

Table B-7: Wave Conditions at Location M6006383

Significant Wave Height (cm) Versus Peak Period (sec)

	0-3	3-4	4-5	5-6	6-7	7-8	8-9	9-10	10-11	11-12	12-13	13-14	14-16	16-18	18-20	20-40	Subtotal
1-25	0.000703	0.000222	0.0001	0.000079	0.000624	0.000699	0.002566	0.001616	0.000693	0.000595	0.00006	0.000044	0.000409	0.000046	0.000012	0	0.008466
25-38	0.000954	0.004109	0.001174	0.001099	0.004445	0.003254	0.007052	0.004266	0.002373	0.000687	0.000193	0.000187	0.000796	0.000083	0.000019	0	0.030691
38-50	0	0.008811	0.004362	0.005096	0.010526	0.006797	0.008973	0.005557	0.003053	0.000734	0.000305	0.000255	0.000867	0.000062	0.000006	0	0.055403
50-62	0	0.0112	0.008321	0.011652	0.020459	0.010331	0.009319	0.006162	0.00359	0.001095	0.00046	0.000282	0.000956	0.000143	0	0	0.083972
62-75	0	0.013558	0.011845	0.01629	0.026034	0.014793	0.00947	0.005837	0.003781	0.001375	0.000429	0.000473	0.001023	0.000058	0	0	0.104966
75-88	0	0.011661	0.016392	0.017991	0.021905	0.016626	0.009755	0.005542	0.003103	0.001751	0.000413	0.000375	0.000799	0.000062	0	0	0.106372
88-100	0	0.005691	0.019455	0.016321	0.01718	0.013142	0.009116	0.004855	0.002783	0.001425	0.000483	0.000382	0.000676	0.000031	0	0	0.091541
100-125	0	0.003673	0.037363	0.029116	0.027472	0.01842	0.018136	0.009485	0.00486	0.002698	0.000776	0.000805	0.00094	0.000021	0.000004	0	0.153768
125-150	0	0.000811	0.021616	0.024597	0.020015	0.012169	0.011959	0.007722	0.004434	0.001865	0.000701	0.000595	0.000556	0.000033	0.000006	0	0.10708
150-175	0	0.000149	0.006042	0.020915	0.018262	0.009914	0.006809	0.005938	0.003995	0.00152	0.000641	0.000363	0.000492	0.000002	0.000004	0	0.075047
175-200	0	0.000027	0.001114	0.012546	0.015809	0.008191	0.005183	0.004132	0.003256	0.000979	0.000463	0.000247	0.000183	0.000008	0	0	0.052137
200-250	0	0	0.000245	0.007384	0.022089	0.011725	0.010045	0.00458	0.0047	0.00141	0.000819	0.000324	0.000305	0.000002	0	0	0.063627
250-300	0	0	0.000023	0.000653	0.008722	0.00627	0.008655	0.003416	0.002781	0.00118	0.000612	0.000226	0.000131	0	0	0	0.032669
300-400	0	0	0	0.000025	0.001921	0.003258	0.009197	0.006152	0.003146	0.001242	0.000589	0.000224	0.000085	0.000002	0	0	0.025841
400-500	0	0	0	0	0	0.000224	0.001207	0.002317	0.00201	0.000485	0.000106	0.000091	0.000021	0.000029	0.000006	0	0.006496
500-600	0	0	0	0	0	0.00001	0.000019	0.000253	0.000612	0.000425	0.000068	0.000027	0.00001	0.000004	0	0	0.001429
600-700	0	0	0	0	0	0	0	0.000008	0.000085	0.000156	0.000073	0.000012	0.000002	0.000004	0	0	0.00034
Subtotal	0.001657	0.059913	0.128051	0.163765	0.215462	0.135823	0.12746	0.077837	0.049256	0.019623	0.007191	0.004911	0.008249	0.000591	0.000058	0	

Significant Wave Height (cm) Versus Vector Mean Direction (to which waves are travelling, clockwise from North)

	22.5	45	67.5	90	112.5	135	157.5	180	202.5	225	247.5	270	292.5	315	337.5	360	Subtotal
1-25	0.00173	0.000857	0.000519	0.000102	0.000048	0.000039	0.000048	0.000068	0.000089	0.000131	0.000139	0.000145	0.000143	0.000212	0.000782	0.003372	0.008423
25-38	0.007877	0.004038	0.002333	0.00083	0.000355	0.000255	0.000288	0.000398	0.000655	0.000616	0.000446	0.000351	0.000394	0.000595	0.002095	0.009029	0.030556
38-50	0.017752	0.010462	0.004298	0.001599	0.000782	0.000436	0.000479	0.000848	0.001141	0.000962	0.000597	0.000512	0.000583	0.000884	0.002711	0.011134	0.055179
50-62	0.031711	0.016448	0.006181	0.00258	0.001217	0.000873	0.000813	0.001435	0.00167	0.001249	0.000709	0.000745	0.000755	0.000996	0.002638	0.01365	0.083669
62-75	0.038811	0.023753	0.00852	0.003775	0.001736	0.001323	0.001367	0.00208	0.002624	0.00152	0.001023	0.000873	0.000896	0.001278	0.003084	0.01186	0.104522
75-88	0.034331	0.027494	0.008991	0.004457	0.002385	0.001674	0.001875	0.002418	0.002949	0.001759	0.001006	0.00102	0.001178	0.001541	0.002526	0.010312	0.105918
88-100	0.025258	0.024908	0.008975	0.004096	0.002302	0.00185	0.001987	0.002362	0.002503	0.001719	0.001103	0.001076	0.001369	0.001487	0.002174	0.007975	0.091146
100-125	0.036328	0.040356	0.016566	0.007815	0.00532	0.004634	0.004586	0.004198	0.004341	0.003464	0.002099	0.002338	0.002837	0.003082	0.004476	0.010715	0.153154
125-150	0.020637	0.025001	0.012565	0.007241	0.00538	0.004432	0.004024	0.002829	0.003138	0.002856	0.002026	0.002082	0.002526	0.002458	0.003005	0.006455	0.106657
150-175	0.012163	0.016491	0.009877	0.006355	0.004911	0.003914	0.002516	0.001896	0.002167	0.001908	0.001587	0.001332	0.001487	0.001686	0.002145	0.004318	0.074753
175-200	0.007392	0.009954	0.007423	0.005718	0.004451	0.002962	0.001589	0.001205	0.001334	0.00128	0.001097	0.000803	0.001076	0.001205	0.001479	0.002951	0.051919
200-250	0.008	0.011571	0.010648	0.008533	0.006612	0.003256	0.001421	0.001155	0.001394	0.001632	0.00118	0.000867	0.000809	0.001124	0.001804	0.003372	0.06338
250-300	0.004009	0.006063	0.005799	0.005428	0.003292	0.00139	0.000469	0.000297	0.000485	0.00085	0.000431	0.000452	0.00029	0.0005	0.000855	0.001935	0.032545
300-400	0.002991	0.004897	0.005573	0.005442	0.002234	0.000496	0.000205	0.000149	0.000224	0.000259	0.000446	0.000257	0.000143	0.000241	0.000558	0.001622	0.025738
400-500	0.000838	0.001365	0.001697	0.001466	0.000336	0.000048	0.000021	0.00001	0.000015	0.000054	0.000054	0.000079	0.000004	0.000048	0.000137	0.000286	0.006457
500-600	0.00018	0.000367	0.00056	0.000189	0.000025	0.000002	0	0	0	0	0	0	0.000006	0.000015	0.000023	0.000058	0.001425
600-700	0.000083	0.000108	0.00011	0.000021	0	0	0	0	0	0	0	0	0	0	0.000002	0.000017	0.00034
Subtotal	0.250091	0.224132	0.110635	0.065647	0.041387	0.027584	0.021687	0.021351	0.02473	0.02026	0.013944	0.012932	0.014498	0.01735	0.030493	0.099061	

Peak Period (sec) Versus Vector Mean Direction (to which waves are travelling, clockwise from North)

	22.5	45	67.5	90	112.5	135	157.5	180	202.5	225	247.5	270	292.5	315	337.5	360	Subtotal
1-3	0.000071	0.000133	0.000278	0.00018	0.000095	0.000075	0.000066	0.000118	0.000189	0.000183	0.000056	0.000062	0.000029	0.000021	0.000052	0.000046	0.001653
3-4	0.004198	0.005411	0.003974	0.003234	0.003138	0.003119	0.00365	0.005739	0.006975	0.003773	0.002659	0.003223	0.003323	0.002508	0.001948	0.002767	0.059639
4-5	0.010157	0.018827	0.012322	0.00694	0.007514	0.010107	0.010978	0.010694	0.010565	0.007531	0.003995	0.00382	0.004434	0.002993	0.002532	0.004059	0.12747
5-6	0.029759	0.046825	0.022906	0.013038	0.009858	0.008153	0.004544	0.002956	0.003831	0.00385	0.002584	0.001456	0.001601	0.002165	0.002727	0.006869	0.163124
6-7	0.06612	0.063387	0.025024	0.018196	0.014513	0.004312	0.00101	0.000612	0.000977	0.001601	0.000906	0.000529	0.000415	0.001261	0.003379	0.012289	0.214531
7-8	0.052363	0.035581	0.016609	0.007859	0.002228	0.000512	0.000224	0.000162	0.000212	0.000311	0.000361	0.000419	0.000438	0.000884	0.002443	0.014699	0.135304
8-9	0.040872	0.024786	0.013936	0.009597	0.002126	0.000315	0.000228	0.000268	0.000409	0.000601	0.000726	0.00074	0.001203	0.002508	0.006816	0.021824	0.126954
9-10	0.022944	0.015039	0.008612	0.003717	0.000732	0.000409	0.000278	0.000324	0.000545	0.000796	0.000871	0.000734	0.000942	0.001883	0.004262	0.015475	0.077563
10-11	0.012387	0.008973	0.004837	0.002055	0.000832	0.000377	0.000388	0.000265	0.000531	0.000898	0.000913	0.000973	0.001132	0.00169	0.003364	0.009439	0.049055
11-12	0.005225	0.002858	0.00123	0.000471	0.000156	0.000079	0.000106	0.000085	0.000172	0.000348	0.000444	0.000465	0.000496	0.00078	0.001622	0.005034	0.019569
12-13	0.002143	0.000989	0.000407	0.000176	0.000091	0.000035	0.000046	0.000031	0.000075	0.000083	0.00012	0.000145	0.000137	0.000209	0.000326	0.002246	0.007259
13-14	0.001902	0.000512	0.000195	0.000089	0.000021	0.000025	0.000046	0.000017	0.000037	0.000066	0.000056	0.000085	0.000058	0.000114	0.000305	0.001412	0.004941
14-16	0.00185	0.000751	0.000317	0.000093	0.000083	0.000062	0.000118	0.000075	0.000168	0.000178	0.000232	0.000253	0.000284	0.000319	0.000693	0.002748	0.008226
16-18	0.000127	0.00012	0.000031	0.000006	0	0.000002	0.000002	0.000004	0.000029	0.000031	0.000017	0.000025	0.000006	0.000015	0.000019	0.000156	0.000589
18-20	0.000015	0.000002	0.000002	0	0	0	0.000002	0.000002	0.000015	0.000008	0.000004	0.000002	0	0	0.000006	0	0.000058
20-40	0	0	0	0	0	0	0	0	0	0	0	0	0	0	0	0	0
Subtotal	0.250131	0.224194	0.11068	0.065652	0.041387	0.027584	0.021687	0.021351	0.02473	0.02026	0.013944	0.012932	0.014498	0.01735	0.030493	0.099063	

B.8 MSC Grid Point M6006974

Table B-8: Wave Conditions at Location M6006974

Significant Wave Height (cm) Versus Peak Period (sec)

	0-3	3-4	4-5	5-6	6-7	7-8	8-9	9-10	10-11	11-12	12-13	13-14	14-16	16-18	18-20	20-40	Subtotal
1-25	0.00213	0.001348	0.000259	0.000307	0.002466	0.002105	0.00442	0.005113	0.003092	0.001135	0.000102	0.000102	0.000709	0.000083	0.00005	0	0.023421
25-38	0.002184	0.010192	0.002887	0.003061	0.011125	0.005225	0.007149	0.007178	0.005142	0.000977	0.000282	0.000168	0.000803	0.000127	0	0	0.056501
38-50	0	0.01602	0.00813	0.00917	0.021336	0.008269	0.00734	0.007407	0.005442	0.001176	0.000367	0.000176	0.000815	0.000071	0	0	0.085721
50-62	0	0.017866	0.009346	0.015311	0.032261	0.009425	0.006274	0.007284	0.004387	0.001551	0.000375	0.000307	0.000863	0.000025	0	0	0.105275
62-75	0	0.018835	0.011484	0.018986	0.039601	0.012664	0.007929	0.00723	0.00392	0.001773	0.000471	0.000438	0.000803	0.000015	0	0	0.12415
75-88	0	0.01432	0.015336	0.018636	0.033914	0.014166	0.009649	0.006529	0.00357	0.001678	0.000438	0.000421	0.000519	0.000012	0	0	0.119186
88-100	0	0.006316	0.017188	0.013784	0.024188	0.011634	0.009692	0.005791	0.003082	0.001437	0.000433	0.000404	0.000317	0.000008	0	0	0.094276
100-125	0	0.003414	0.031479	0.0202	0.029761	0.019874	0.019214	0.011352	0.005633	0.001931	0.00073	0.000701	0.000575	0	0	0	0.144864
125-150	0	0.000604	0.014793	0.014683	0.016236	0.015232	0.013457	0.008844	0.004978	0.001636	0.000614	0.00038	0.000371	0	0.000002	0	0.091829
150-175	0	0.000133	0.004893	0.009132	0.009692	0.009404	0.010539	0.006295	0.003773	0.001097	0.000552	0.000259	0.000193	0.000008	0	0	0.05597
175-200	0	0.000012	0.000969	0.005461	0.005019	0.005849	0.008384	0.004279	0.003053	0.000869	0.000438	0.000174	0.000102	0	0	0	0.034608
200-250	0	0	0.000166	0.004036	0.003464	0.006206	0.008717	0.007154	0.004648	0.001545	0.000562	0.000241	0.000095	0	0	0	0.036834
250-300	0	0	0.000002	0.000421	0.000799	0.002404	0.003395	0.003827	0.003491	0.000871	0.000355	0.000147	0.000041	0	0	0	0.015753
300-400	0	0	0	0.000023	0.000168	0.000823	0.001668	0.002454	0.003066	0.001004	0.000191	0.000093	0.000021	0.000002	0	0	0.009512
400-500	0	0	0	0	0.000002	0.000081	0.000114	0.000284	0.000541	0.000529	0.000095	0.000019	0.000012	0.000006	0	0	0.001684
500-600	0	0	0	0	0	0	0.000002	0.000006	0.000085	0.000102	0.000091	0.00001	0.000002	0	0	0	0.000299
600-700	0	0	0	0	0	0	0	0	0.000006	0.000021	0.000044	0.000031	0	0	0	0	0.000102
Subtotal	0.004314	0.08906	0.116932	0.133211	0.230033	0.123361	0.117944	0.091026	0.057909	0.019333	0.006139	0.004071	0.006241	0.000357	0.000052	0	

Significant Wave Height (cm) Versus Vector Mean Direction (to which waves are travelling, clockwise from North)

	22.5	45	67.5	90	112.5	135	157.5	180	202.5	225	247.5	270	292.5	315	337.5	360	Subtotal
1-25	0.00644	0.002713	0.000823	0.000108	0.000019	0.000017	0.000021	0.000031	0.000046	0.000044	0.000102	0.000581	0.001278	0.001338	0.001981	0.007826	0.023365
25-38	0.018704	0.011206	0.004192	0.000753	0.000288	0.000176	0.000151	0.000172	0.000334	0.000465	0.000956	0.001771	0.001987	0.002228	0.002605	0.010273	0.056262
38-50	0.029122	0.023748	0.006934	0.001738	0.000757	0.000442	0.00045	0.000427	0.00094	0.001595	0.001788	0.001595	0.001622	0.00208	0.002669	0.009423	0.085331
50-62	0.030784	0.037315	0.008838	0.002408	0.001255	0.000577	0.000653	0.00068	0.001257	0.003014	0.002516	0.001495	0.001728	0.002157	0.002806	0.007293	0.104775
62-75	0.031265	0.050139	0.010447	0.003153	0.001607	0.001012	0.001068	0.001255	0.0018	0.003696	0.003182	0.001751	0.001616	0.002439	0.00279	0.00633	0.12355
75-88	0.025379	0.04966	0.011839	0.003302	0.001813	0.001273	0.001147	0.001527	0.002107	0.003528	0.003084	0.001908	0.001639	0.003024	0.002821	0.004621	0.118672
88-100	0.017456	0.039528	0.009522	0.00279	0.001653	0.001473	0.001184	0.001371	0.001831	0.002356	0.002495	0.00162	0.001412	0.002906	0.002688	0.003634	0.09392
100-125	0.024661	0.055739	0.016091	0.005026	0.003026	0.002769	0.00252	0.002136	0.002236	0.003495	0.004565	0.003086	0.002674	0.005229	0.005274	0.005712	0.144239
125-150	0.013687	0.033764	0.011733	0.003711	0.002667	0.002072	0.00145	0.000989	0.000952	0.001848	0.003132	0.002553	0.001829	0.003507	0.004065	0.003497	0.091458
150-175	0.008139	0.019789	0.008066	0.002858	0.001856	0.001025	0.000653	0.000425	0.000373	0.000726	0.001848	0.001804	0.0013	0.002006	0.002491	0.002356	0.055717
175-200	0.004953	0.012374	0.005521	0.001908	0.000993	0.00044	0.000253	0.000172	0.000193	0.000284	0.001126	0.001213	0.000782	0.000996	0.001612	0.001632	0.034453
200-250	0.005888	0.013451	0.00611	0.002383	0.000761	0.000259	0.000122	0.000118	0.000097	0.000224	0.000873	0.001298	0.000998	0.000865	0.00141	0.001802	0.036662
250-300	0.002644	0.006367	0.002956	0.000697	0.000133	0.000052	0.000029	0.000029	0.000035	0.000062	0.000224	0.000535	0.000355	0.000315	0.00045	0.000815	0.015699
300-400	0.002004	0.004451	0.001338	0.000232	0.000046	0.000025	0.000002	0.000002	0.00001	0.00001	0.000091	0.000286	0.00016	0.000129	0.000232	0.000463	0.009481
400-500	0.000463	0.000828	0.000156	0.000006	0	0	0	0	0	0	0.000002	0.000041	0.000064	0.000023	0.000033	0.000062	0.001678
500-600	0.000124	0.000143	0.000012	0	0	0	0	0	0	0	0	0	0	0	0.000004	0.000015	0.000299
600-700	0.000054	0.000046	0	0	0	0	0	0	0	0	0	0	0	0	0	0.000002	0.000102
Subtotal	0.221767	0.361263	0.104578	0.031072	0.016875	0.011611	0.009705	0.009336	0.012212	0.021347	0.025984	0.02154	0.019443	0.029241	0.033932	0.065755	

Peak Period (sec) Versus Vector Mean Direction (to which waves are travelling, clockwise from North)

	22.5	45	67.5	90	112.5	135	157.5	180	202.5	225	247.5	270	292.5	315	337.5	360	Subtotal
1-3	0.000334	0.000678	0.000531	0.000216	0.000054	0.000035	0.000025	0.000041	0.000127	0.000112	0.000232	0.000458	0.000755	0.00029	0.000185	0.000228	0.004302
3-4	0.005171	0.012509	0.006152	0.004721	0.004385	0.002804	0.003059	0.003868	0.006477	0.00773	0.006581	0.005115	0.005384	0.009043	0.003829	0.001773	0.088602
4-5	0.002101	0.028424	0.015776	0.002313	0.006075	0.007149	0.005685	0.004692	0.004644	0.010889	0.009983	0.004702	0.00258	0.005617	0.004988	0.000807	0.116424
5-6	0.01528	0.059923	0.024265	0.006838	0.001916	0.000705	0.000326	0.000191	0.000122	0.001446	0.005901	0.00464	0.002176	0.002107	0.0033	0.003505	0.132641
6-7	0.061514	0.139763	0.012347	0.000933	0.000212	0.000097	0.000056	0.000056	0.000147	0.00016	0.000498	0.00078	0.000801	0.001253	0.003072	0.007218	0.228906
7-8	0.038288	0.045865	0.019026	0.004725	0.000803	0.00016	0.000095	0.000073	0.000127	0.000272	0.000481	0.001033	0.000948	0.001294	0.002491	0.007234	0.122913
8-9	0.039537	0.032605	0.013488	0.008097	0.00242	0.000245	0.000129	0.000068	0.000095	0.00011	0.000301	0.000676	0.001259	0.002028	0.004142	0.012246	0.117446
9-10	0.032601	0.023041	0.007315	0.001775	0.000529	0.000153	0.000124	0.000116	0.000158	0.000226	0.000755	0.001462	0.002043	0.002821	0.004573	0.012982	0.090676
10-11	0.015589	0.012884	0.004418	0.001085	0.000357	0.000166	0.000108	0.000131	0.000166	0.000187	0.00078	0.00169	0.00197	0.002812	0.004372	0.010972	0.057687
11-12	0.005926	0.003611	0.000792	0.000259	0.000073	0.000035	0.000023	0.000044	0.000058	0.000075	0.000245	0.00051	0.000668	0.000979	0.001713	0.004248	0.019258
12-13	0.002149	0.00095	0.000183	0.000062	0.000029	0.000029	0.000021	0.000021	0.000021	0.000015	0.000058	0.000143	0.00029	0.000317	0.000415	0.001431	0.006133
13-14	0.00174	0.000494	0.000108	0.000021	0.00001	0.000017	0.000017	0.000019	0.000033	0.000033	0.00005	0.00006	0.000129	0.000141	0.000274	0.000917	0.004061
14-16	0.001464	0.000475	0.000178	0.000025	0.00001	0.000015	0.000029	0.000017	0.000037	0.000093	0.00012	0.000257	0.000398	0.000487	0.000539	0.002076	0.006222
16-18	0.000079	0.000041	0	0	0	0	0	0	0	0	0	0.000012	0.000037	0.000046	0.000033	0.000106	0.000355
18-20	0.000004	0.000008	0	0.000002	0.000002	0	0.000008	0	0	0	0	0	0.000004	0.000004	0.000006	0.000012	0.000052
20-40	0	0	0	0	0	0	0	0	0	0	0	0	0	0	0	0	0
Subtotal	0.221776	0.361272	0.104578	0.031072	0.016875	0.011611	0.009705	0.009336	0.012212	0.021347	0.025984	0.02154	0.019443	0.029241	0.033932	0.065755	

B.9 MSC Grid Point M6007354

Table B-9: Wave Conditions at Location M6007354

Significant Wave Height (cm) Versus Peak Period (sec)

	0-3	3-4	4-5	5-6	6-7	7-8	8-9	9-10	10-11	11-12	12-13	13-14	14-16	16-18	18-20	20-40	Subtotal
1-25	0.016033	0.006027	0.005511	0.004571	0.021946	0.006554	0.009089	0.015705	0.003978	0.002248	0.000431	0.000243	0.002296	0.000353	0.000077	0	0.095062
25-38	0.007351	0.019279	0.016477	0.012322	0.038354	0.008151	0.003719	0.008693	0.000823	0.000946	0.000467	0.000496	0.000767	0.0001	0	0	0.117944
38-50	0	0.027635	0.012501	0.020077	0.048318	0.009489	0.004551	0.007309	0.000838	0.000558	0.000504	0.000442	0.00027	0.000004	0	0	0.132496
50-62	0	0.02917	0.00936	0.020503	0.040262	0.011592	0.005509	0.007355	0.00112	0.000386	0.000392	0.000201	0.000153	0.000019	0	0	0.126023
62-75	0	0.031815	0.011352	0.017217	0.029909	0.013168	0.006343	0.008305	0.001213	0.000348	0.000222	0.000255	0.000104	0.000008	0	0	0.120259
75-88	0	0.024794	0.015908	0.011696	0.018364	0.012472	0.004443	0.007533	0.001095	0.00033	0.00017	0.00018	0.00006	0.000006	0	0	0.097051
88-100	0	0.011532	0.019403	0.007035	0.010161	0.010358	0.004327	0.005075	0.000991	0.000216	0.000147	0.000087	0.000097	0.000004	0	0	0.069435
100-125	0	0.005861	0.036413	0.011069	0.01002	0.016054	0.009927	0.006809	0.001473	0.000452	0.000236	0.000102	0.000029	0.000012	0	0	0.098458
125-150	0	0.00102	0.017242	0.010404	0.004343	0.008197	0.010758	0.003951	0.00084	0.000369	0.000193	0.000129	0.000012	0	0	0	0.057459
150-175	0	0.000137	0.004437	0.00997	0.002437	0.003738	0.009124	0.0033	0.00061	0.000255	0.000095	0.000023	0.000002	0	0	0	0.034127
175-200	0	0.000025	0.000747	0.00632	0.001682	0.001887	0.006486	0.002833	0.000575	0.000135	0.000091	0.000023	0.000002	0	0	0	0.020805
200-250	0	0.000002	0.000147	0.004484	0.00245	0.001527	0.004941	0.004142	0.00185	0.000205	0.000023	0.000027	0	0	0	0	0.019797
250-300	0	0	0.000004	0.000353	0.001375	0.00073	0.001058	0.001493	0.001792	0.000247	0.000019	0.000008	0.000002	0.000006	0	0	0.007087
300-400	0	0	0	0.000004	0.000446	0.000529	0.000599	0.000502	0.000767	0.000512	0.000073	0.000008	0	0.000002	0	0	0.003443
400-500	0	0	0	0	0.000002	0.000073	0.000077	0.000068	0.000081	0.000108	0.000056	0	0	0	0	0	0.000465
500-600	0	0	0	0	0	0	0	0.000006	0.000008	0.000029	0.000041	0	0	0	0	0	0.000085
600-700	0	0	0	0	0	0	0	0	0	0	0.000004	0	0	0	0	0	0.000004
Subtotal	0.023383	0.157298	0.149501	0.136026	0.23007	0.104518	0.080948	0.08308	0.018055	0.007344	0.003165	0.002223	0.003796	0.000514	0.000077	0	

Significant Wave Height (cm) Versus Vector Mean Direction (to which waves are travelling, clockwise from North)

	22.5	45	67.5	90	112.5	135	157.5	180	202.5	225	247.5	270	292.5	315	337.5	360	Subtotal
1-25	0.006376	0.055443	0.01444	0.001251	0.000344	0.000249	0.0004	0.000514	0.000699	0.001201	0.002499	0.002962	0.002508	0.001817	0.001674	0.002423	0.094799
25-38	0.003292	0.063918	0.027304	0.003574	0.00124	0.000817	0.000923	0.001643	0.002555	0.003306	0.001887	0.001512	0.001894	0.001319	0.000983	0.001448	0.117614
38-50	0.002831	0.06526	0.03477	0.005237	0.002389	0.001452	0.001386	0.002416	0.003487	0.003696	0.001489	0.001363	0.002095	0.001437	0.001271	0.001342	0.131921
50-62	0.00279	0.048932	0.041055	0.006747	0.003061	0.00185	0.001761	0.002856	0.004105	0.003416	0.001394	0.0014	0.002192	0.001423	0.001126	0.00124	0.125348
62-75	0.002205	0.035552	0.04242	0.008415	0.003764	0.002868	0.002622	0.003547	0.004683	0.004098	0.001566	0.001535	0.002792	0.001377	0.001029	0.001116	0.119589
75-88	0.001504	0.021239	0.035743	0.007857	0.003982	0.002831	0.002659	0.003466	0.004822	0.003713	0.001585	0.001751	0.00235	0.001468	0.000799	0.000832	0.096599
88-100	0.001155	0.012426	0.024856	0.005841	0.003213	0.002698	0.002783	0.002808	0.003876	0.002871	0.001479	0.001271	0.001605	0.000998	0.000626	0.000552	0.069059
100-125	0.001821	0.013635	0.035117	0.008867	0.005563	0.00487	0.004683	0.004076	0.004847	0.00441	0.00263	0.001863	0.002317	0.001421	0.000894	0.000954	0.097966
125-150	0.001054	0.00645	0.020397	0.005857	0.003727	0.003841	0.002767	0.002201	0.002323	0.002584	0.001798	0.00112	0.00096	0.001008	0.000554	0.000554	0.057195
150-175	0.000618	0.003331	0.01214	0.003854	0.00296	0.002394	0.001535	0.001101	0.000962	0.001535	0.001396	0.000697	0.000375	0.00038	0.000377	0.000346	0.034001
175-200	0.000382	0.002022	0.007597	0.00279	0.002182	0.001356	0.000693	0.000498	0.00045	0.000755	0.000857	0.000357	0.000176	0.000199	0.000191	0.000228	0.020733
200-250	0.000243	0.001699	0.007674	0.003236	0.002049	0.001247	0.00067	0.000346	0.000305	0.000498	0.000869	0.000353	0.000174	0.000114	0.000127	0.000127	0.019729
250-300	0.000104	0.000803	0.00297	0.001215	0.000606	0.000305	0.000168	0.000114	0.000114	0.000131	0.000297	0.000137	0.000052	0.000021	0.000017	0.000021	0.007073
300-400	0.000025	0.000377	0.001587	0.000514	0.000255	0.000095	0.000093	0.000066	0.000025	0.000075	0.00017	0.000114	0.000017	0.000002	0.000008	0.000006	0.003431
400-500	0.000006	0.000077	0.000203	0.000089	0.000046	0.000015	0.000002	0	0	0	0.000021	0.000004	0	0	0	0	0.000463
500-600	0	0.000025	0.000048	0.00001	0	0	0	0	0	0	0	0	0	0	0	0	0.000083
600-700	0	0.000004	0	0	0	0	0	0	0	0	0	0	0	0	0	0	0.000004
Subtotal	0.024404	0.331193	0.30832	0.065353	0.035382	0.026889	0.023145	0.025653	0.033254	0.032288	0.019936	0.016437	0.019507	0.012984	0.009676	0.011188	

Peak Period (sec) Versus Vector Mean Direction (to which waves are travelling, clockwise from North)

	22.5	45	67.5	90	112.5	135	157.5	180	202.5	225	247.5	270	292.5	315	337.5	360	Subtotal
1-3	0.000726	0.004472	0.002914	0.001327	0.000417	0.000359	0.000535	0.000836	0.00134	0.001989	0.002209	0.002452	0.00185	0.000863	0.000496	0.000519	0.023303
3-4	0.003823	0.017877	0.018545	0.008591	0.00862	0.007461	0.008487	0.013971	0.021158	0.014232	0.0052	0.006181	0.011916	0.005592	0.002661	0.002286	0.156599
4-5	0.00163	0.02434	0.051556	0.005949	0.004999	0.009487	0.009141	0.007504	0.007774	0.010688	0.005851	0.00319	0.001873	0.001954	0.001489	0.00133	0.148753
5-6	0.001095	0.023701	0.073342	0.012604	0.004644	0.004136	0.00252	0.001471	0.001141	0.002846	0.00335	0.001813	0.000948	0.000666	0.000577	0.000543	0.135395
6-7	0.005702	0.141806	0.063069	0.005681	0.001856	0.00112	0.000886	0.000703	0.000558	0.000604	0.001058	0.000747	0.000581	0.001079	0.001417	0.002186	0.229052
7-8	0.001537	0.034229	0.049696	0.010493	0.002661	0.000927	0.000485	0.000303	0.000295	0.000386	0.000554	0.000506	0.000292	0.000417	0.000504	0.00073	0.104014
8-9	0.001883	0.023549	0.023744	0.015259	0.010215	0.002609	0.000496	0.000247	0.000176	0.00018	0.000245	0.000214	0.000297	0.000467	0.000425	0.000635	0.080641
9-10	0.004988	0.043693	0.019302	0.003238	0.00133	0.000558	0.000438	0.000431	0.000545	0.000817	0.000923	0.000892	0.001161	0.001265	0.001361	0.001867	0.082809
10-11	0.001332	0.007678	0.003959	0.00189	0.000504	0.000162	0.000106	0.000114	0.000158	0.000278	0.000278	0.000197	0.000278	0.000307	0.000313	0.000429	0.017982
11-12	0.000778	0.003881	0.001226	0.000214	0.000066	0.000023	0.000012	0.000029	0.000037	0.000095	0.00012	0.0001	0.000135	0.000139	0.000174	0.000301	0.00733
12-13	0.000295	0.001964	0.000409	0.000056	0.000029	0.000019	0.000019	0.000015	0.000027	0.000035	0.000031	0.000039	0.000027	0.000029	0.00006	0.000095	0.003148
13-14	0.000153	0.0014	0.000207	0.000025	0.00001	0.00001	0.00001	0.000019	0.000021	0.000035	0.000027	0.000008	0.000017	0.000058	0.000068	0.000143	0.002213
14-16	0.000409	0.002333	0.000288	0.000025	0.000029	0.000017	0.000008	0.00001	0.000021	0.000089	0.000081	0.000087	0.000091	0.0001	0.000093	0.000106	0.003787
16-18	0.000054	0.000261	0.000044	0.000002	0.000002	0.000002	0.000002	0	0.000004	0.000012	0.00001	0.00001	0.000025	0.000023	0.000033	0.000019	0.000504
18-20	0	0.000008	0.000019	0	0	0	0	0	0	0	0	0.000002	0.000017	0.000027	0.000004	0	0.000077
20-40	0	0	0	0	0	0	0	0	0	0	0	0	0	0	0	0	0
Subtotal	0.024404	0.331193	0.30832	0.065353	0.035382	0.026889	0.023145	0.025653	0.033254	0.032288	0.019936	0.016437	0.019507	0.012984	0.009676	0.011188	

B.10 MSC Grid Point M6007721

Table B-10: Wave Conditions at Location M6007721

Significant Wave Height (cm) Versus Peak Period (sec)

	0-3	3-4	4-5	5-6	6-7	7-8	8-9	9-10	10-11	11-12	12-13	13-14	14-16	16-18	18-20	20-40	Subtotal
1-25	0.0497	0.008305	0.033356	0.010273	0.061655	0.038622	0.007465	0.025574	0.001502	0.001035	0.000915	0.001027	0.002709	0.00027	0.000023	0	0.242427
25-38	0.017478	0.038054	0.018679	0.02138	0.027834	0.037998	0.0005	0.009674	0.000614	0.000102	0.000195	0.000247	0.000172	0.00001	0	0	0.172937
38-50	0	0.059913	0.010835	0.011379	0.008921	0.028664	0.000701	0.006542	0.000259	0.000046	0.000124	0.000166	0.00012	0.000004	0	0	0.127674
50-62	0	0.057345	0.016101	0.004636	0.002796	0.021411	0.001408	0.003648	0.000135	0.000021	0.000031	0.000068	0.000031	0	0	0	0.107631
62-75	0	0.044668	0.026453	0.001813	0.000881	0.017055	0.00246	0.00262	0.000077	0.000021	0.000033	0.000041	0.000017	0	0	0	0.096139
75-88	0	0.022888	0.030118	0.001529	0.000216	0.011671	0.003136	0.001896	0.000039	0.000019	0.000033	0.000027	0.00001	0	0	0	0.071581
88-100	0	0.00778	0.027546	0.001929	0.000085	0.006527	0.003283	0.001639	0.000046	0.000008	0.000029	0.00001	0.000002	0	0	0	0.048885
100-125	0	0.003619	0.037827	0.00739	0.000129	0.006351	0.005801	0.00313	0.000048	0.000037	0.000017	0.000012	0.000002	0	0	0	0.064364
125-150	0	0.000392	0.012144	0.012316	0.000193	0.001495	0.003115	0.002574	0.000205	0.000019	0	0.000006	0	0.000002	0	0	0.032462
150-175	0	0.000021	0.001317	0.010435	0.0005	0.00051	0.000767	0.002072	0.000328	0.000021	0	0.000006	0	0	0	0	0.015977
175-200	0	0	0.000133	0.004849	0.002043	0.000297	0.000118	0.000937	0.000483	0.000044	0	0.000006	0	0	0	0	0.00891
200-250	0	0	0.000008	0.001369	0.005053	0.000149	0.000033	0.000243	0.000363	0.000054	0.000019	0.000008	0	0	0	0	0.007299
250-300	0	0	0	0.000029	0.001941	0.000247	0.000015	0.00001	0.000033	0.000052	0	0	0	0	0	0	0.002327
300-400	0	0	0	0.000002	0.000361	0.000622	0.00022	0	0.000023	0.000006	0.000002	0	0	0	0	0	0.001236
400-500	0	0	0	0	0	0.000004	0.000137	0.00001	0	0	0	0	0	0	0	0	0.000151
500-600	0	0	0	0	0	0	0	0	0	0	0	0	0	0	0	0	0
600-700	0	0	0	0	0	0	0	0	0	0	0	0	0	0	0	0	0
Subtotal	0.067178	0.242983	0.214518	0.089327	0.112607	0.171624	0.02916	0.060568	0.004154	0.001483	0.001398	0.001626	0.003063	0.000286	0.000023	0	

Significant Wave Height (cm) Versus Vector Mean Direction (to which waves are travelling, clockwise from North)

	22.5	45	67.5	90	112.5	135	157.5	180	202.5	225	247.5	270	292.5	315	337.5	360	Subtotal
1-25	0.002441	0.020397	0.138699	0.039601	0.005453	0.001699	0.00157	0.00189	0.003781	0.007365	0.006757	0.005637	0.002371	0.001255	0.001099	0.001363	0.241378
25-38	0.001386	0.005233	0.085839	0.039929	0.008603	0.002922	0.002317	0.002642	0.006282	0.006027	0.001247	0.003453	0.003034	0.001323	0.001014	0.000985	0.172238
38-50	0.001319	0.004405	0.043471	0.035227	0.009763	0.004476	0.003113	0.00273	0.006585	0.006212	0.001222	0.002462	0.002846	0.00158	0.000896	0.000817	0.127124
50-62	0.001068	0.004646	0.030386	0.028247	0.011171	0.004652	0.002918	0.002649	0.005946	0.006533	0.001267	0.002024	0.002956	0.001267	0.000709	0.000738	0.107179
62-75	0.001049	0.004325	0.025028	0.023703	0.010543	0.004594	0.002566	0.002628	0.006515	0.006782	0.001311	0.001993	0.002308	0.001124	0.000601	0.000649	0.09572
75-88	0.000946	0.002974	0.01623	0.017414	0.007539	0.004227	0.002485	0.002325	0.005274	0.005538	0.001211	0.001417	0.001676	0.001	0.00046	0.000548	0.071264
88-100	0.000776	0.001844	0.010848	0.011435	0.004864	0.003263	0.00202	0.001666	0.003248	0.00381	0.000989	0.000987	0.001209	0.000879	0.000392	0.000419	0.048648
100-125	0.000925	0.002114	0.01299	0.015259	0.006529	0.005704	0.00314	0.00223	0.003663	0.005059	0.001634	0.001294	0.001431	0.001103	0.000477	0.000525	0.064077
125-150	0.000473	0.000913	0.005523	0.008344	0.004022	0.003603	0.001634	0.000991	0.00107	0.002342	0.001247	0.000599	0.000483	0.000525	0.000336	0.000228	0.032333
150-175	0.000118	0.000365	0.002717	0.004694	0.002671	0.001549	0.00066	0.000355	0.000348	0.000844	0.000825	0.000259	0.000166	0.000141	0.0001	0.000095	0.015908
175-200	0.000064	0.000224	0.001583	0.002624	0.001597	0.000925	0.000398	0.000141	0.00012	0.000348	0.000579	0.000104	0.000056	0.000048	0.000029	0.000039	0.008879
200-250	0.000044	0.000127	0.001091	0.002087	0.00146	0.000805	0.000261	0.000162	0.000129	0.000255	0.000635	0.000062	0.000062	0.000023	0.000021	0.000035	0.007257
250-300	0.000015	0.000029	0.000334	0.0009	0.000363	0.000205	0.000097	0.000031	0.000035	0.000104	0.00017	0.000021	0.000004	0.000006	0.000002	0.000004	0.002321
300-400	0	0.000029	0.000153	0.000367	0.000282	0.000118	0.000056	0.000002	0.000006	0.0001	0.000108	0.00001	0	0	0	0	0.001232
400-500	0	0	0.000025	0.000052	0.000068	0.000006	0	0	0	0	0	0	0	0	0	0	0.000151
500-600	0	0	0	0	0	0	0	0	0	0	0	0	0	0	0	0	0
600-700	0	0	0	0	0	0	0	0	0	0	0	0	0	0	0	0	0
Subtotal	0.010624	0.047623	0.374917	0.229881	0.074929	0.038748	0.023236	0.02044	0.043004	0.05132	0.019202	0.020324	0.018603	0.010275	0.006137	0.006446	

Peak Period (sec) Versus Vector Mean Direction (to which waves are travelling, clockwise from North)

							157.5	180	202.5	225	247.5	270	292.5	315	337.5	360	Subtotal
1-3	0.000799	0.001873	0.006907	0.018412	0.00649	0.001804	0.001678	0.002167	0.004839	0.006637	0.005511	0.005258	0.002236	0.000886	0.000707	0.000682	0.066886
3-4	0.004853	0.015234	0.038197	0.036147	0.024006	0.012063	0.00913	0.010213	0.028235	0.025377	0.004553	0.008954	0.012886	0.006189	0.002987	0.00285	0.241874
4-5	0.0013	0.004227	0.067321	0.056333	0.019575	0.016562	0.008784	0.005546	0.006793	0.014722	0.004526	0.003306	0.001261	0.001396	0.000898	0.000929	0.213479
5-6	0.000185	0.001365	0.037338	0.030589	0.007338	0.003993	0.001489	0.000637	0.000479	0.001713	0.001927	0.000927	0.000519	0.000197	0.000104	0.000147	0.088946
6-7	0.000967	0.0042	0.079337	0.017935	0.003298	0.001273	0.000463	0.00034	0.000398	0.000745	0.00135	0.00033	0.000413	0.000463	0.000348	0.000431	0.11229
7-8	0.001079	0.005102	0.104607	0.044585	0.006579	0.001742	0.001014	0.000917	0.001126	0.000888	0.000684	0.000597	0.000485	0.00051	0.00046	0.000651	0.171029
8-9	0.000205	0.002854	0.006942	0.011779	0.005569	0.000687	0.000249	0.000127	0.000081	0.000025	0.000023	0.000137	0.000089	0.000073	0.000079	0.000073	0.02899
9-10	0.001041	0.010636	0.028944	0.011488	0.001724	0.000514	0.000365	0.000417	0.000884	0.000925	0.000523	0.000697	0.000593	0.000458	0.000475	0.000579	0.060263
10-11	0.000081	0.000855	0.001126	0.001408	0.000243	0.000041	0.000021	0.000025	0.000075	0.000124	0.000019	0.000017	0.000021	0.000019	0.000023	0.000035	0.004132
11-12	0.000027	0.000463	0.000562	0.000226	0.000023	0.00001	0.000012	0.000004	0.000012	0.000027	0.000012	0.000027	0.000021	0.000027	0.000004	0.000012	0.001471
12-13	0.000027	0.000363	0.000695	0.000147	0.000031	0.000015	0.00001	0.00001	0.000015	0.000023	0.000008	0.000004	0.000004	0.000004	0.000012	0.000021	0.00139
13-14	0.000015	0.000207	0.000942	0.000189	0.000019	0.000021	0.000015	0.000017	0.000015	0.000023	0.000012	0.00001	0.000054	0.000033	0.000025	0.00001	0.001605
14-16	0.000037	0.000236	0.001836	0.000554	0.000031	0.000019	0.000006	0.000019	0.000052	0.000083	0.000044	0.00006	0.000019	0.000019	0.000015	0.000021	0.003049
16-18	0.000008	0.000008	0.000156	0.000075	0.000004	0.000004	0	0.000002	0.000002	0.000008	0.00001	0	0.000002	0.000002	0	0.000004	0.000286
18-20	0	0	0.000008	0.000015	0	0	0	0	0	0	0	0	0	0	0	0	0.000023
20-40	0	0	0	0	0	0	0	0	0	0	0	0	0	0	0	0	0
Subtotal	0.010624	0.047623	0.374917	0.229881	0.074929	0.038748	0.023236	0.02044	0.043004	0.05132	0.019202	0.020324	0.018603	0.010275	0.006137	0.006446	